ELECTRIC ANALOG COMPUTER STUDY OF SUPERSONIC FLUTTER OF ELASTIC DELTA WINGS

Thesis by

Michael Abram Basin

In Partial Fulfillment of the Requirements

for the Degree of

Doctor of Philosophy

California Institute of Technology

Pasadena, California

1954

ACKNOWLEDGMENTS

I wish to express my deepest appreciation to Dr. Gilbert D. McCann who initiated and directed this research project.

I should like to express my sincerest gratitude and appreciation to those who have helped in carrying on this project:

To Dr. Charles H. Wilts for his many valuable suggestions, encouragement, and continued interest throughout the course of the project.

To Dr. Richard H. MacNeal for his aid in developing the electric analog for the elastic wing structure.

To Vance W. Smith for assisting in the maintenance of the electronic equipment.

To Jeanne Shacklett for her patience with the author in typing this thesis.

Michael A. Basin

ABSTRACT

This thesis presents a method for the solution of the supersonic flutter problem for elastic delta wings with supersonic leading edges.

In Part I, the necessary aerodynamic equations are developed, first in integral form, and then in a power series expansion in order to obtain a practical expression for the pressure at a point on the wing due to the motion of the wing surface in a supersonic air stream.

Part II gives a method for computing the lifts on a partitioned wing, and sets up cell division criteria. These methods are then applied to a specific wing form.

Parts III and IV present the electrical analogs for the aerodynamic lifts, and for the elastic wing structure respectively. These analogs are then applied to the example of part II.

Part V presents the results of the actual flutter study performed on the above wing on the California Institute of Technology Electric Analog Computer.

Part VI contains the conclusions of the study, and recommendations and suggestions for further research.

TABLE OF CONTENTS

LIST OF ILLUSTRATIONS

LIST OF TABLES

LIST OF SYMBOLS

ϕ	disturbance - velocity potential
x', y', z'	rectangular coordinates for fixed system
x, y, z	rectangular coordinates attached to source moving in negative x direction; also represents field point being influenced
ξ', η', ζ'	rectangular coordinates used to represent space coordinates in fixed system
$\xi, \eta, \zeta,$	rectangular coordinates used to represent space location at source distribution $A(\xi, \eta, \zeta)$
t, t'	time
v	velocity of main stream
c	velocity of sound 1,100 ft/sec
M	Mach number v/c
β =	$\sqrt{M^2 - 1}$
θ	variable used instead of ζ
P	pressure
L_i	lift
ρ	density of air = 2.378×10^{-3} lb-ft^{-4}sec^2
α	angle of attack (pitch) = $\alpha_o\, e^{j\omega t}$
ω	angular frequency $\bar{\omega} = \dfrac{\omega M}{c\beta^2}$
h	vertical displacement = $h_o\, e^{j\omega t}$
$\bar{\beta}$	spanwise motion = $\beta_o\, e^{j\omega t}$
δ	coordinate difference = $\dfrac{\bar{\omega}}{c\beta^2}(x - \xi)$
$w(x,z,t)$	vertical velocity at surface of wing = $W(x,z)w(t)$
λ	angle of leading edge of wing
b	semichord of midspan wing section
$\bar{s}$	semispan of wing

p	$\frac{d}{dt}$
$A = -\theta_1$	velocity potential coefficients
$B = -\frac{\sin 2\theta_1}{2}$	velocity potential coefficients
$D = -\theta_1 + \frac{\sin 2\theta_1}{2}$	velocity potential coefficients
K, a, N, P_1, b'	scale factors
τ	time constant
L	inductance
R	resistance
C	capacitance
K_o	fraction of potentiometer setting
T	transformer
k_o	radius of gyration
$\bar{m}$, $\bar{M}$	mass
E	Young's modulus
I	moment of inertia
G	torsion modulus
M_x, M_y, M_s	moments
D_o	Stiffness coefficient of plate $\frac{Et_o^3}{12(1-\nu^2)}$
ν	Poisson's Ratio
A_i	wing cell area $(\bar{c}\,\bar{d})$
$\bar{c}$	spanwise dimension of wing cell
$\bar{d}$	chordwise dimension of wing cell
n	number of cells along trailing edge of semi-span of wing
Γ	lift coefficient = (Area of cell) x $\frac{\rho c}{\pi}$
e,g,k,m	aerodynamic lag (lead) function coefficients

d	separation of wing cover plates
t_o	thickness of wing cover plate
$\bar{\theta}$	angle of leading edge of wing $= \frac{\pi}{2} - \lambda$
$Z_m(x,z,t)$	vertical motion of a point on the wing
E_h, E_α	voltages
i, I_x, I_y, I_s	currents
s	distance along leading edge
ω'	equivalent width of leading edge beam
q	load per unit area on a plate

I THE AERODYNAMIC PROBLEM

A. Introduction

In high-speed-aircraft design, a knowledge of the air forces that act on various types of oscillating-wing plan forms is often desired. Such information is used in the solution of general instability problems such as wing flutter and low-frequency instability of aircraft involving control-surface deflections. The usual line of approach lies in the solution of the linearized partial differential equation for the disturbance velocity potential for compressible flow.

The solution of the compressible flow equation for a purely "supersonic wing", namely one in which the upper and lower surfaces of the wing can be assumed to act independently of one another (Refs. 1,2), is usually given in terms of a Green's function type solution, the potential of a point being represented by an integral equation (Abel's Equation) integrated over a wing surface.

This thesis is concerned with developing an integrated form of this solution in such a manner that the resulting air forces can be represented electrically on an analog computer, thus making possible a supersonic flutter analysis of an arrowhead type wing.

The treatment used for the purely supersonic case, involving source and sink distributions to account for the motion of the body, is believed to be exact within the framework of the linearized theory. The problem is analogous to that of sound in a moving medium generated by the motion of pistons imbedded in an infinite plane. For a treatment of the aerodynamic equations in a mixed supersonic case the reader is referred to Stewart's work (ref. 3).

It should be recognized at the start that the small-disturbance linearized theory being much less complicated than a more rigorous nonlinear theory, is to be regarded as an expedient which allows an initial theoretical solution. This theory permits the occurrence of weak shocks and thus the basic effects and trends can be studied. In view of the restriction on the theory that only small disturbances in an ideal fluid can be allowed, only thin, nearly flat wings at a small angle of attack situated in a nonviscous flow, free of strong shocks, can be analyzed. In view of the above restrictions and assumptions in the analysis, important modifications may be required in certain cases for thick finite airfoils, but even here, the simple theory for thin wings may serve as a basis.

B. The Wave Equation

In the linearized theory based on small disturbances, the equation satisfied by the velocity potential for the propogation of sound waves of small amplitude is the wave equation:

$$\frac{1}{c^2}\frac{\partial^2 \phi}{\partial t'^2} = \frac{\partial^2 \phi}{\partial x'^2} + \frac{\partial^2 \phi}{\partial y'^2} + \frac{\partial^2 \phi}{\partial z'^2} \tag{1}$$

the fluid being at rest at infinity. For completeness, the derivation of this equation as given by Baker and Copson (Ref. 4) is presented in Appendix A.

Fundamental solutions of equation (1) are of the form of spherical waves

$$\phi_o = \frac{A}{r'}\, f(t' - \frac{r'}{c}) + \frac{A}{r'}\, f(t' + \frac{r'}{c}) \tag{2}$$

where

$$r' = \sqrt{(x'-\xi')^2 + (y'-\eta')^2 + (z'-\zeta')^2}$$

the source being at the point (ξ', η', ζ'), the source strength being $A(\xi', \eta', \zeta')f(t')$.

The outward moving wave of equation (2) represents a "retarded" potential, while the incoming wave is known as an "advanced" potential.

The following problem will now be analyzed: consider a thin lifting surface of small curvature moving forward at a constant supersonic velocity v, which may be performing small oscillations normal to the direction of v (Ref. 1).

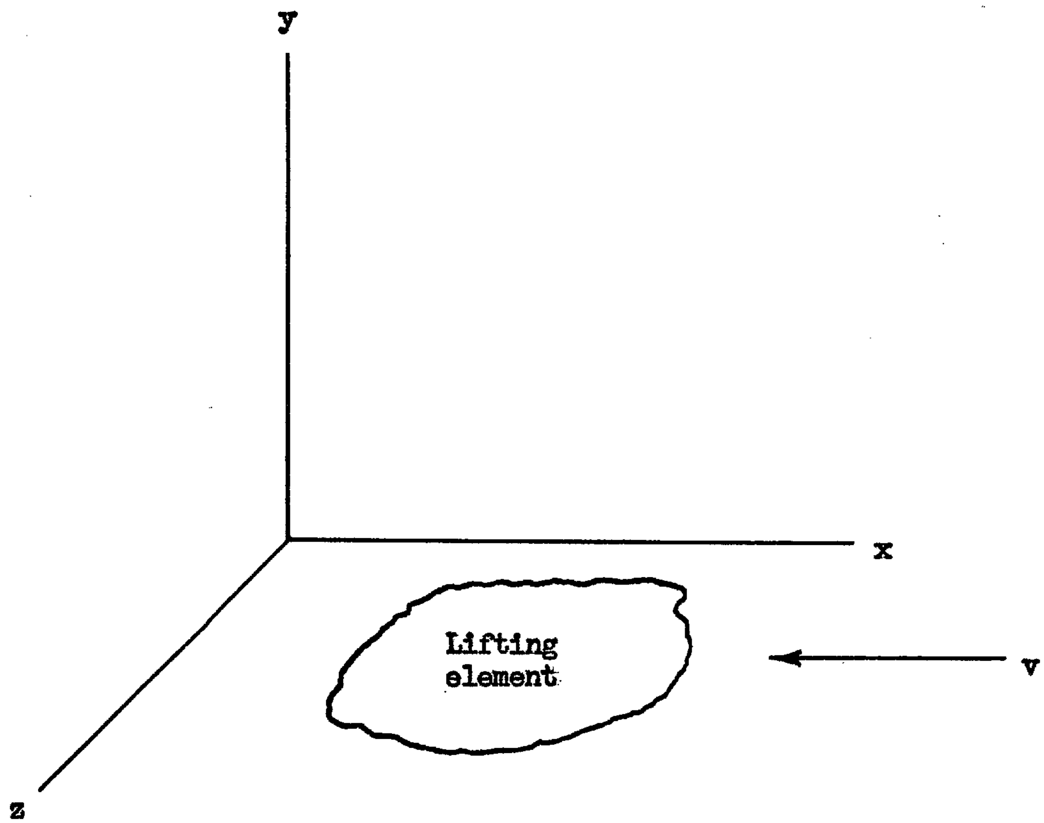

Foil moving in a negative x direction
with a constant supersonic velocity v

FIGURE 1

If a new coordinate system x, y, z is attached to the foil, then the equations of transformation between coordinates are:

$$\begin{aligned} x &= x' + v\,t' \\ y &= y' \\ z &= z' \\ t &= t' \end{aligned} \qquad (3)$$

under this transformation, equation (1) becomes:

$$\frac{1}{c^2}\frac{\partial^2\phi}{\partial t^2} + \left(\frac{2v}{c^2}\right)\frac{\partial^2\phi}{\partial x\partial t} + \left(\frac{v^2}{c^2} - 1\right)\frac{\partial^2\phi}{\partial x^2} - \frac{\partial^2\phi}{\partial y^2} - \frac{\partial^2\phi}{\partial z^2} = 0 \qquad (4)$$

Now Küssner (Ref. 5) shows that a solution of (1) can be transformed to a solution of (4) by the following combination of Lorentz transformations and Galilean transformations:

$$\begin{aligned} x' &= \frac{x}{1 - M^2} \\ y' &= \frac{y}{\sqrt{1 - M^2}} \\ z' &= \frac{z}{\sqrt{1 - M^2}} \\ t' &= t + \frac{xM}{c(1 - M^2)} \end{aligned} \qquad (5)$$

where $M = v/c$ is the Mach number. With the aid of equations (5), the solution of equation (2) may be written in the form:

$$\phi_o = \frac{A(\xi,\eta,\zeta)}{r}\left[f(t - \tau_2) + f(t - \tau_1)\right] \qquad (6)$$

where

$$r = \frac{1}{M^2 - 1} \sqrt{(x - \xi)^2 - (M^2 - 1)\left[(y - \eta)^2 + (z - \zeta)^2\right]}$$

$$\tau_2 = \frac{M}{c} \frac{x - \xi}{M^2 - 1} + \frac{r}{c}$$

$$\tau_1 = \frac{M}{c} \frac{x - \xi}{M^2 - 1} - \frac{r}{c}$$

At this point it should be noted that equation (6) is valid in a conical region called a "Mach Cone" opening aft of the moving source. Outside of this region ($r = 0$) the flow is undisturbed. It should also be noted that the line $r = 0$ is a singularity.

Physical meaning may be attributed to the "Mach Cone" in the following manner. Consider a spherical source moving at a constant supersonic velocity v. The radius vector R of a point x, y, z with respect to the center is

$$R = \sqrt{\left[x - (\xi + vt)\right]^2 + (y - \eta)^2 + (z - \zeta)^2}$$

The time the spherical wave passes the field point x, y, z is given as

$$t = \frac{R}{c}$$

eliminating R gives

$$c^2t^2 = (x - \xi - vt)^2 + (y - \eta)^2 - (z - \zeta)^2 = 0 \qquad (7)$$

This quadratic in t has two real roots ($v > c$), the τ_1 and τ_2 of equation (6). This indicates that two waves pass the point x, y, z at time t, namely the ones originating at times τ_1 and τ_2 earlier (Figure 2).

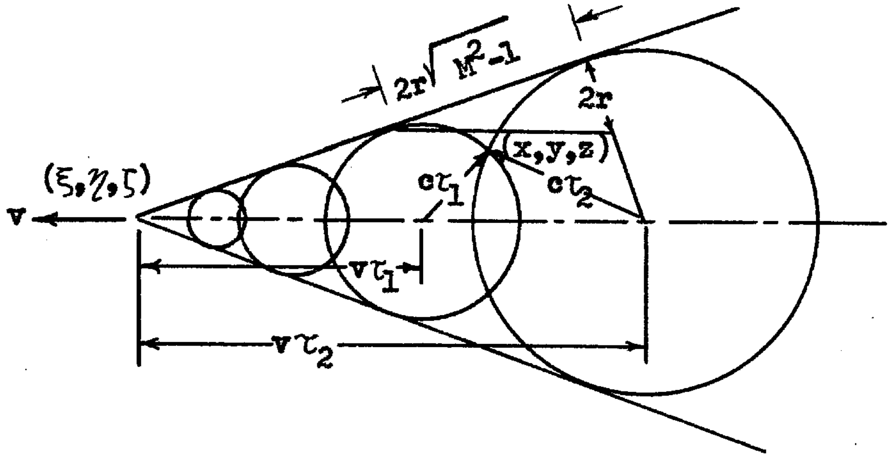

MACH CONE FIELD OF INFLUENCE

FIGURE 2

The next obvious step in the development of the problem is to superimpose solutions of the type of equation (6) and to evaluate A by using the boundary condition of tangential flow over the air foil surface. This is quite adequately carried out in reference 1 and will not be repeated here. The result of such a development gives for y = 0 (surface of the foil)

$$\phi(x,z,t) = -\frac{1}{2\pi\beta}\int_0^x\int_{\zeta_1}^{\zeta_2}\frac{W(\xi,\zeta)\left[w(t-\tau_1)+w(t-\tau_2)\right]}{\sqrt{(\zeta-\zeta_1)(\zeta_2-\zeta)}}\,d\zeta\,d\xi \tag{8}$$

where

$$\tau_1 = \frac{M(x-\xi)}{c\beta^2} - \frac{\sqrt{(\zeta-\zeta_1)(\zeta_2-\zeta)}}{c\beta}$$

$$\tau_2 = \frac{M(x-\xi)}{c\beta^2} + \frac{\sqrt{(\zeta-\zeta_1)(\zeta_2-\zeta)}}{c\beta}$$

$$\zeta_1 = z - \zeta_o$$

$$\zeta_2 = z + \zeta_o$$

$$\zeta_o = \frac{x - \xi}{\beta}$$

$$\beta = \sqrt{M^2 - 1}$$

$W(x,z)$ space function part of vertical velocity

$w(t)$ time function part of vertical velocity

$w(x,z,t) = W(x,z)w(t)$ vertical velocity

Equation (8) is Abel's Equation. Herbert Nelson (Ref. 6) has expanded this equation in a power series of ω (for low frequency flutter) and was thus able to obtain closed expressions for section force and moment coefficients for any arrowhead wing. His expressions were however quite involved and laborious, hence a slightly different approach was attempted here.

In order to simplify the coordinate system, a new coordinate θ was introduced

$$\theta = \cos^{-1}\left[\frac{\zeta - z}{x - \xi}\beta\right] \tag{9}$$

The convenience of such a coordinate system is apparent from inspection of figure (3).

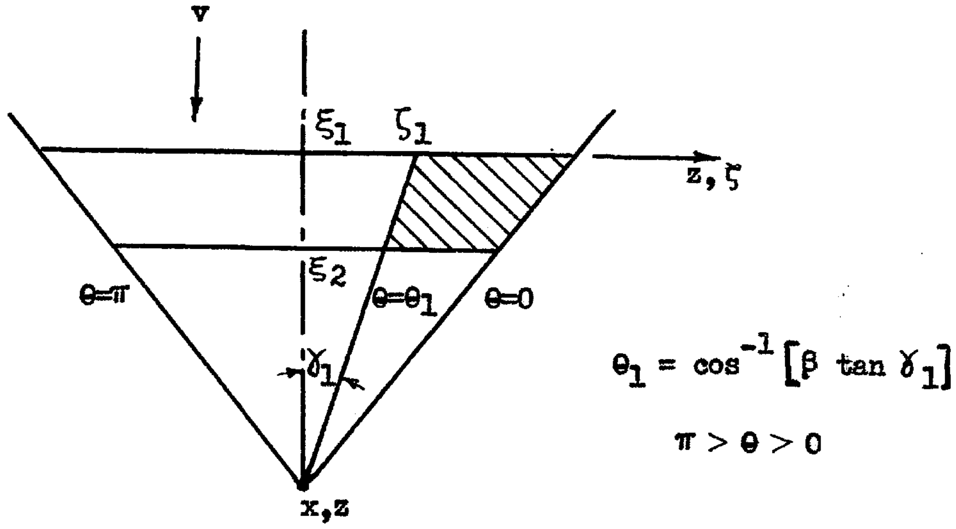

MACH LINE COORDINATES

FIGURE 3

Using equations (8) and (9) the following equation is obtained

$$\phi = -\frac{1}{2\pi\beta} \int_0^x \int_0^\pi W[\xi, \zeta(\theta)] \left[w(t - \tau_1) + w(t - \tau_2) \right] d\theta \, d\xi \qquad (10)$$

where

$$\tau_1 = \frac{x - \xi}{c\,\beta^2} (M - \sin\theta)$$

$$\tau_2 = \frac{x - \xi}{c\,\beta^2} (M + \sin\theta)$$

Now considering the motion of the strip bounded by $\theta_1 \geqslant \theta \geqslant 0$ and $\xi_1 > \xi > \xi_2$ as uniform, an assumption about the nature of $W[\xi, \zeta(\theta)]$ may be made. Since the ultimate objective is to analyze a delta wing on the electric analog computer, it is seen that a reasonable assumption would be to suppose that the wing is composed of cells, each one moving with a uniform motion. Hence for a strip in a given cell

$$W\left[\xi\,,\ \zeta(\theta)\right] = \text{constant}$$

and may be removed from inside the integral signs in equation (10).

Now the vertical velocity $w(x,z,t)$ is given by

$$w(x,z,t) = v\frac{\partial Z_m}{\partial x} + \frac{\partial Z_m}{\partial t} \tag{11}$$

where Z_m is the vertical motion of a point on the wing. For the present problem of a wing performing small harmonic torsional oscillations of amplitude α_o about some spanwise axis x_o, and small harmonic vertical translations of amplitude h_o, Z_m is given by

$$Z_m = \left[h_o + (x - x_o)\,\alpha_o\right]\, e^{j\omega t} \tag{12}$$

then

$$W_{strip}w(t) = \left[j\omega\, h_o + v\,\alpha_o + (x - x_o)j\omega\,\alpha_o\right]\, e^{j\omega t} \tag{13}$$

(note - this neglects spanwise motion). Now using $w(t) = e^{j\omega t}$ and the fact that W_{strip} = constant, equation (10) gives the expression for the potential at a point (x,z) due to a radially cut strip source as

$$\phi(x,\theta,t) = -\frac{e^{j\omega t}\, W_{strip}}{\pi\beta}\int_{\xi_1}^{\xi_2} d\,\xi \int_0^{\theta_1} e^{-\frac{j\omega M(x-\xi)}{c\,\beta^2}} \cos\left[\frac{\omega}{c\beta^2}(x-\xi)\sin\,\theta\right] d\theta \tag{14}$$

Now for simplicity the following substitution is made

$$\delta = \frac{\omega}{c\,\beta^2}\,(x - \xi\,)$$

$$d\delta = -\frac{\omega}{c\,\beta^2}\ d\xi$$

Equation (14) then becomes

$$\phi(x,\theta,t) = \frac{e^{j\omega t}}{\pi} W_{strip} \frac{c\beta}{\omega} \int_{\delta_1}^{\delta_2} \int_0^{\theta_1} e^{-jM\delta} \cos\left[\delta \sin\theta\right] d\theta \, d\delta \qquad (14a)$$

It can at this point be noted that the integral over θ is an "incomplete Bessel function integral of zero order," since for $\theta_1 = \pi$ this integration produces a Bessel function of zero order. However, such integrals are not tabulated, and it becomes necessary to resort to other methods in order to integrate equation (14a).

C. The Integrated Solution

An examination of equation (14a) discloses the inherent difficulty involved in the further solution of the velocity potential problem. Namely, an integration of the above equation with an arbitrary θ limit is quite involved if not impossible to perform in closed form. The integrand can however be expanded in a power series in powers of δ, and then integrated term by term. This technique is not new and is often used when other methods of integration fail. The only drawback to such a method is the limitation that is imposed on the final answer if only a few terms in the series are used, namely

$$\delta = \frac{\omega}{c\,\beta^2}(x - \xi) \ll 1 \qquad (15)$$

For practical systems in low frequency flutter, equation (15) will be satisfied with ease. Expanding the integrand of (14a) gives

$$\phi(\delta,\theta,t) = \frac{e^{j\omega t}W_s\,c\beta}{\pi\,\omega}\int_{\delta_1}^{\delta_2}\int_{0}^{\theta_1}\left(1 - jM\delta - \frac{M^2\delta^2}{2!}\cdots\right)\left(1 - \frac{\delta^2}{4}(1-\cos 2\theta)\ldots\right)d\theta d\delta \tag{16a}$$

now keeping only powers of δ up to δ^2, equation (16a) becomes

$$\phi(\delta,\theta,t) \doteq \frac{e^{j\omega t}W_s\,c\beta}{\pi\,\omega}\int_{\delta_1}^{\delta_2}\int_{0}^{\theta_1}\left[1 - jM\delta - \frac{\delta^2}{4}(2M^2+1-\cos 2\theta)\right] d\theta d\delta$$

carrying out the integration first with respect to θ gives

$$\phi(\delta,\theta,t) \doteq \frac{e^{j\omega t}W_s\,c\beta}{\pi\,\omega}\int_{\delta_1}^{\delta_2}\left[\theta_1\left(1 - jM\delta - \frac{\delta^2}{4}\{2M^2+1\}\right) + \frac{\delta^2}{4}\left(\frac{\sin 2\theta_1}{2}\right)\right] d\delta$$

Now integrating this once more, this time with respect to δ gives:

$$\phi(\delta,\theta,t) = -\frac{e^{j\omega t}W_s\,c\beta}{\pi\,\omega}\left[(\delta_1 - \delta_2)\theta_1 - j\frac{M}{2}\theta_1(\delta_1^{\,2} - \delta_2^{\,2}) - \frac{\delta_1^{\,3} - \delta_2^{\,3}}{12}\left\{(2M^2+1)\theta_1 - \frac{\sin 2\theta_1}{2}\right\}\right] \tag{16b}$$

For convenience in numerical evaluation of equation (16b), the following parameters will be defined:

$$A = -\theta_1$$

$$B = -\frac{\sin 2\theta_1}{2} \tag{16c}$$

$$D = -\theta_1 + \frac{\sin 2\theta_1}{2} = A - B$$

then equation (16b) is given in its final form as :

$$\phi(\delta,\theta,t) = \frac{e^{j\omega t}W_s\, d\beta}{\pi\,\omega}\left[A(\delta_1-\delta_2) - j\,\frac{MA}{2}(\delta_1{}^2-\delta_2{}^2) - \frac{\delta_1{}^3-\delta_2{}^3}{12}\quad(2M^2A+D)\right] \tag{17}$$

Equation (17) will be the starting equation for the work to follow.

D. THE DETERMINATION OF PRESSURE AT A POINT

Now that a workable expression in closed form has been derived for the velocity potential at a point of a wing due to the influence of a radial segment inside the Mach Cone, the next logical step in the solution is to determine the pressure at that point due to the segment.

Bernoulli's equation for pressure in a stream is

$$P = -\frac{1}{2}\,\rho\,V_T{}^2$$

where V_T is the total velocity.

Now since the velocity potential of equation (17) is a disturbance potential, the total velocity may be written as:

$$V_T = v + \frac{d\phi}{dx}$$

and the square of this velocity may be written as:

$$V_T{}^2 \doteq v^2 + 2v\,\frac{\partial\phi}{\partial x} + 2\,\frac{\partial\phi}{\partial t}$$

If it is recognized that $v \gg \frac{d\phi}{dx}$, namely the velocity in the main stream is much larger than the disturbance velocity, then the disturbance pressure (local static pressure minus the pressure in the undisturbed stream) is given by:

$$P = -\rho \frac{d\phi}{dt} = -\rho\left[\frac{\partial\phi}{\partial t} + v\frac{\partial\phi}{\partial x}\right]$$

while the total pressure difference (positive in the downward direction) is just twice the pressure on one side of the foil and is:

$$P_T = -2\rho\left[\frac{\partial\phi}{\partial t} + v\frac{\partial\phi}{\partial x}\right] \tag{18}$$

It is now apparent that by a combination of equations (18) and (17) the pressure at a point may be computed. Before this is done however, a physical interpretation of the partial derivative with respect to x in equation (18) must be given.

The definition of $\frac{\partial\phi}{\partial x}$ is obviously the usual one

$$\frac{\partial\phi}{\partial x} = \lim_{\Delta x \to 0} \frac{\phi[(x+\Delta x), \xi, \zeta] - \phi[x, \xi, \zeta]}{\Delta x}$$

The difficulty that arises however, is best seen by examination of the following geometrical figure (Figure 4):

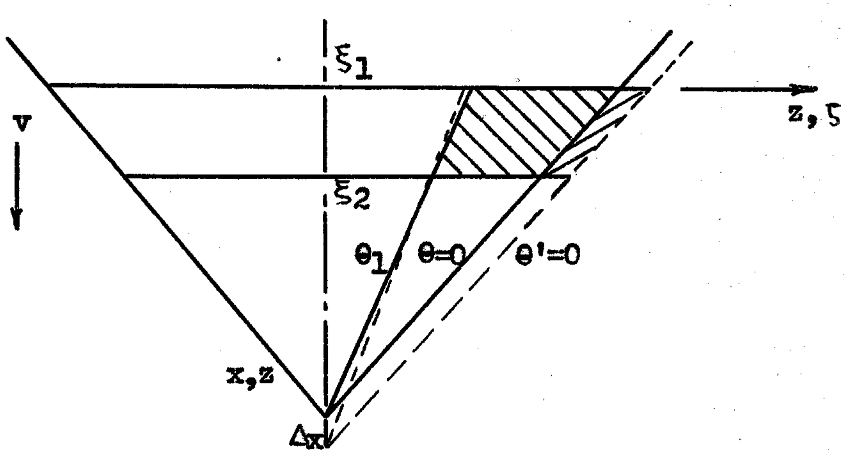

PHYSICAL INTERPRETATION OF $\frac{\partial\phi}{\partial x}$

FIGURE 4

It is thus seen from figure 4 that a slightly different geometrical area causes the ϕ at $(x + \Delta x)$ than the one that causes the ϕ at the point (x). It is this physical fact that places a singularity at the line $\theta = 0$. However, if it is assumed (as is physically reasonable), that the wing is continuous and that the region between $\theta = 0$ and $\theta' = 0$ moves in the same way as the sector in question, the singularity along the mach line is removed. Thus in evaluating equation (18) only partial derivatives with respect to $\theta_1(x)$, $\delta_1(x)$, and $\delta_2(x)$ will be taken. The singularity was automatically removed when the θ limits in equation (14) were chosen from $0 < \theta < \theta_1$ and not $\theta_2 < \theta < \theta_1$. This procedure does not limit the resulting equation in any way because a solution for the region $\theta_2 < \theta < \theta_1$ is easily obtained by subtracting the solution for $0 < \theta < \theta_2$ from that of $0 < \theta < \theta_1$.

Now evaluating equation (18) with the aid of equation (17), the following relation is obtained:

$$P_T = -2\rho\left[j\omega\phi + Mc\frac{\partial\phi}{\partial\delta_1}\frac{\partial\delta_1}{\partial x} + Mc\frac{\partial\phi}{\partial\delta_2}\frac{\partial\delta_2}{\partial x} + Mc\frac{\partial\phi}{\partial\theta_1}\frac{\partial\theta_1}{\partial x}\right] \tag{19a}$$

Putting in the values of the partial derivatives gives:

$$P_T = -\frac{2\rho e^{j\omega t}W_s c\beta}{\pi}\left[\left\{jA(\delta_1-\delta_2)+\frac{MA}{2}(\delta_1{}^2-\delta_2{}^2)-j(2M^2A+D)\frac{\delta_1{}^3-\delta_2{}^3}{12}\right\}\right.$$

$$\left.+\frac{M}{\beta^2}\left\{-jMA(\delta_1-\delta_2)-(2M^2A+D)\frac{\delta_1{}^2-\delta_2{}^2}{4}\right\}\right]-2\rho Mc\frac{\partial\phi}{\partial\theta_1}\frac{\partial\theta_1}{\partial x}$$

collecting terms gives:

$$P_T = -\frac{2\rho e^{j\omega t} c W_s M}{\pi \beta}\left[\frac{\delta_1{}^2 - \delta_2{}^2}{4}(-2A-D) - j\left\{(\delta_1 - \delta_2)\frac{A}{M} + \frac{(\delta_1{}^3 - \delta_2{}^3)}{12}\,\frac{\beta^2}{M}(2M^2A+D)\right\}\right]$$

$$-\,2\,\rho Mc\,\frac{\partial\phi}{\partial\theta_1}\,\frac{\partial\theta_1}{\partial x} \qquad (19b)$$

Now since θ_1 is given by the relation

$$\theta_1 = \cos^{-1}\left[\beta\,\frac{\zeta_1 - z}{x - \xi_1}\right]$$

the partial of θ_1 with respect to x is:

$$\frac{\partial\theta_1}{\partial x} = \left\{\frac{d}{d(\beta\,\frac{\zeta_1 - z}{x - \xi_1})}\ \cos^{-1}\left[\beta\,\frac{\zeta_1 - z}{x - \xi_1}\right]\right\}\left\{+\beta\,\frac{\zeta_1 - z}{(x - \xi_1)^2}\right\}$$

$$\frac{\partial\theta_1}{\partial x} = -\frac{1}{\sqrt{1 - \beta^2(\frac{\zeta_1 - z}{x - \xi_1})^2}}\ \left\{+\beta\,\frac{\zeta_1 - z}{(x - \xi_1)^2}\right\}$$

$$\frac{\partial\theta_1}{\partial x} = \left[\beta\,\frac{\zeta_1 - z}{x - \xi_1}\right]\left[\frac{1}{x - \xi_1}\right]\frac{1}{\sqrt{1 - \beta^2\,(\frac{\zeta_1 - z}{x - \xi_1})^2}}$$

which may be recognized to be:

$$\frac{\partial\theta_1}{\partial x} = \cos\theta_1\ \frac{1}{x - \xi_1}\ \frac{1}{\sqrt{1 - \cos^2\theta_1}} = \frac{\omega\cot\theta_1}{c\,\beta^2\,\delta_1} \qquad (20)$$

With the use of equation (20), the last term in equation (19b) then becomes:

$$- 2\, \rho Mc \frac{\partial \phi}{\partial \theta_1} \frac{\partial \theta_1}{\partial x} = \frac{2\, \rho M c W_s e^{j\omega t}}{\pi \beta} (\cot \theta_1) \Big[(1 - \frac{\delta_2}{\delta_1}) - j\frac{M}{2}(\delta_1 - \frac{\delta_2^{\,2}}{\delta_1})$$

$$- \frac{1}{12} (\delta_1^{\,2} - \frac{\delta_2^{\,3}}{\delta_1})(2M^2 + 1 - \cos 2\,\theta_1) \Big]$$

where $\qquad \pi > \theta_1 > 0 \qquad$ (20a)

Using equation (20a) and (19b) and collecting terms, gives the final desired expression for the total pressure at a point (x) due to the influence of a radially cut strip of width $(\delta_1 - \delta_2)$, moving with a sinusoidal uniform motion $W_s e^{j\omega t}$, $(\theta = 0 \text{ to } \theta = \theta_1)$

$$P_T = - \frac{2\, \rho M c W_s e^{j\omega t}}{\pi \beta} \Big[\frac{\delta_1^{\,2} - \delta_2^{\,2}}{4} (-2A-D) - j \Big\{ (\delta_1 - \delta_2) \frac{A}{M} + \frac{\delta_1^{\,3} - \delta_2^{\,3}}{12} \left(\frac{\beta^2}{M} \right) (2M^2A + D) \Big\}$$

$$- \cot \theta_1 \Big\{ (1 - \frac{\delta_2}{\delta_1}) - j\, \frac{M}{2}(\delta_1 - \frac{\delta_2^{\,2}}{\delta_1}) - \frac{1}{12}(\delta_1^{\,2} - \frac{\delta_2^{\,3}}{\delta_1})(2M^2 + 1 - \cos 2\theta_1) \Big\} \Big]$$

where $\qquad \pi > \theta_1 > 0 \qquad$ (21)

It can be noted that for one half of a complete strip enclosed by the mach lines the $\frac{\partial \phi}{\partial \theta_1}$ terms do not contribute any pressure terms as

$$\cot \theta_1 \Big|_{\theta_1 = \pi/2} = 0$$

The pressure due to a complete segment by symmetry then is simply equal to twice the pressure contributed by the segment contained in $0 \leq \theta \leq \pi/2$ namely

$$P_{segment} = 2P_{\theta_1 = \frac{\pi}{2}} = -\frac{2\rho M c W_s e^{j\omega t}}{\beta}\left[\frac{3}{4}(\delta_1^2-\delta_2^2)+j\left\{\frac{\delta_1-\delta_2}{M}+\frac{\delta_1^3-\delta_2^3}{12}\left(\frac{\beta^2}{M}\right)(2M^2+1)\right\}\right] \tag{22}$$

Equation (22) is of particular interest as it may be used to derive the pressure at a point x due to its own motion. This pressure will be called the self pressure term. The derivation is carried out as follows: consider the triangular area bounded by the mach lines $\theta = 0$, $\theta = \pi$, δ_1 and $\delta_2 = 0$, Figure 5.

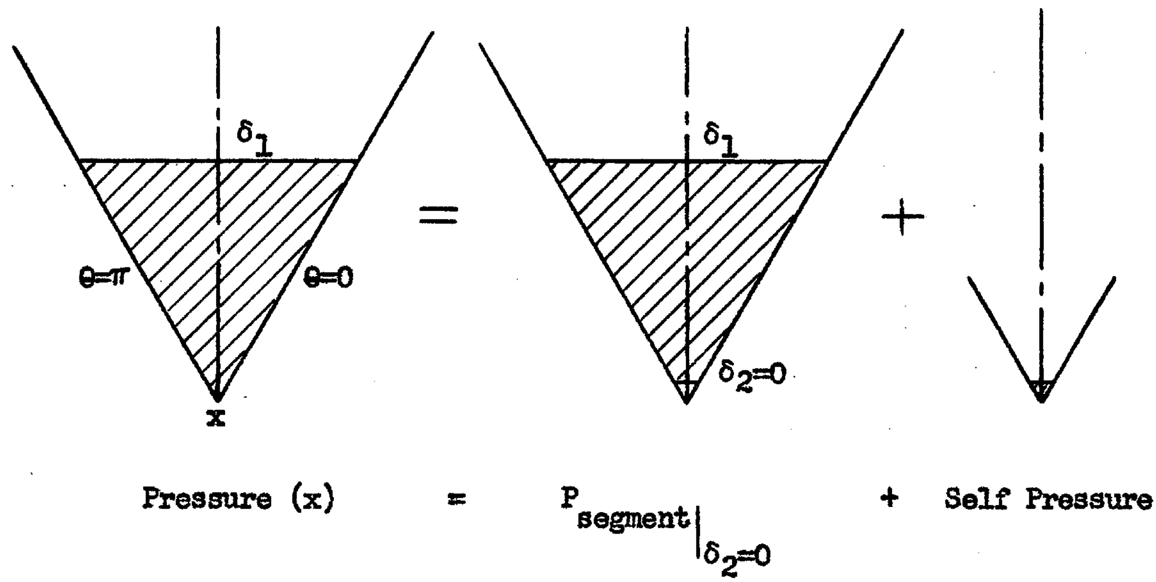

SELF PRESSURE DETERMINATION

FIGURE 5

The pressure of the triangular segment, not including the self pressure term, is given by evaluating equation (22) with $\delta_2 = 0$ namely

$$P_{segment}\Big|_{\delta_2=0} = -\frac{2\rho M c W_s e^{j\omega t}}{\beta}\left[\frac{3}{4}\delta_1^2 + j\left\{\frac{\delta_1}{M} + \frac{\delta_1^3}{12}\left(\frac{\beta^2}{M}\right)(2M^2+1)\right\}\right] \tag{23}$$

To find the total pressure at the point x the potential ϕ must be evaluated at $\delta_2 = 0$, thus from equation (17) for $\delta_2 = 0 \quad \theta_1 = \pi$

$$\phi_\Delta = -\frac{e^{j\omega t} W_s c\beta}{\omega}\left[\delta_1 - j\,\frac{M}{2}\,\delta_1^2 - (2M^2+1)\,\frac{\delta_1^3}{12}\right]$$

then using equation (18), to find the total pressure

$$P_\Delta = -\frac{2\rho M c W_s e^{j\omega t}}{\beta}\left[\frac{3}{4}\delta_1^2 + j\left\{\frac{\delta_1}{M} + \frac{\delta_1^3}{12}\left(\frac{\beta^2}{M}\right)(2M^2+1)\right\} - 1\right] \tag{24}$$

The self pressure $P_{s.p.}$ then is equal to

$$P_{s.p.} = P_\Delta - P_{segment}$$

or subtracting equation (23) from equation (24) gives for the self pressure

$$P_{s.p.} = \frac{2\rho M c W_s e^{j\omega t}}{\beta} \tag{25}$$

An examination of equation (25) shows that this is just the result of the Ackeret theory for wings of infinite span and zero sweep. It states that the pressure at a point is proportional to the angle of attack at that point. Thus for example for a wing having identical motion in every chordwise section, in the steady case $\omega = 0$

$$W_s = v\,\frac{dy}{dx} \qquad \text{(local angle of attack)}$$

and

$$P = 2\,\rho\,\left(\frac{v^2}{\beta}\right)\,\frac{dy}{dx} \tag{25a}$$

which is exactly the Ackeret result.

II AERODYNAMIC LIFTS

A. Cell Division Criteria

The principal results of the aerodynamic analysis of Part I of this thesis are contained in equations (21), (22) and (25) which give the pressure at a point (x) due to the motion of a segment, of a strip, and of the point itself respectively. These results are not an end in themselves, but are a stepping stone to the next step in the procedure, namely that of calculating the lifts on an oscillating elastic airfoil. Since the ultimate objective of this work is to analyze a delta wing in supersonic flutter on an electric analog computer, the aerodynamic lifts on sections of the wing will have to be determined.

The important factor that must be recognized at this point is that the electrical analogy for a triangular plate or delta wing is obtained by dividing this plate into a number of cells each of which is moving with a uniform motion. If such an analogy is used, the problem of lifts is one of finding the lift on a cell due to itself and adding to it the lift due to the motion of the other cells which lie within the mach lines. It should be noted that different cells can contribute lift terms to the lift on one cell as the Mach number is varied.

The first thing that must be done before the lifts are computed, is to subdivide the wing to be analyzed into a number of cells, each moving as a rigid body and possessing its own vertical (h), chordwise pitching (α), and spanwise pitching ($\bar{\beta}$) motions. In order to have the area of the cells equal the actual area of the wing, the criteria for cell division as given in a report at Republic Aircraft by Pines, will be used (Ref. 7).

1. The cells should be rectangles of equal size, except at the trailing edge where the cell width should be half size. (So that exactly the area of the wing is covered.)

2. The cell size should be the same for all Mach numbers for which the edges are supersonic, and all Mach cones should produce essentially the same types of cuts.

3. The triangular part of the cell cut out by the leading edge (or trailing edge) should be equal to the adjacent triangle within the wing not covered by a cell. Thus the area covered by cells will equal the area of the wing.

4. The dimensions of the cell should be such that the approximations used in evaluating the integrals will be valid for all Mach numbers for which the leading edges are supersonic and for the proper range of values of the frequency-distance parameter δ.

Applying these criteria to a wing with a straight trailing edge (Figure 6), the cell dimensions are given as

$$\bar{d} = \bar{c} \tan \lambda \tag{26}$$

where

$\bar{d}$ = chordwise dimension of full cell

$\bar{c}$ = spanwise dimension of full cell

λ = sweep angle of leading edge

and

$$\bar{s} = n\bar{c} \tag{27}$$

where

$\bar{s}$ = semi-span

n = number of cells along trailing edge of semi-span

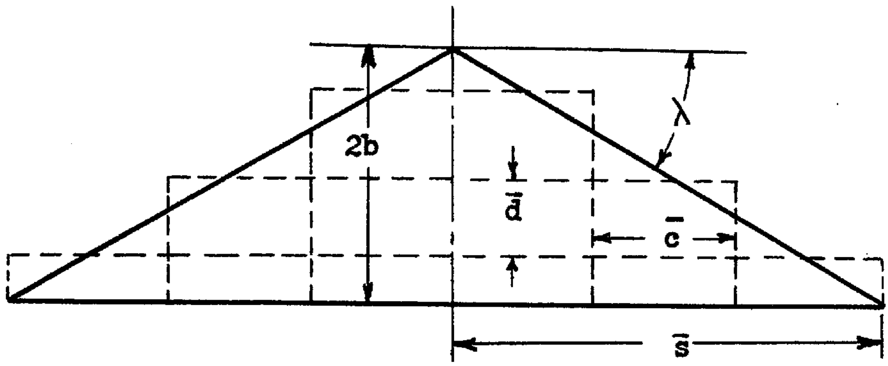

CELL DIVISION OF DELTA WING

FIGURE 6

B. Determination of Cell Lifts

Once the wing of Figure 6 is divided into a number of cells, it becomes necessary to determine the aerodynamic lift per cell in order to perform a flutter analysis on the electric analog computer. Strictly speaking, it is necessary to actually integrate equation (21) for the pressure at a point over the entire cell. Such an integration is not feasible at this point, hence an approximate numerical method will be used. It will be assumed that the pressure at the centroid of a cell is approximately equal to the average pressure on the cell. The lift will then be given as the product of this pressure and the cell area. As the number of cells in the wing increases, this approximation becomes increasingly better. Based on this assumption, a set of rules for the determination of cell lifts can be formulated:

1. Divide the wing into a number of cells such that the cell area is equal to the wing area.

2. Compute the pressure at the centroid of each cell with the use of equations (21), (22) and (25). Then the lift per cell will be given as the product of this pressure multiplied by the area of the cell.

3. In computing the pressure at the centroid, angular segments of influencing cells, such as shown in figure 3, will be used, each possessing the h and α motion of the centroid of the appropriate cell.

4. In the construction of these segments, the area of the segments should equal the area of the wing inside the mach lines which are centered at the centroid of the cell at which the lift is being computed.

5. For practical flutter analyses, symmetrical and anti-symmetrical flutter will be considered one at a time. Hence, only one half of the wing has to be represented electrically since full advantage can be taken of symmetry.

Using the above set of computing rules the procedure can be outlined as follows:

1. Draw a planform of the wing to a convenient scale, and divide it into cells.

2. Construct graphically the angular segments affecting each cell (this has to be done for each mach number of interest).

3. From the above construction, values of θ_1, δ_1, and δ_2 can be determined. (δ_1 and δ_2 will be functions of ω).

4. Using equations (21), (22) and (25), the pressure at the centroid can be computed as a function of ω.

5. The lifts are then given as the product of the cell area by the centroid pressure.

C. A Six Cell Wing Analysis

In order to clearly illustrate the procedure outlined in the above section, and to get an idea of the order of magnitude of the terms involved, a specific planform will be considered (see Figure 7). This planform is the same one as considered by Nelson (Ref. 6) and by Pines (Ref. 7). The following parameter values will be used:

$$M^2 = 1.75$$

$$b = 1/2 \text{ ft.}$$

$$\lambda = 30^\circ$$

The cell dimensions as given by equations (27) and (26) are

$$\bar{c} = \frac{\bar{s}}{n} = \frac{\sqrt{3}}{3} = .576 \text{ ft.}$$

$$\bar{d} = \bar{c} \tan \lambda = .333 \text{ ft.}$$

It will now be formulated that in the study to follow, only symmetrical flutter will be analyzed. A study of the anti-symmetrical motion is quite similar and will not be performed at this time as no new information would be obtained from such an analysis. The motion of the "left cells" marked with an L in figure 7 will thus be identical with that of the corresponding cells on the right side. Figure 7 represents the first step in the procedure for calculating the desired cell lifts.

It should be pointed out, that the ultimate number of cells per half wing is primarily determined by the capacity of the computer that is available. Six cells were chosen for this study due to the limitations on the number of operational amplifiers that were available. It is firmly believed by the author that such a six cell structure, crude

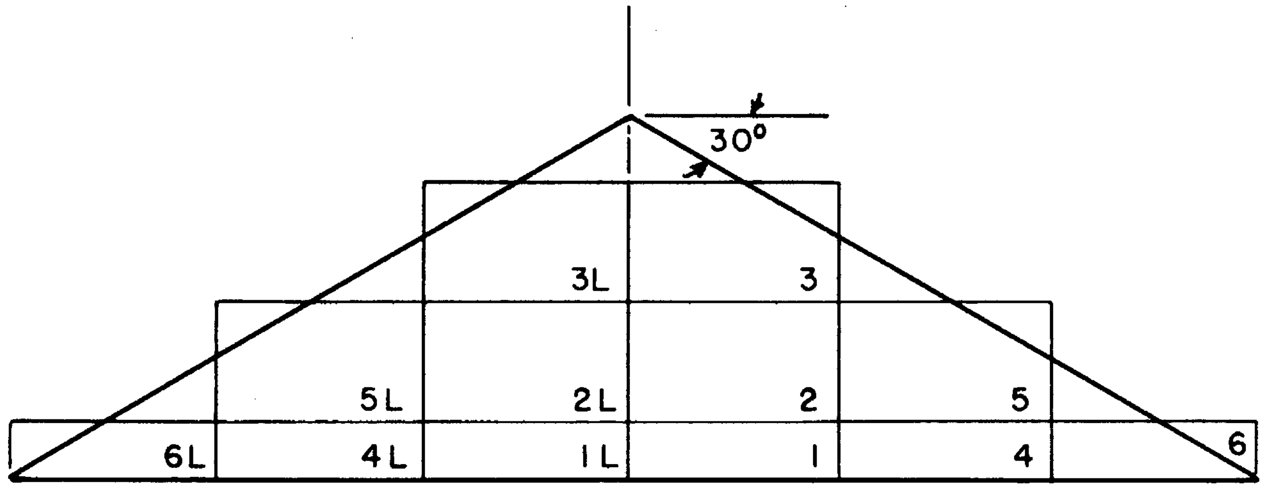

SCALE: $\frac{3''}{16} = \frac{1'}{10}$

CELL REPRESENTATION OF WING

FIGURE 7

as it may appear to be, will still give a satisfactory first order engineering result.

The second step of the procedure for the determination of lifts calls for a graphical determination of the influencing angular segments. Such a construction for all six cells is presented in figures (8) - (10).

Now, placing the available numerical values into equations (21), (22) and (25) so as to get them to be functions of $x - \xi_1$, $x - \xi_2$, θ_1, and $\bar{\omega} = \frac{\omega M}{c\beta^2}$ only, the following equations with numerical coefficients are obtained (neglecting terms in δ^3).

$$P_T = -\frac{2\rho McW_s e^{j\omega t}}{\pi\beta}\Bigg[\left(\frac{x-\xi_2}{x-\xi_1} - 1\right)\cot\theta_1 + \bar{\omega}^2\Big\{.14285(2A+D)\left[(x-\xi_2)^2-(x-\xi_1)^2\right]$$

$$+\left[(x-\xi_1)^2 - \frac{(x-\xi_2)^3}{x-\xi_1}\right]\cot\theta_1\left[.21428 - .047616\cos 2\theta_1\right]\Big\}$$

$$+ j\bar{\omega}\Big\{.5\cot\theta_1\left[(x-\xi_1) - \frac{(x-\xi_2)^2}{x-\xi_1}\right] - .5714\,A\left[(x-\xi_1)-(x-\xi_2)\right]\Big\}\Bigg] \tag{21'}$$

and the pressure due to a triangular segment plus the self pressure is given by:

$$P_\Delta = -\frac{2\rho McW_s e^{j\omega t}}{\pi\beta}\left[\left\{-\pi + 1.3463\,\bar{\omega}^2(x-\xi_1)^2\right\} + j\,1.7951\,\bar{\omega}(x-\xi_1)\right] \tag{24'}$$

while the pressure due to a complete strip is given by

$$P_{segment} = -\frac{2\rho McW_s e^{j\omega t}}{\pi\beta}\Big[1.3463\,\bar{\omega}^2\left\{(x-\xi_1)^2-(x-\xi_2)^2\right\} + j1.7951\,\bar{\omega}\left\{(x-\xi_1) - (x-\xi_2)\right\}\Big] \tag{22'}$$

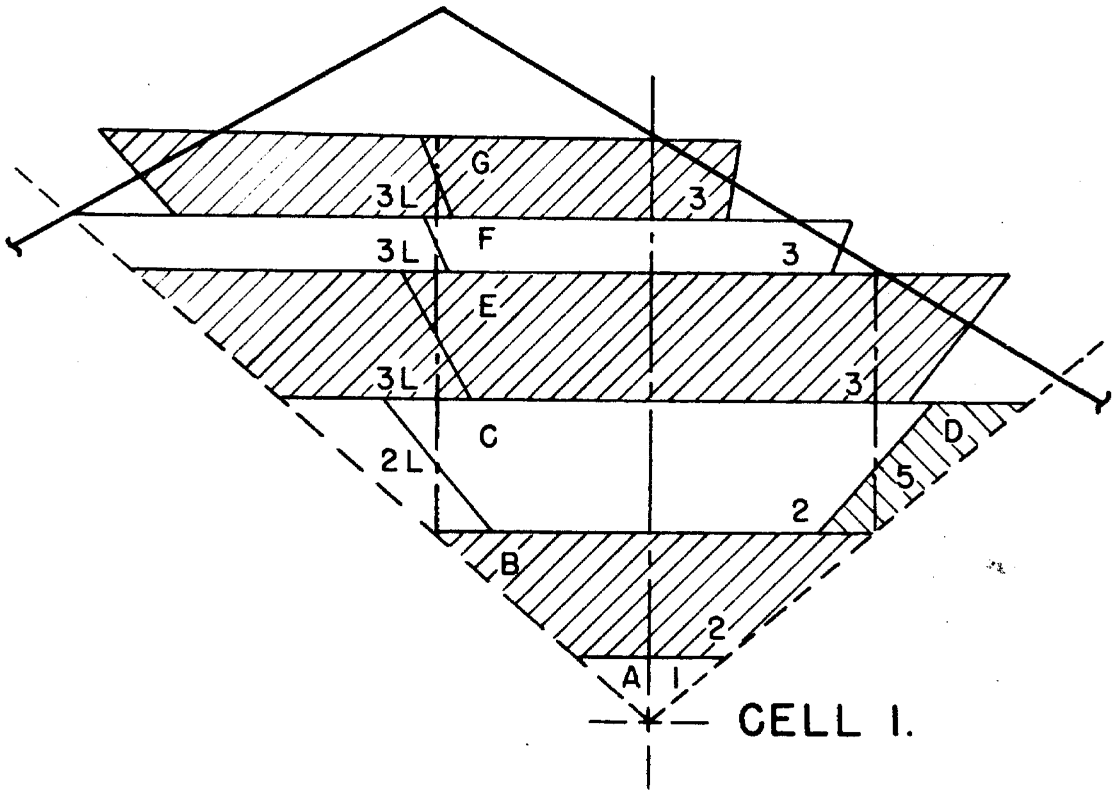

CELL 1.

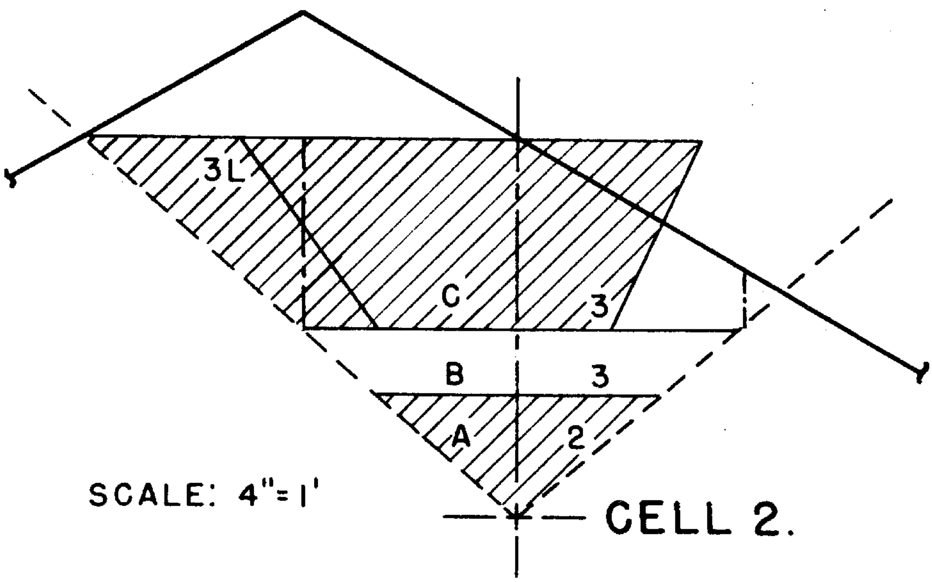

SCALE: 4"=1'

CELL 2.

CELL INFLUENCES M^2=1.75

FIGURE 8

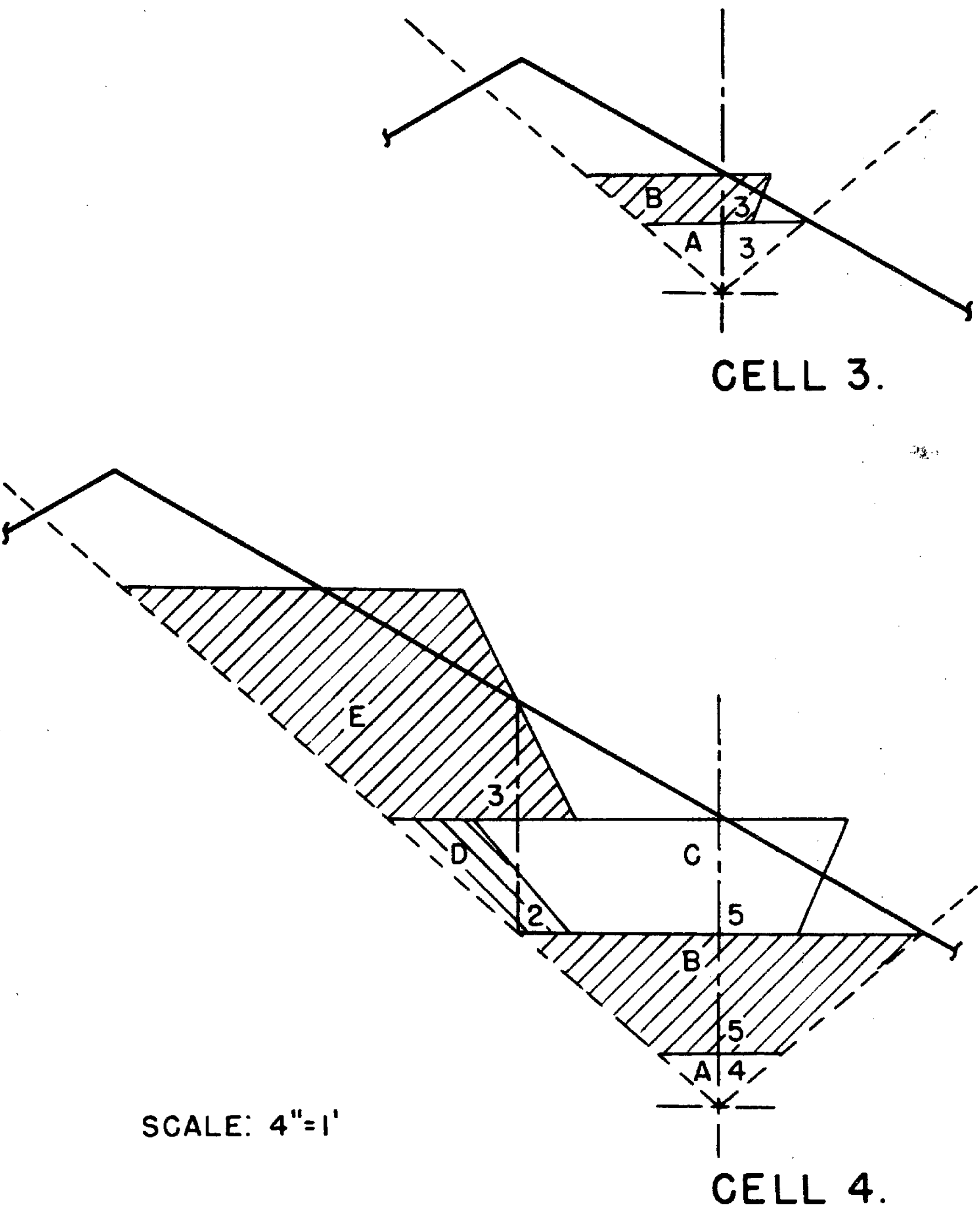

CELL INFLUENCES $M^2 = 1.75$

FIGURE 9

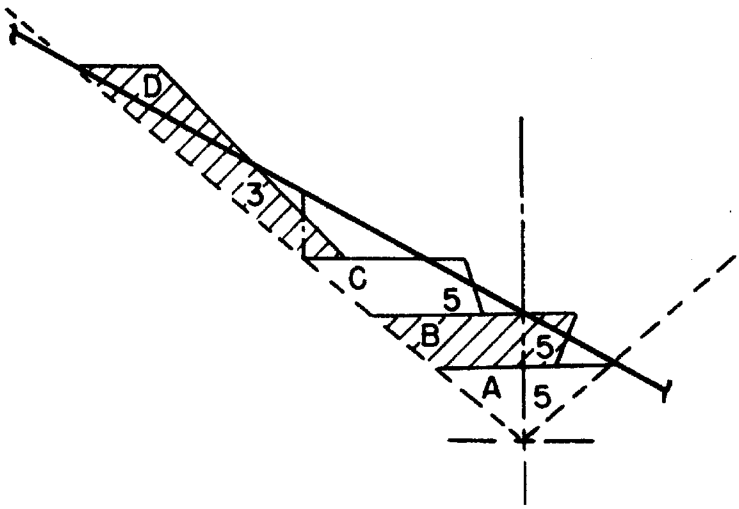

CELL 5.

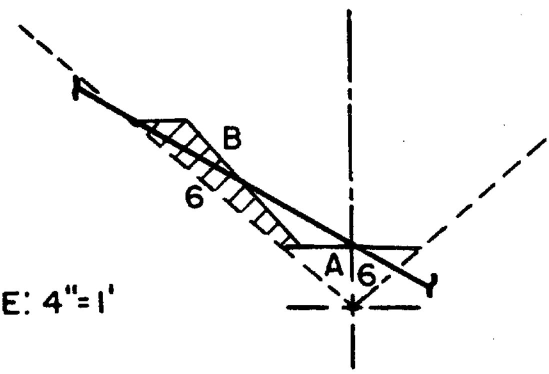

SCALE: 4"=1'

CELL 6.

CELL INFLUENCES $M^2 = 1.75$

FIGURE 10

Now with the aid of the above equations, and with the scale drawings (Figures 8-10), the calculation of the lifts on each cell is carried out (See table 1B, Appendix B). The pressures as computed in Table 1B of Appendix B are summarized below:

$\frac{\pi \beta P}{-2\rho McW_s}$	Contributing Cells	Numerical Value
P_{1-1}	1a	$-\pi + \bar{\omega}^2\ .006956\ + j\ \bar{\omega}\ .1497$
P_{1-2}	1b + 1c	$.5009 + \bar{\omega}^2\ .1652\ + j\ \bar{\omega}\ .3692$
P_{1-3}	1e + 1f + 1g - 1g'	$.5611 + \bar{\omega}^2\ .2245\ + j\ \bar{\omega}\ .0472$
P_{1-5}	1d	$-.4884 + \bar{\omega}^2\ .0586\ + j\ \bar{\omega}\ .2278$
P_{2-2}	2a	$-\pi + \bar{\omega}^2\ .02789\ + j\ \bar{\omega}\ .2998$
P_{2-3}	2b + 2c	$.2296 + \bar{\omega}^2\ .1935\ + j\ \bar{\omega}\ .3486$
P_{3-3}	3a + 3b	$-2.9747 + \bar{\omega}^2\ .0137\ + j\ \bar{\omega}\ .23246$
P_{4-2}	4d	$-.4239 + \bar{\omega}^2\ .05806\ + j\ \bar{\omega}\ .2136$
P_{4-3}	4e	$-.2133 + \bar{\omega}^2\ .2200\ + j\ \bar{\omega}\ .3381$
P_{4-4}	4a	$-\pi + \bar{\omega}^2\ .006956\ + j\ \bar{\omega}\ .14971$
P_{4-5}	4b + 4c - 4c'	$.5919 + \bar{\omega}^2\ .1021\ + j\ \bar{\omega}\ .2172$
P_{5-3}	5d	$-.7159 + \bar{\omega}^2\ .10658\ + j\ \bar{\omega}\ .3569$
P_{5-5}	5a + 5b + 5c	$-3.0610 + \bar{\omega}^2\ .04338\ + j\ \bar{\omega}\ .30846$
P_{6-6}	6a + 6b	$-3.8439 + \bar{\omega}^2\ .02848\ + j\ \bar{\omega}\ .3391$

TABLE 1

Now it should be noted that in the computation of the centroid pressures given in Table 1, the assumption of $\delta \ll 1$ was used. This in effect places an upper limit on $\bar{\omega}$. The maximum value of $(x - \xi_1)$ that was used was .770 ft. hence if δ^2_{max} is taken as .1,

$$\delta_{max} = \sqrt{.1} = \frac{\omega_{max}(x - \xi_1)_{max}}{M} = (.75591)(.770)\,\bar{\omega}_{max}$$

or

$$\bar{\omega} \leq .547 \qquad \text{for validity of equations.}$$

Now an examination of Table 1 shows that as a first approximation, the real part of the pressure ratio may be considered a constant. In most cases the $\bar{\omega}^2$ term contributes a negligible error. The largest deviation comes in the P_{4-3} term where at $\bar{\omega}_{max}$ the error is approximately 25%. However this is a "mutual" pressure and is not as significant as a self pressure. If desired, the effect of the $\bar{\omega}^2$ term may be partially included by adding to the constant real term a term in $\bar{\omega}^2$ evaluated at approximately the expected flutter frequency, for example $\bar{\omega} \doteq .35$. This correction was not used in the analysis to follow.

Before computing the lifts on each cell, it is desirable to evaluate the W_s that appears in the pressure relationship. Equation (13) gives W_s as

$$W_s e^{j\omega t} = \left[j\,\omega\, h_o + v\, \alpha_o + (x - x_o)\, j\, \alpha_o\, \omega \right] e^{j\omega t} \qquad (13)$$

where spanwise motion has been neglected. Now for a small cell size, the $\dot{\alpha}(x - x_o)$ term or the pitching about the centroid will be neglected in comparison to the other terms and

$$W_s\, e^{j\omega t} \doteq \dot{h} + Mc\, \alpha \qquad (13')$$

will be used. Equation (13') states that the lift is proportional to the vertical velocity and to the angle of attack of the wing. An examination of the pressures of Table 1 then indicates that the lift on a cell (i) with area A_i is of the form

$$L_i = -\frac{\rho c\, A_i}{\pi}\left[\frac{2M}{\beta}\dot{h}_i + \frac{2M^2 c}{\beta}\alpha_i\right]\left[e - j\, g\, \omega\right] + \frac{\rho c\, A_j}{\pi}\left[\frac{2M}{\beta}\dot{h}_j + \frac{2M^2 c}{\beta}\alpha_j\right]\left[k + j\, m\, \omega\right] + \ldots \qquad (28)$$

where the coefficients e, g, k, m are determined from Table 1. Now evaluating the coefficients of $\dot{h}_i$ and α_i gives

$$\frac{2M}{\beta} = 3.055$$

$$\frac{2M^2 c}{\beta} = 4445.5$$

while the unit of area (area of small cell like cell 1) is $A_1 = .09622\ ft^2$. If the symbol Γ is now introduced as

$$\Gamma = \text{Area of Small Cell}\ \frac{\rho c}{\pi} = .080115$$

and the conversion is made from ϖ to ω, the results of Table 1 may be used to obtain the cell lifts. If $p = \frac{d}{dt}$ the following expressions are obtained:

Lift	Numerical Value
L_{1-1}	$-(\Gamma)(\pi)(3.055\,\dot{h}_1 + 4445.5\,\alpha_1)(1 - p\,.76413 \times 10^{-4})$
L_{1-2}	$(\Gamma)(.5009)(3.055\,\dot{h}_2 + 4445.5\,\alpha_2)(1 + p\,11.82 \times 10^{-4})$
L_{1-3}	$(\Gamma)(.5611)(3.055\,\dot{h}_3 + 4445.5\,\alpha_3)(1 + p\,1.349 \times 10^{-4})$
L_{1-5}	$-(\Gamma)(.4884)(3.055\,\dot{h}_5 + 4445.5\,\alpha_5)(1 - p\,7.479 \times 10^{-4})$
L_{2-2}	$-(\Gamma)(2\pi)(3.055\,\dot{h}_2 + 4445.5\,\alpha_2)(1 - p\,1.5302 \times 10^{-4})$
L_{2-3}	$(\Gamma)(.4592)(3.055\,\dot{h}_3 + 4445.5\,\alpha_3)(1 + p\,24.35 \times 10^{-4})$
L_{3-3}	$-(\Gamma)(5.9494)(3.055\,\dot{h}_3 + 4445.5\,\alpha_3)(1 - p\,1.253 \times 10^{-4})$
L_{4-2}	$-(\Gamma)(.4239)(3.055\,\dot{h}_2 + 4445.5\,\alpha_2)(1 - p\,8.080 \times 10^{-4})$
L_{4-3}	$-(\Gamma)(.2133)(3.055\,\dot{h}_3 + 4445.5\,\alpha_3)(1 - p\,25.41 \times 10^{-4})$
L_{4-4}	$-(\Gamma)(\pi)(3.055\,\dot{h}_4 + 4445.5\,\alpha_4)(1 - p\,.7641 \times 10^{-4})$
L_{4-5}	$(\Gamma)(.5919)(3.055\,\dot{h}_5 + 4445.5\,\alpha_5)(1 + p\,5.884 \times 10^{-4})$
L_{5-3}	$-(\Gamma)(1.4318)(3.055\,\dot{h}_3 + 4445.5\,\alpha_3)(1 - p\,7.995 \times 10^{-4})$
L_{5-5}	$-(\Gamma)(6.1220)(3.055\,\dot{h}_5 + 4445.5\,\alpha_5)(1 - p\,1.6159 \times 10^{-4})$
L_{6-6}	$-(\Gamma)(3.8439)(3.055\,\dot{h}_6 + 4445.5\,\alpha_6)(1 - p\,1.4146 \times 10^{-4})$

TABLE 2

Table 2 serves to illustrate the fact that all lifts on each cell are given by equations of the form of equation (28). Some cells like cells one and four have as many as four contributing cells, however the contribution of each cell takes one of two possible forms, namely a time lag $(e - j\,g\,\omega)$ or a time lead $(k + j\,m\,\omega)$. The next obvious step in the solution of the supersonic flutter problem is to derive an electric analog for equations of the form of equation (28). The desired circuit is one which will produce a current which has the form of equation (28), namely an analogy between current and lift will be used.

III ELECTRICAL ANALOGY FOR AERODYNAMIC LIFTS

A. Operational Amplifiers and Computing Circuits

In order to represent the lifts on an oscillating airfoil electrically it is necessary to generate a current of the form of equation (28) namely:

$$L_i = -\frac{\rho c\, A_i}{\pi}\left[\frac{2M}{\beta}\dot{h}_i + \frac{2M^2 c}{\beta}\alpha_i\right]\left[e - jg\omega\right] + \frac{\rho c\, A_j}{\pi}\left[\frac{2M}{\beta}\dot{h}_j + \frac{2M^2 c}{\beta}\alpha_j\right]\left[k + jm\omega\right] \tag{28}$$

The desired electrical circuit should operate on the available wing coordinates namely $\dot{h}$ and $\dot{\alpha}$, and by a system of operational amplifiers and passive computing networks, generate a lift current. For the sake of completeness, the following derivations for operational elements are presented below (Ref. 8).

1. The Integrator

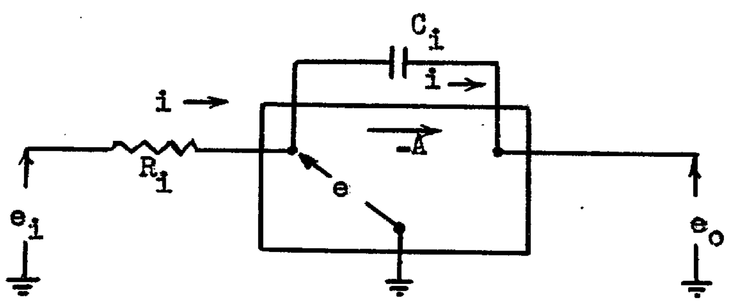

$$\frac{e_o}{e_i} \doteq -\frac{1}{\tau_i p}$$

FIGURE 11

The amplifier used in the above circuit was a Model 3 C.I.T. Analysis Laboratory chopper-stabilized Direct Current Amplifier. Such an amplifier has low drift (less than 5×10^{-5} v/hour), and a wide frequency response (from d-c to about 70 kc for a gain of 100). The gain A can be adjusted by choice of internal feedback network. For an integrator, it was set to approximately 100, while for an adder a higher gain, 20,000, was used.

The governing equations for an integrator are

$$e = e_i - R_i\, i = -\frac{e_o}{A}$$

$$e - e_o = \frac{i}{C_i \bar{p}}$$

solving for the transfer function

$$\frac{e_o}{e_i} = -\frac{A}{R_i\, C_i (A+1)\bar{p}+1}$$

now for $A \doteq 100$ $\quad A + 1 \doteq A$

$$\frac{e_o}{e_i} \doteq -\frac{1}{R_i C_i \bar{p}} = -\frac{1}{\tau_1 \bar{p}} \qquad (29)$$

2. <u>The Summer</u>

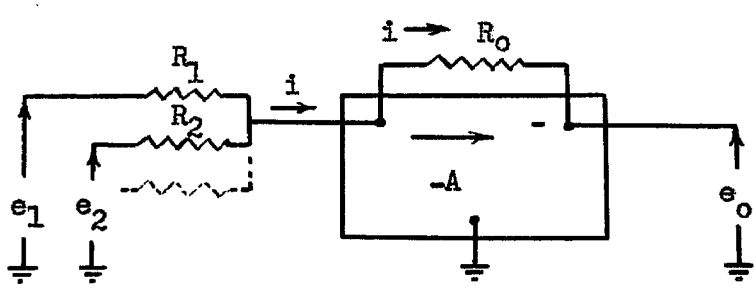

$$e_o = -R_o\left[\frac{e_1}{R_1} + \frac{e_2}{R_2} + \ldots\right]$$

FIGURE 12

The amplifier used for the above circuit was a Model 4 C.I.T. Analysis Laboratory amplifier with a gain of about 20,000. The negative gain amplifier is followed by an amplifier with a gain of +1 so that an additional sign reversal is available if necessary.

The governing equations for a summer are:

$$(e_1 + \frac{e_o}{A}) \frac{1}{R_1} + (e_2 + \frac{e_o}{A}) \frac{1}{R_2} + \ldots = (- e_o - \frac{e_o}{A}) \frac{1}{R_o}$$

or

$$\frac{e_o}{A}(\frac{A+1}{R_o} + \frac{1}{R_2} + \frac{1}{R_1} + \ldots) = - (\frac{e_1}{R_1} + \frac{e_2}{R_2} + \ldots)$$

now if $\frac{1}{R_2}, \frac{1}{R_1} << \frac{A+1}{R_o}$ (use $A \doteq 20,000$) then

$$e_o \doteq - R_o (\frac{e_1}{R_1} + \frac{e_2}{R_2} + \ldots) \qquad (30)$$

3. <u>The Current Generator</u>

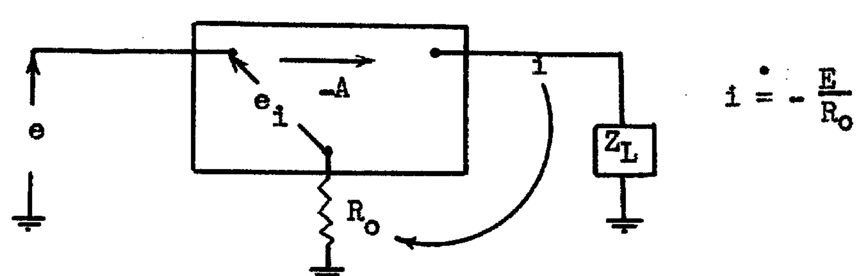

FIGURE 13

The amplifier used for this purpose was a Model 1 C.I.T. Analysis Laboratory negative gain amplifier with a separate power supply so that the amplifier chassis could be floated above ground.

The governing equations for a current generator are:

$$e_i = e + i\,R_o$$

$$-A\,e_i = (Z_L + R_o)i$$

or

$$i = \frac{-A\,e}{(A+1)R_o + Z_L}$$

for a high gain where $(A+1)\,R_o \gg Z_L$ $\qquad A \doteq 2000$

$$i \doteq -\frac{e}{R_o} \qquad (31)$$

4. <u>Passive Computing Circuits</u>

a. The Lag Function

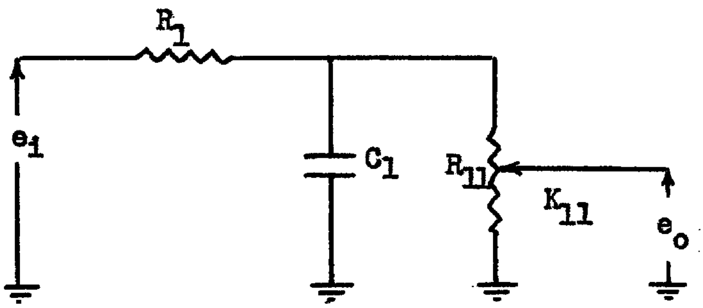

FIGURE 14

$$\frac{e_o}{e_i} = K_{11}\left(\frac{R_{11}}{R_1+R_{11}}\right)\left(\frac{1}{\tau_2\bar{p}+1}\right)$$

where

$$\tau_2 = \frac{C_1R_1R_{11}}{R_1+R_{11}}$$

now if $\tau_2^{\,2}\,\omega^2 \ll 1$

$$\frac{e_o}{e_i} \doteq K_{11}\left(\frac{R_{11}}{R_1+R_{11}}\right)\left(1 - \bar{p}\tau_2\right) \qquad (32)$$

b. The Lead Function

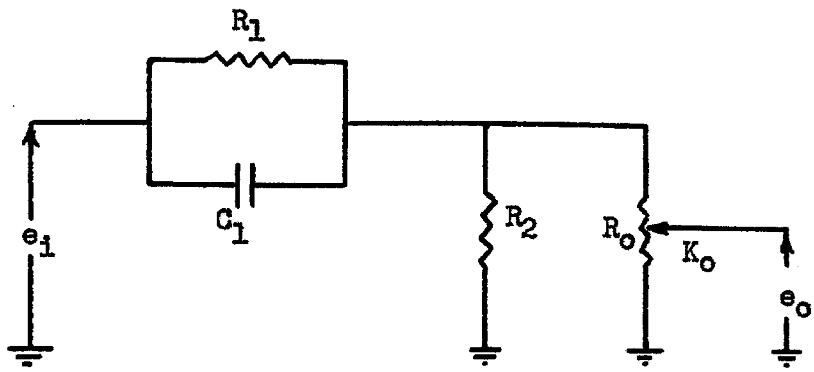

FIGURE 15

$$\frac{e_o}{e_i} = K_o \left(\frac{\tau_2}{\tau_1}\right)\left(\frac{\tau_1 \bar{p}+1}{\tau_2 \bar{p}+1}\right)$$

where $\tau_1 = R_1 C_1$ $\qquad$ $\tau_2 = \frac{R_1 \bar{R}_2}{R_1+\bar{R}_2} C_1$

$$\bar{R}_2 = \frac{R_2 R_0}{R_2+R_0}$$

now if $\quad 1 \gg \tau_2^{\,2} \omega^2$ $\quad$ and $\quad \tau_1 \tau_2 \omega^2 \ll 1$

$$\frac{e_o}{e_i} \doteq K_o \left(\frac{\tau_2}{\tau_1}\right)\left(1 + \bar{p}\left[\tau_1 - \tau_2\right]\right) \qquad (33)$$

An examination of equations (29) through (33) shows that equations of the form of equation (28) can now be analyzed.

The complete circuit for the aerodynamic lifts on the six cell wing for $M^2 = 1.75$ is presented in figure 16. As an example of the process involved in the derivation of this circuit, the equation for the output current (lift) of cell two will now be presented:

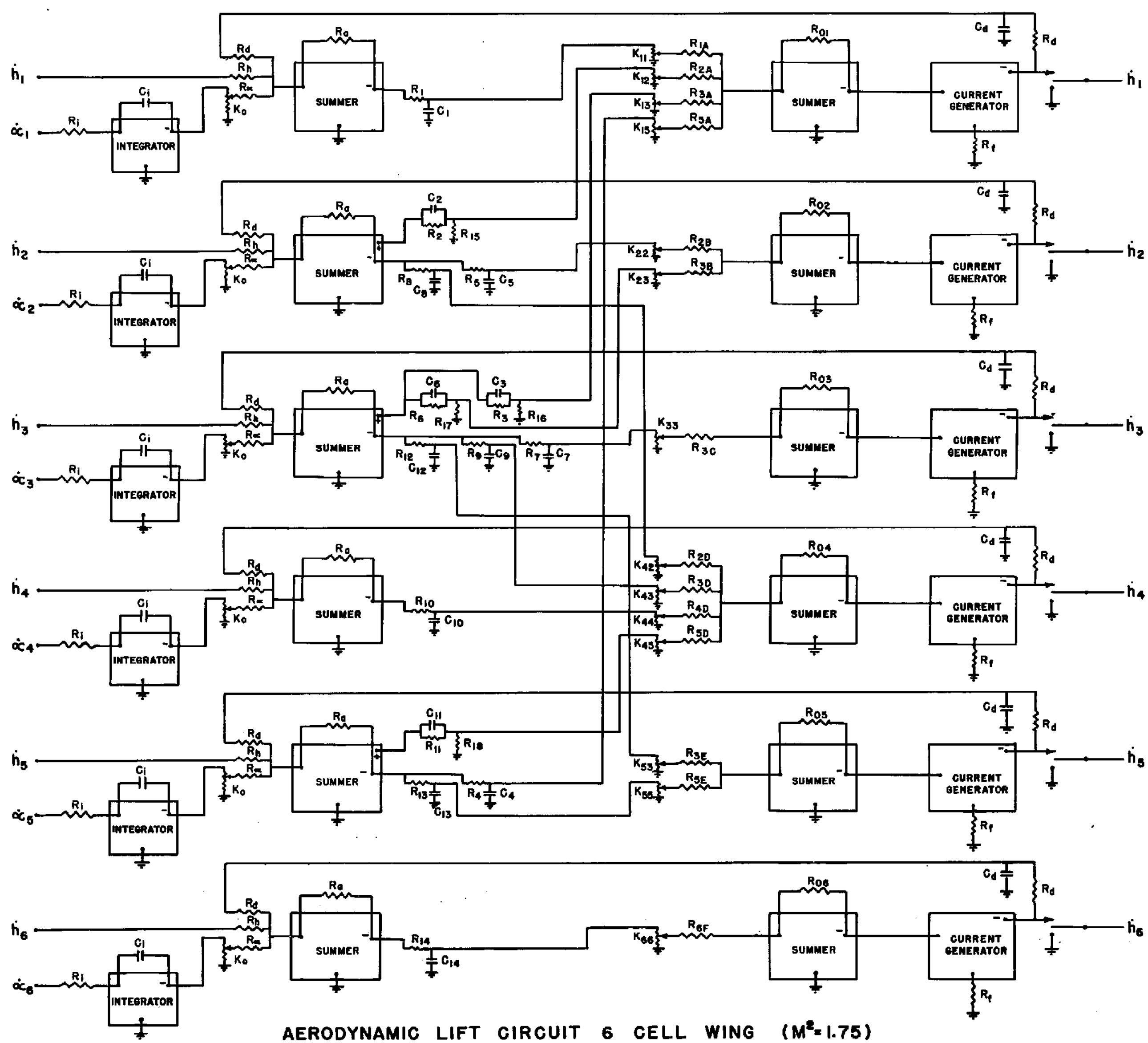

AERODYNAMIC LIFT CIRCUIT 6 CELL WING ($M^2 = 1.75$)

FIGURE 16

The equation for the output current of current generator (2) using equations (29)-(33) is

$$i_{h_2} \doteq -\frac{1}{R_f}\left[\frac{R_a R_{o_2}}{R_{2B}R_h}\ \frac{K_{22}R_{22}}{R_5+R_{22}}\ (1-\tau_5\bar{p})(E_{h_2}-\frac{R_h}{R_\alpha}\frac{K_o}{\tau_1\bar{p}}E_{\alpha_2})\right.$$

$$\left. -\frac{R_a R_{o_2}}{R_{3B}R_h}K_{23}\left(\frac{\tau_6'}{\tau_6}\right)\left\{1+(\tau_6-\tau_6')\bar{p}\right\}\left\{E_{h_3}-\frac{R_h}{R_\alpha}\frac{K_o}{\tau_1\bar{p}}E_{\alpha_3}\right\}\right] \tag{34}$$

where

$$\tau_5 = \frac{R_{22}R_5}{R_5+R_{22}}C_5 \qquad \tau_6 = R_6C_6$$

$$\tau_6' = \frac{R_6\bar{R}_{17}}{R_6+\bar{R}_{17}}C_6 \qquad \bar{R}_{17} = \frac{R_{17}R_{23}}{R_{17}+R_{23}}$$

Now, making sure that all of the above approximations are observed, an analogy, with the aid of artfully chosen scale factors, can be made between equations (28) and (34).

Before this analogy is made however, a few words of explanation should be written about the R_d-C_d-R_d feedback circuit from the output of the current generator to the input of the first adder. The capacitor C_d is so chosen as to trap all but the very low frequencies, hence the overall transfer function of the circuit is unchanged. This feedback does however tend to eliminate drift at very low frequencies. The practical values for these elements are

$$C_d = 2\ \mu f \qquad R_d = 1.8\ \text{meg}$$

or

$$\tau_d = R_dC_d = 3.6\ \text{seconds}$$

B. The Introduction of Scale Factors

The following analogy will be made between the electrical quantities of figure (16) and the physical quantities of the wing being studied:

$$ph = \frac{Ka}{N} E_h$$

$$p\alpha = -\frac{Ka}{P_1 N} E_\alpha$$

$$p = \frac{\bar{p}}{N}$$

$$\text{Lift} = \frac{K}{a} \; i_h$$

Now using equation (35) and equation (28) the following expression for the lift current is obtained:

$$i_{h_i} = -\frac{2M}{\beta} a^2 \frac{\rho c}{\pi N} \left[A_i e\left(1 - \frac{g}{e}\frac{\bar{p}}{N}\right)\left(E_{h_i} - \frac{N\, Mc}{P_1\, \bar{p}} E_{\alpha_i}\right) + A_j k\left(1 + \frac{m}{k}\frac{\bar{p}}{N}\right)\left(E_{h_j} - \frac{N\, Mc}{P_1\, \bar{p}} E_{\alpha_j}\right) \right] \qquad (36)$$

comparing equation (36) with equation (34) for i_{h_2}, the lift on cell 2 (for example), the following correspondences can be seen:

$$\tau_5 = \frac{g}{eN} \qquad\qquad (\tau_6 - \tau'_6) = \frac{m}{kN}$$

$$\frac{2a^2 \rho c M A_2}{\pi\, N\, \beta} e = \frac{1}{R_f} \frac{R_a R_{o2}}{R_{2B} R_h} K_{22} \frac{R_{22}}{R_5 + R_{22}} \qquad (37)$$

$$\frac{2a^2 \rho c M A_3 k}{\pi\, N\, \beta} = \frac{1}{R_f} \frac{R_a R_{o2}}{R_{3B} R_h} K_{23} \frac{\tau_6'}{\tau_6}$$

$$\frac{NM_c}{P_1} = \frac{R_h}{R_\alpha} \frac{K_o}{\tau_i}$$

Equations (37) therefore give a complete set of relationships between the parameters of the electrical circuit representing the aerodynamic lifts, and the actual lifts as given in Table 2 and as characterized in equation (28).

C. Numerical Determination of Circuit Parameters for Lifts on a Six Cell Wing

Values for the circuit parameters shown on the circuit diagram for the aerodynamic lifts on a six cell wing (figure 16) will now be determined. The lifts are those given in Table 2.

Where:

$M^2 = 1.75$ $\qquad$ $\rho = 2.378 \times 10^{-3}$ lb-ft^{-4}-sec^2

$c = 1.1 \times 10^3$ ft-sec^{-1}

$\Gamma = .080115$

for these equations, the following selection of scale factors was made:

Scale Factor	Value
N	4
P_1	.576
a^2	.002

Table 3

Now for the sake of convenience, all potentiometers indicated on figure 16 will be 10,000 ohm helipots. The time constants of the integrators τ_i will be set to

$$\tau_i = .01 \text{sec. with } R_i = 1 \text{ meg. } C_i = .01\ \mu f$$

so that the approximation of equation (29) is valid. The resistance R_f of the current generators will be 500 Ω (a standard analysis-lab. value) while the ratio of

$$\frac{R_h}{R_u} = \frac{NMc}{P_1}\frac{\tau_1}{K_o} = 101.04 \quad \text{for} \quad K_o = 1$$

Also, the feedback resistors R_{o1} - R_{o6} will be set to 10 meg. (All resistors being within ± 1% of nominal value.) Summarizing these values in table form gives:

Parameter	Value
R_i	1 M
C_i	.01 µf
All helipots	10 K
R_h	10 M
R_u	.1 M
R_f	500 Ω
R_d	1.8 M
C_d	2 µf
R_{o1} through R_{o6}	2 M
K_o	1.00
R_a	5 M

Table 4

Once the above elements have been selected, the remaining part of the calculation is to determine the values of the elements in the lag (lead) functions from equations of the form of equation (37) and to evaluate the gains of the second summers so as to give the correct overall gain.

The first step in this procedure is to rewrite the equations of Table 2 in a slightly different form, namely in terms of the voltages, thus, making use of the scale factor equations (35), the following expressions are obtained:

TABLE 5

Lift	Value
L'_{1-1}	$-.4\text{x}10^{-3}(1.2585)(.76375\ E_{h_1} - \frac{7710E_{\alpha_1}}{\bar{p}})(1-\bar{p}\ .19103\text{x}10^{-4})$
L'_{1-2}	$-.4\text{x}10^{-3}(.2007)(.76375\ E_{h_2} - \frac{7710E_{\alpha_2}}{\bar{p}})(1+\bar{p}\ 2.955\text{x}10^{-4})$
L'_{1-3}	$.4\text{x}10^{-3}(.2248)(.76375\ E_{h_3} - \frac{7710E_{\alpha_3}}{\bar{p}})(1+\bar{p}\ .33725\text{x}10^{-4})$
L'_{1-5}	$-.4\text{x}10^{-3}(.1957)(.76375\ E_{h_5} - \frac{7710E_{\alpha_3}}{\bar{p}})(1-\bar{p}\ 1.86975\text{x}10^{-4})$
L'_{2-2}	$-.4\text{x}10^{-3}(2.517)(.76375\ E_{h_2} - \frac{7710E_{\alpha_2}}{\bar{p}})(1-\bar{p}\ .38255\text{x}10^{-4})$
L'_{2-3}	$.4\text{x}10^{-3}(.18396)(.76375\ E_{h_3} - \frac{7710E_{\alpha_3}}{\bar{p}})(1+\bar{p}\ 6.0875\text{x}10^{-4})$
L'_{3-3}	$-.4\text{x}10^{-3}(2.3833)(.76375\ E_{h_3} - \frac{7710E_{\alpha_3}}{\bar{p}})(1-\bar{p}\ .31325\text{x}10^{-4})$
L'_{4-2}	$-.4\text{x}10^{-3}(.1698)(.76375\ E_{h_2} - \frac{7710E_{\alpha_2}}{\bar{p}})(1-\bar{p}\ 2.020\text{x}10^{-4})$
L'_{4-3}	$-.4\text{x}10^{-3}(.08545)(.76375\ E_{h_3} - \frac{7710E_{\alpha_3}}{\bar{p}})(1-\bar{p}\ 6.3525\text{x}10^{-4})$
L'_{4-4}	$-.4\text{x}10^{-3}(1.2585)(.76375\ E_{h_4} - \frac{7710E_{\alpha_4}}{\bar{p}})(1-\bar{p}\ .19103\text{x}10^{-4})$
L'_{4-5}	$.4\text{x}10^{-3}(.2371)(.76375\ E_{h_5} - \frac{7710E_{\alpha_5}}{\bar{p}})(1+\bar{p}\ 1.471\text{x}10^{-4})$
L'_{5-3}	$-.4\text{x}10^{-3}(.5736)(.76375\ E_{h_3} - \frac{7710E_{\alpha_3}}{\bar{p}})(1-\bar{p}\ 1.9988\text{x}10^{-4})$
L'_{5-5}	$-.4\text{x}10^{-3}(2.452)(.76375\ E_{h_5} - \frac{7710E_{\alpha_5}}{\bar{p}})(1-\bar{p}\ .40398\text{x}10^{-4})$
L'_{6-6}	$-.4\text{x}10^{-3}(1.5399)(.76375\ E_{h_6} - \frac{7710E_{\alpha_6}}{\bar{p}})(1-\bar{p}\ .35365\text{x}10^{-4})$

These lifts are analogous to the lift currents of equations of the type of equation (34). As an example of the computations involved, the relations for the lift L'_{1-1} will be carried out in detail:

$$L'_{1-1} = -.4\times10^{-3}(1.2585)(.76375\ E_{h_1} - \frac{7710E_{a_1}}{\bar{p}})(1-\bar{p}\ .19103\times10^{-4})$$

now $\tau_1 = .19103 \times 10^{-3} = R_1C_1$ from the above expression

set $C_1 = .05\ \mu f$ (available in 1% tolerance polystyrene plug-in capacitors)

then $R_1 = 397.2\ \Omega$

The overall "h" gain is

$$.4\times10^{-3}(1.2585)(.76375) = \frac{1}{R_f}\ \frac{R_{11}}{R_{11}+R_1}\ K_{11}\left(\frac{R_a}{R_h}\right)\frac{R_{o1}}{R_{1A}}$$

but $R_f = 500\ \Omega$ $\quad R_a/R_h = 1/2$ $\quad R_{o1} = 2\ M\Omega$ $\quad R_1 = 397.2\ \Omega$

then

$$\frac{.96118}{5} = .9618\ K_{11}\left(\frac{1}{2}\right)\frac{2M\Omega}{R_{1A}}$$

thus select $R_{1A} = 5M\Omega$

then $K_{11} = .9993$

Using a procedure similar to the one outlined above, the following parameter values, in addition to the ones presented in Table 4, were computed: See Table 6.

Cell 1		Cell 2		Cell 3		Cell 4		Cell 5		Cell 6	
R_1	397.2	R_2	7910	R_6	6337.5	R_{10}	397.2	R_{11}	3442	R_{14}	761
C_1	.05μf	C_2	.05μf	C_6	.1 μf	C_{10}	.05μf	C_{11}	.05μf	C_{14}	.05μf
K_{11}	.9993	R_{15}	3656	R_{17}	267.2	K_{44}	.9995	R_{18}	621.3	K_{66}	.5062
R_{1A}	5 M	K_{12}	.6070	K_{23}	.7123	R_{2D}	10 M	K_{45}	.4986	R_{6F}	2 M
R_{2A}	5 M	R_8	6778.5	R_3	1000	R_{3D}	10 M	R_{13}	879		
R_{3A}	10 M	C_8	.05μf	C_3	.1 μf	R_{4D}	5 M	C_{13}	.05μf		
R_{5A}	5 M	K_{42}	.4352	R_{16}	2175	R_{5D}	2 M	K_{55}	.8149		
		R_5	828.4	K_{13}	.5181			R_4	3739.6		
		C_5	.05μf	R_{12}	6663.4			C_4	.05μf		
		K_{22}	.8326	C_{12}	.05μf			K_{15}	.5027		
		R_{2B}	2 M	K_{53}	.730			R_{5E}	5 M		
		R_{3B}	1 M	R_9	4654			R_{5E}	2 M		
				C_9	.2 μf						
				K_{43}	.1912						
				R_7	668.2						
				C_7	.05μf						
				K_{33}	.7768						
				R_{3C}	2 M						

COMPUTER AERO ELEMENT SETTINGS

Table 6

D. Computer Aero Cell Test Procedure

Once a circuit of the form of figure 16 is physically set up on an electric analog computer (like the computer in the Analysis Laboratory at the California Institute of Technology), and the parameters are computed (see Tables 4 and 5), the next obvious step is to devise a test procedure in order to insure the proper performance of the equipment being used. With such an object in mind, the following procedure is established:

1. Check the gains of each individual amplifier for numerical gain, and for phase shifts at 10 kc. If phase shift exists on summers, compensate for it by placing capacitors in parallel with channel adding resistors (capacitors will usually be of the order of magnitude $1\mu\mu f$ - $250\ \mu\mu f$). Ten kc square wave testing is to be used. Thus for example:

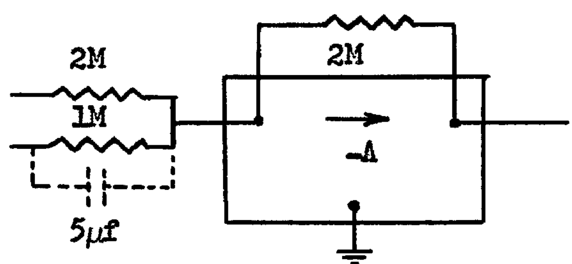

Compensation of Summers

FIGURE 17

2. In order to check the overall performance of the aerodynamic circuit, the lift currents should be measured for a specific frequency, with unit voltage inputs on each h and α input terminal in turn. Thus, it is necessary to compute the expected magnitude and phase of the lift currents from the equations of Table 5 at a fixed frequency (say

100 cps). These then are the desired lifts. They differ from the expected lifts by the approximations made in the lag functions, namely by assuming that

$$\frac{\tau_1\bar{p} + 1}{\tau_2\bar{p} + 1} \doteq 1 + \bar{p}(\tau_1 - \tau_2) \tag{33}$$

and

$$\frac{1}{\tau_2\bar{p} + 1} \doteq 1 - \bar{p}\tau_2 \tag{32}$$

Thus, for example, for the lift current i_{h_1} due to 5 volts (100 cps) impressed on the h_2 terminal namely $i_{h_{1-2}}$, the desired current from Table 5 is given by:

$$i_{h_{1-2_d}} = .4x10^{-3}(.2007)\left[.76375 \cdot (5\text{volts})\right]\left[1+j\ 2\pi(100)(2.955x10^{-4})\right]$$

$$= .313 \angle 10.5^{\circ}$$

while the expected lift current is:

$$i_{h_{1-2_e}} = (\text{Gain})(\text{Phase Shift})$$

$$= .3066\ \frac{1+j(2\pi \times 100)3.955x10^{-4}}{1+j(2\pi \times 100)\ 10^{-4}} = .316 \angle 10.4^{\circ}$$

which shows that the appoximation to the lag (lead) function at such frequencies ($\bar{\omega} = 1.6035 \times 10^{-3}\ \frac{\omega}{N} = .25$) is quite good. Using such a calculating procedure, the numerical test table (7) was computed.

TEST PROCEDURE FOR AERODYNAMIC CELLS

$M^2 = 1.75$ $N = 4$ $a^2 = .002$ $P_1 = .576$ $f = 100$ cps

Input Volts	Volts	Expected Lift Current (Ma)	Desired Lift Current (MA)	Cell
E_{h_1}	5	$-1.922 \angle -.688°$	$-1.922 \angle -.688°$	1
E_{h_2}	5	$.316 \angle 10.4$	$.313 \angle 10.5$	1
E_{h_3}	5	$.3434 \angle 1.21$	$.3434 \angle 1.21$	1
E_{h_5}	5	$-.7260 \angle -6.7$	$-.7376 \angle -6.7$	1
E_{h_2}	5	$-3.845 \angle -1.38$	$-3.845 \angle -1.38$	2
E_{h_3}	10	$.3021 \angle 20.8$	$.3007 \angle 20.95$	2
E_{h_3}	5	$-3.640 \angle 1.065$	$-3.640 \angle 1.065$	3
E_{h_2}	10	$-.2565 \angle -7.25$	$-.2605 \angle -7.25$	4
E_{h_3}	10	$-.1212 \angle -21.8$	$-.1406 \angle -21.8$	4
E_{h_4}	10	$-1.923 \angle -.688$	$-1.923 \angle -.688$	4
E_{h_5}	10	$.3640 \angle 5.28$	$.3623 \angle 5.3$	4
E_{h_3}	5	$-.8698 \angle -7.16$	$-.8820 \angle -7.16$	5
E_{h_5}	5	$-3.745 \angle -1.46$	$-3.745 \angle -1.46$	5
E_{h_6}	5	$-2.352 \angle -1.27$	$-2.352 \angle -1.27$	6

TABLE 7

In order to check the α channel, it can be noted that the ratio of lift current due to an "α" voltage to that due to an "h" voltage is:

$$\frac{i_{h_\alpha}}{i_{h_h}} = 16.08\ j \quad \text{(a constant for all channels)}$$

IV THE ELASTIC WING ANALOGY

A. The Analogy for an Elastic Beam in Bending

The equation for the vibration of a beam with moment of inertia I and distributed mass $\bar{m}$ per unit length is given as

$$\frac{\partial^2}{\partial y^2}\left(EI\,\frac{\partial^2 h}{\partial y^2}\right) + \bar{m}\,\frac{\partial^2 h}{\partial t^2} = 0 \tag{38}$$

The electrical analogy for this equation was derived by Dr. G. D. McCann and is fully outlined in Reference 9. The circuit is given below:

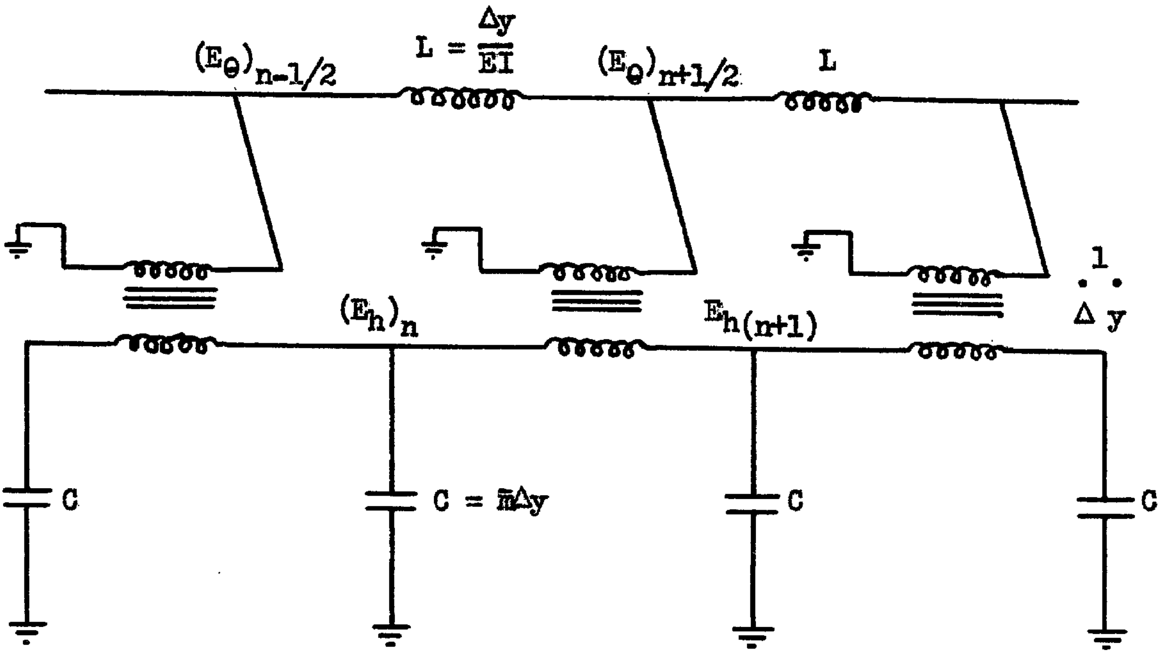

THE ELECTRICAL ANALOGY FOR THE

BENDING OF A BEAM

FIGURE 18

B. The Analogy for the Plate Equation

The differential equation for the dynamic deflection of a constant thickness elastic plate can be written in the following form (Ref. 10):

$$\nabla^4 h = q/D_o$$

or

$$\frac{\partial}{\partial x}\left[\frac{\partial^2}{\partial x^2} + \frac{\partial^2}{\partial y^2}\right]\frac{\partial h}{\partial x} + \frac{\partial}{\partial y}\left[\frac{\partial^2}{\partial x^2} + \frac{\partial^2}{\partial y^2}\right]\frac{\partial h}{\partial y} = q/D_o \qquad (39)$$

where q is a load per unit area and D_o is the stiffness constant for the plate

$$D_o = \frac{E\, t_o^3}{12(1 - \nu^2)}$$

where t_o is plate thickness, and ν is Poisson's ratio.

In deriving an analogy for equation (39), it was pointed out in reference 10 that equation (38) is similar in form to the first term on the left side of equation (39). Thus it may be deduced that an analogy for the first term of equation (39) will be similar to the circuit of figure 18, with stiffness inductors going in both (x) and (y) directions.

Consider the following network:

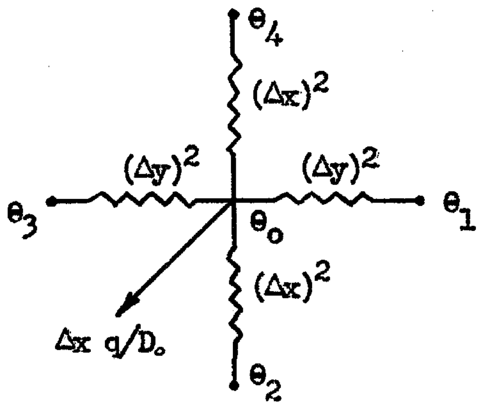

$$\frac{\theta_4+\theta_2}{(\Delta x)^2} + \frac{\theta_1+\theta_3}{(\Delta y)^2} - \frac{2\,\theta_o}{(\Delta x)^2} - \frac{2\,\theta_o}{(\Delta y)^2} = \Delta x\, q/D_o$$

DERIVATION OF PLATE CIRCUIT

FIGURE 19

now if
$$\frac{h_n - h_{n-1}}{\Delta x} = \theta_x$$

then the following equation is obtained

$$\frac{\partial}{\partial x}\left[\frac{\partial^2}{\partial x^2} + \frac{\partial^2}{\partial y^2}\right]\frac{\partial h}{\partial x} = q/D_o \tag{39a}$$

Thus the following circuit for equation (39a) may be deduced:

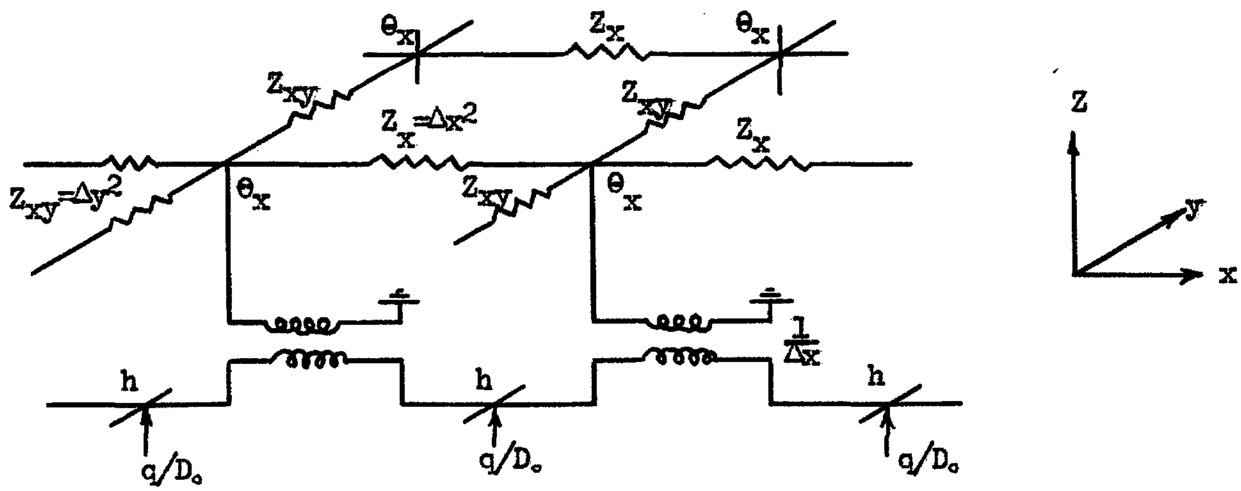

DYNAMIC ANALOG FOR EQUATION (39a)

FIGURE 20

Obviously, a similar circuit can be derived for the second term of equation (39). Hence a circuit for the complete equation is best represented by three planar diagrams.

C. The Elastic Wing

A wing such as the elastic wing of Part III is composed of intersecting beams covered with thin plates on both the top and bottom surfaces. Thus using the theory outlined above, the structure can be represented electrically by the circuits of figures 21, 22, and 23.

Now if the following definitions are made:

T_x h circuit/α circuit transformer

T_y h circuit/$\bar{\beta}$ circuit transformer

L_x α inductor

L_y $\bar{\beta}$ inductor

L_{yx} α inductors in y direction

C mass capacitors

$$D_o = EI = \frac{td^2}{2} E$$

where wing cross section may be represented as:

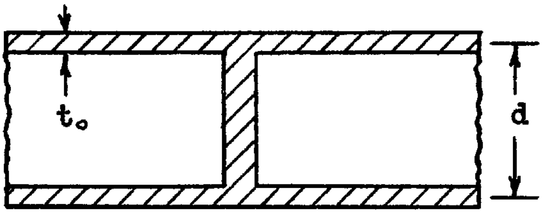

WING CROSS SECTION

FIGURE 20(a)

The equations for the circuit parameters then are:

Transformers:

$$T_x = \frac{\Delta x}{P_1} = \frac{.333}{.576} = .5781 \qquad T_y = \frac{\Delta y}{P_1} = \frac{.576}{.576} = 1.0$$

$$= .5/.85 \qquad = 1.0/1.0$$

Bending Inductors:

$$L_x = \frac{\Delta x}{\Delta y} \frac{P_1^2}{a^2} \frac{1}{D_o} \qquad L_y = \frac{\Delta y}{\Delta x} \frac{P_1^2}{a^2} \frac{1}{D_o}$$

Torsion Inductors:

$$\text{for } G = \frac{E}{2(1+\nu)} \doteq \frac{E}{2}$$

$$L_{yx} = \frac{\Delta y}{\Delta x} \frac{P_1^2}{a^2} \frac{1}{4GI} = \frac{\Delta y}{\Delta x} \frac{P_1^2}{a^2} \frac{1}{2D_o}$$

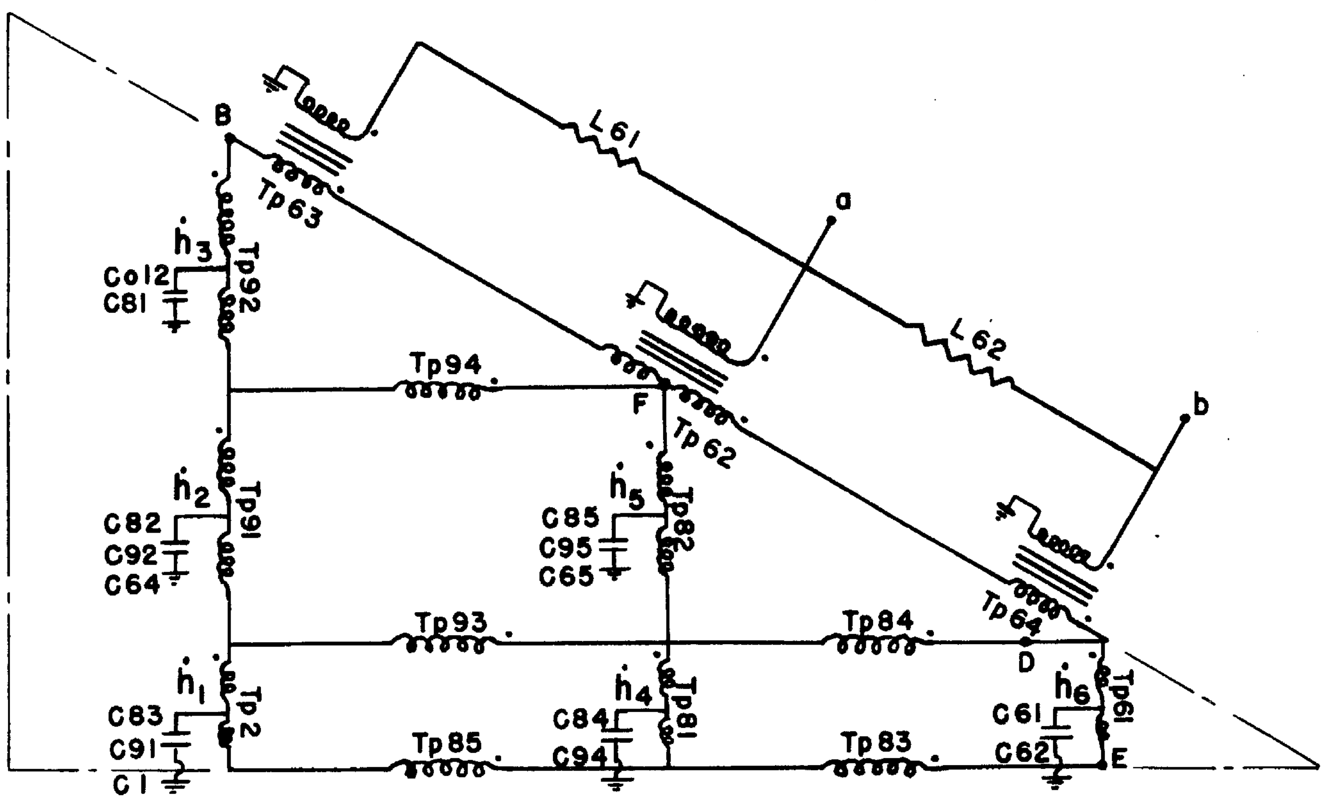

"h" CIRCUIT 6 CELL WING

FIGURE 21

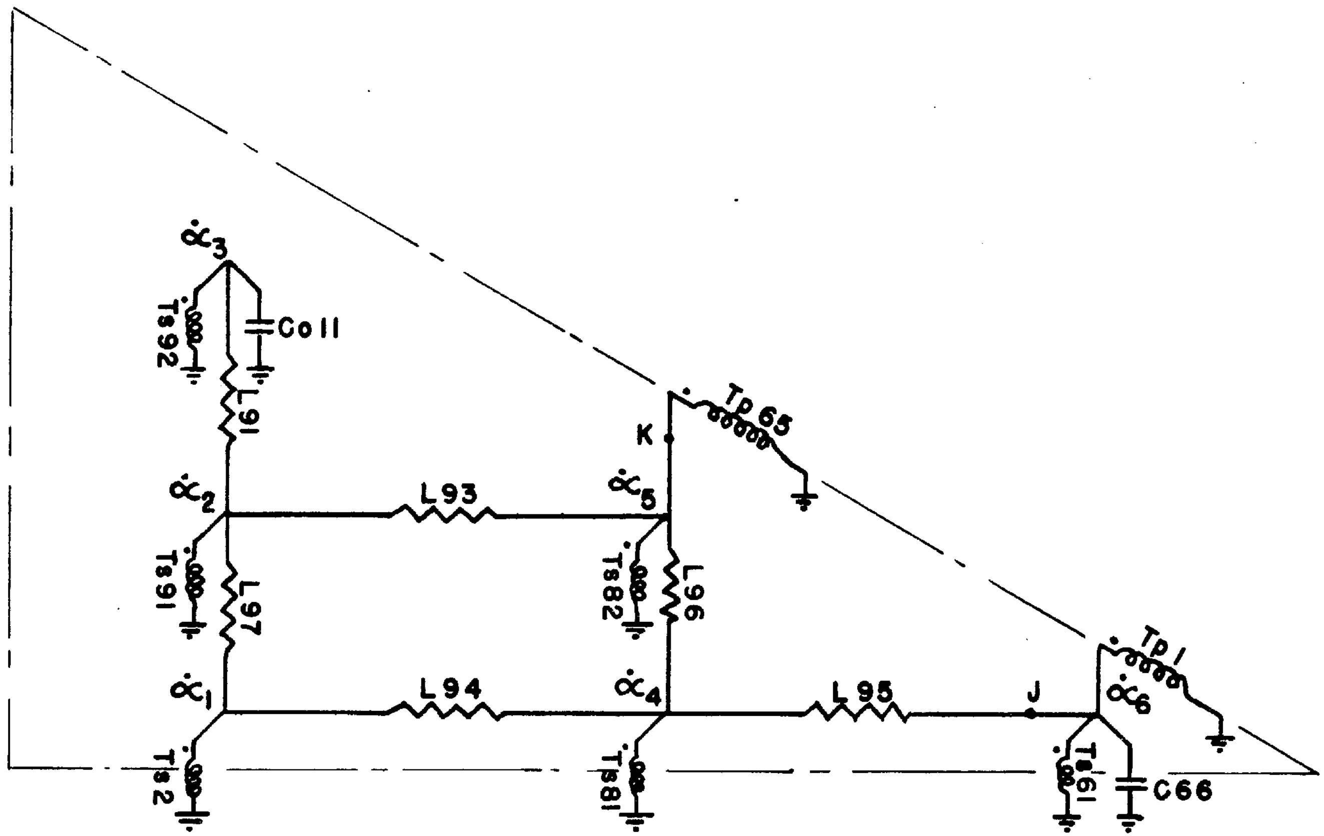

"α" CIRCUIT 6 CELL WING

FIGURE 22

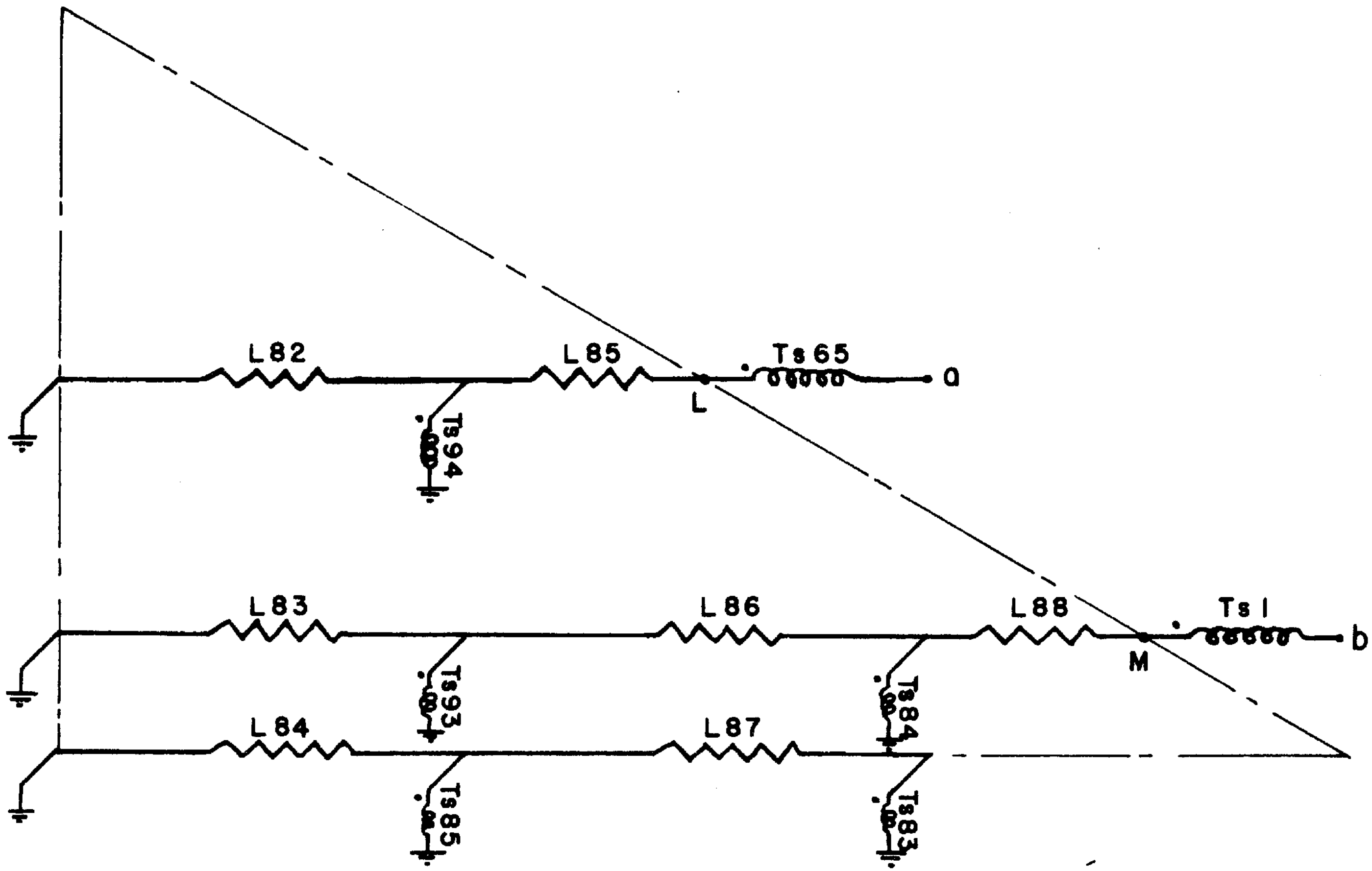

"$\bar{B}$" CIRCUIT 6 CELL WING

FIGURE 23

The leading edge circuit however requires special attention. Consider the following diagram:

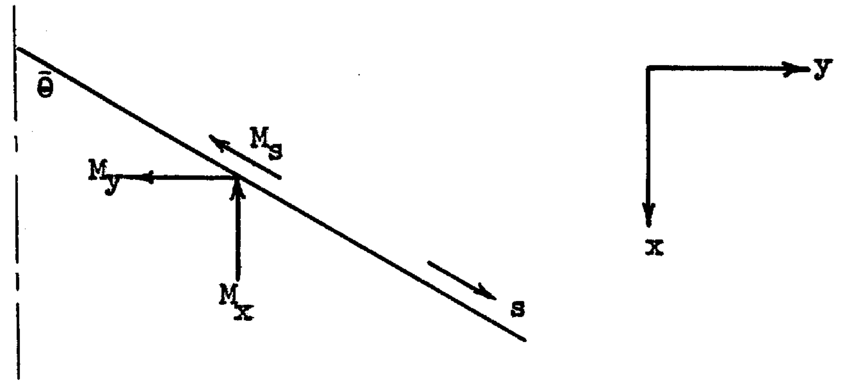

MOMENT EQUILIBRIUM IN LEADING EDGE CIRCUIT

FIGURE 24

$$M_y = M_s \sin \bar{\theta}$$

$$M_x = M_s \cos \bar{\theta}$$

Now if the following scale factors are introduced:

$$M_s = K/b' I_s$$

$$M_y = K/a \; I_y \qquad M_x = K/a \; I_x$$

while

$$\frac{ph}{p\alpha} = - \frac{E_h}{E_\alpha} P_1 = \Delta x$$

or

$$\frac{E_h}{E_\alpha} = - \frac{\Delta x}{P_1}$$

then using the scale factor equations and figure 24:

$$I_y = \frac{a}{b'} I_s \sin \bar{\theta}$$

$$I_x = \frac{a}{b'} I_s \cos \bar{\theta}$$

then let the scale factor (b') be:

$$b' = a \sin \bar{\theta}$$

then

$$I_y = I_s$$

$$I_x = I_s/\tan\bar{\theta}$$

The turns ratio of the $\bar{\beta}/\alpha$ transformers in the leading edge is:

$$\bar{\beta}/\alpha = \frac{1}{\tan\bar{\theta}} = \frac{1}{\sqrt{3}} = \frac{.55}{.95} \tag{41}$$

While the bending inductors in the leading edge are given by:

$$L_z = \frac{\Delta s}{\omega'}\frac{P_1^2}{a^2\sin^2\bar{\theta}}\frac{1}{D_o} \tag{42}$$

where Δs is 1/2 length of leading edge = .667' and ω' is an equivalent width of the leading edge beam chosen as .15 feet.

The h/α transformers in the leading edge are given by

$$T = \frac{E_h}{E_\alpha} = \frac{\Delta s\sin\bar{\theta}}{P_1} = T_y = \frac{1.0}{1.0} \tag{43}$$

Using equations (40)-(43), the following parameter values can be tabulated:

Element	Quantity	Primary	Secondary	Pri. Tap
T_{61}	h/α T_x	.35	1.0	.15
T_{62}	leading edge	1.0	1.0	.5
T_{63}	leading edge	.5	1.0	
T_{64}	leading edge	.5	1.0	
T_{65}	α/β coupling	.95	.55	
T_2	h/α T_x	.35	1.0	.15
T_{91}	h/α T_x	.5	.85	.25
T_{92}	h/α T_x	.5	.85	.25
T_{81}	h/α T_x	.35	1.0	.15
T_{82}	h/α T_x	.5	.85	.25
T_{85}	h/β̄ T_y	1.0	1.0	
T_{93}	h/β̄ T_y	1.0	1.0	
T_{94}	h/β̄ T_y	1.0	1.0	
T_{83}	h/β̄ T_y	1.0	1.0	
T_{84}	h/β̄ T_y	1.0	1.0	
T_1	α/β̄ coupling	.95	.55	

ELASTIC WING TRANSFORMER VALUES
TABLE 8

The mass capacitors of figure 21 are given by:

$$C = \frac{a^2}{N^2}\bar{M} = 1.25 \times 10^{-4}\,\bar{M} \qquad (44)$$

where $\bar{M}$ is the mass per cell which is the mass of the beams and plates per cell. In computing the inductors, the following expressions will be used (see figure 20a)

$$D_o = \frac{td^2}{2}E$$

where

$$E = 1.05 \times 10^7 \text{ lb/in}^2$$

The values for the L's and C's will be determined in part V.

In order to compute the values for the capacitors in the α circuit, the following equation may be used

$$\frac{I}{\bar{M}} = k_o^2 = P_1^{\,2}\frac{C_\alpha}{C_h} \qquad (45)$$

where k_o is the radius of gyration.

D. Test Procedure for Elastic Wing Circuit

Once the circuits of figures (21)-(23) are set up on the electric analog computer, a test procedure for the validity of the circuit should be formulated.

1. First, measure the currents at all nodes in the circuit. Then
   a. Kirchhoff's Law should be satisfied, namely, the sum of the currents at a node should be zero.
   b. Ampere turns on each side of a transformer should be equal.
2. Second, measure the h circuit voltages at mode frequencies. This gives the mode shapes of the wing which should check with physical

intuition. The sum of $\sum_i C_i V_i$ in the h circuit (the total charge) must be zero - this is equivalent to the conservation of linear momentum. A mode frequency is one at which the driving current is a minimum (maximum circuit impedance).

V THE ELECTRIC ANALOG COMPUTER STUDY

A. Equipment

In order to complete the analysis of the last four sections, an actual computer study was performed on the planform of figure 7 using the circuits of figures (16), (21), (22), (23). The elastic structure was set up on the California Institute of Technology Electric Analog computer, a picture of which is presented in figure 25. Thus all of the passive elements, with the exception of T_1 and T_2, indicated in figures 21 - 23 were computer elements with tolerances of $\pm$ 1%. (T_1 and T_2 also had similar tolerances.)

The principal equipment problem lay in the construction of the six aero cells represented in figure 16. Three different types of amplifiers had to be used in this circuit. This fact was dictated not by circuit needs, but by existing equipment in the Analysis Laboratory and the Servomechanisms Laboratory at the California Institute of Technology. Pictures of these amplifiers are presented in figures (26) - (28). The plug-in units for these operational amplifiers are shown in figure (29), while a complete assembled view of two out of the six aerodynamic cells is shown in figures (30) and (31).

It should be mentioned at this point that all resistors and capacitors used in the plug-in units were precision elements ($\pm$ 1% tolerances). The specifications of the amplifiers were already presented in Section III under a discussion of operational amplifiers.

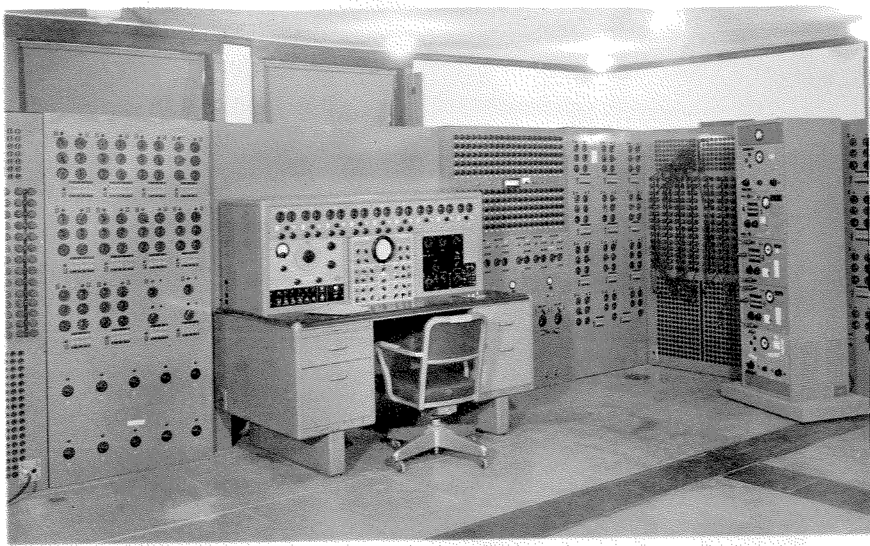

CONTROL DESK OF CIT ELECTRIC ANALOG COMPUTER

FIGURE 25

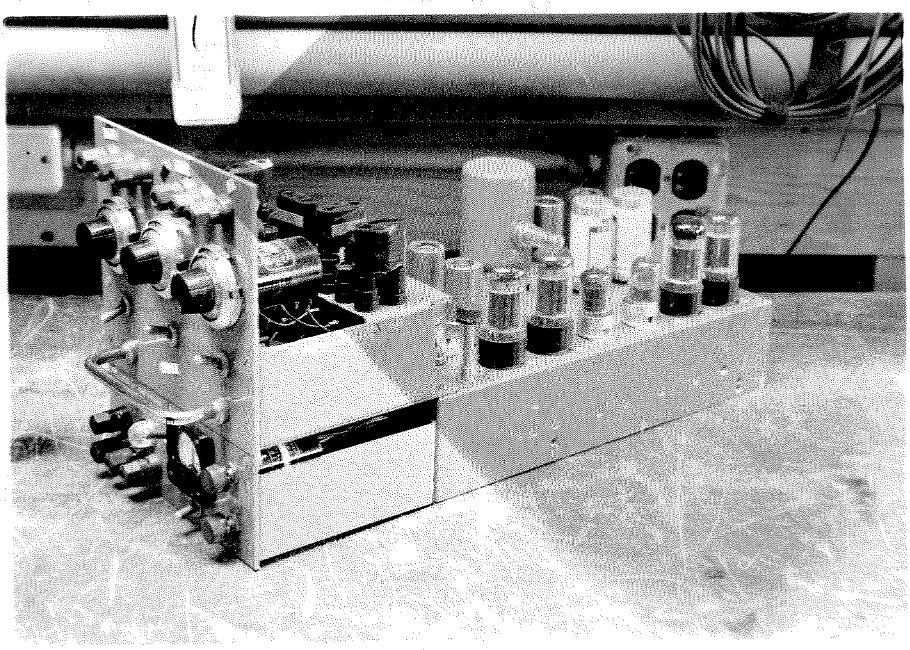

SUMMER WITH NEGATIVE AND POSITIVE OUTPUTS (WITH PLUG-IN UNIT IN PLACE) SERVOMECHANISMS LABORATORY

FIGURE 26

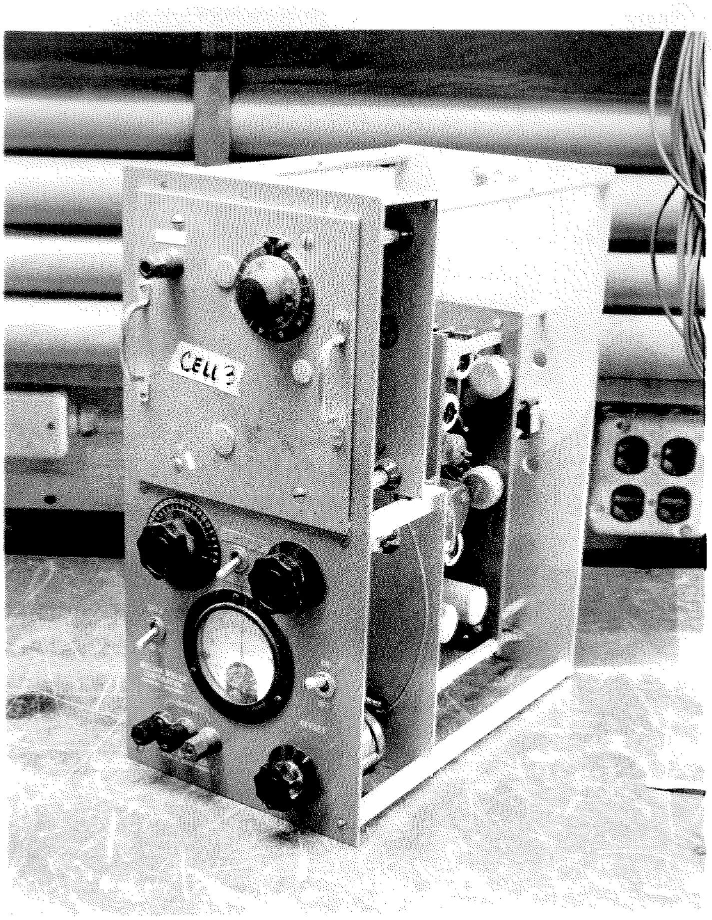

INTEGRATOR AMPLIFIER NEGATIVE GAIN WITH INTEGRATOR PLUG-IN UNIT IN PLACE ANALYSIS LABORATORY

FIGURE 27

CURRENT GENERATOR AMPLIFIER (WITH POWER SUPPLY) ANALYSIS LABORATORY

FIGURE 28

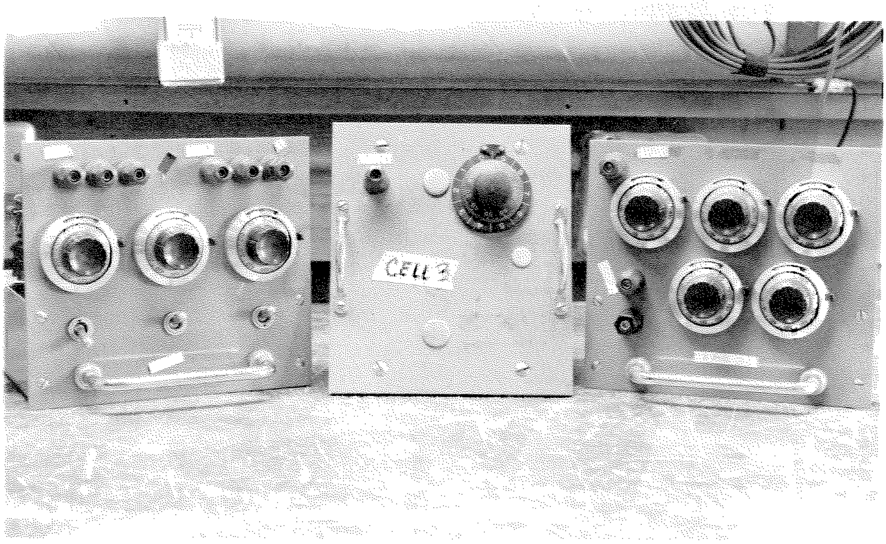

SUMMER INTEGRATOR LAG (LEAD) FUNCTION

PLUG-IN UNITS

FIGURE 29

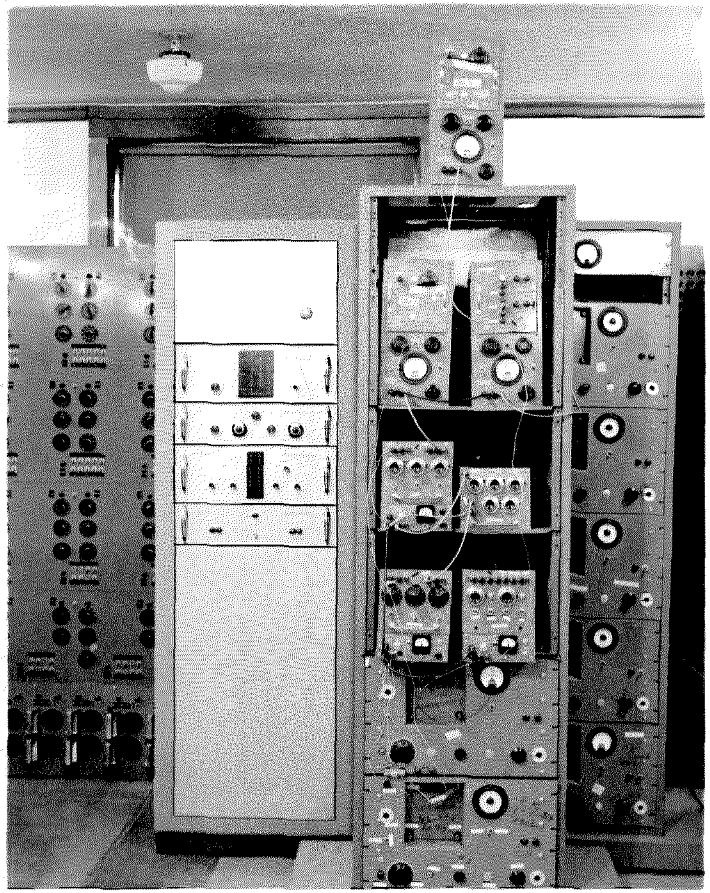

VIEW OF 2 AERO CELLS

FIGURE 30

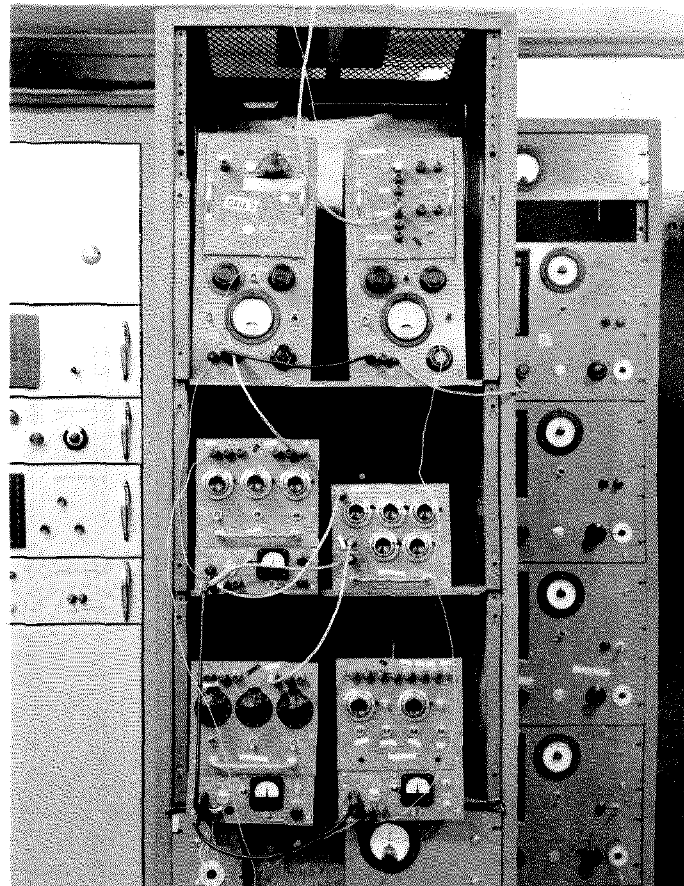

CLOSE UP VIEW OF 2 AERO CELLS

FIGURE 31

C. I. T. ANALYSIS LABORATORY

B. Analysis of Three Wings

In order to perform a thorough flutter analysis at a fixed Mach number ($M^2 = 1.75$), it was decided to analyze three wings of identical planform but with different mass distributions and stiffnesses. By such a procedure, a range of flutter frequencies could be obtained, thus covering the allowable values of $\bar{\omega}$ in the aerodynamic lift equations.

For each wing three cases were investigated. These were:

1. Wing and complete aerodynamic lift circuit (basic case).

2. Wing and aerodynamic lift circuit with lag (lead) function capacitors removed. This illustrates the effects of phase shift as compared to magnitude of the lifts on supersonic flutter in the allowable frequency range.

3. Wing and aerodynamic lifts due to "self-cell motion" only. Namely, in figure 16 set R_{2A}, R_{3A}, R_{5A}, R_{3B}, R_{2D}, R_{3D}, R_{5D}, R_{3E} to infinity. This illustrates the effect of the mutual terms on supersonic flutter.

Tables 9 and 10 present the values of the capacitors and stiffness inductors used for the three basic wing cases respectively. It should be noted that the effects of a fuselage were included by distributing its mass near the centerline of the wing at stations 1, 2, and 3. The effects of rotary inertia were included by having an "α" mass at cell (3), the assumed center of gravity of the wing and fuselage. In order to obtain desirable flutter mode shapes and frequencies, a tip mass was included at cell (6) with an appropriate rotary inertia C_α included at "α_6" coordinate.

CAPACITOR VALUES FOR WINGS 1, 2, 3

Capacitors	Wing 1	Wing 2	Wing 3
C1 + C83 + C91	2 μf	5 μf	8 μf
C64 + C82 + C92	4 μf	8 μf	12 μf
C81 + C_o12	42 μf	42 μf	42 μf
C84 + C94	2 μf	4 μf	7 μf
C65 + C85 + C95	4 μf	8 μf	12 μf
C61 + C62	3 μf	4 μf	7 μf
C66	.46 μf	.69 μf	1.06 μf
C_o11	80 μf	80 μf	80 μf

TABLE 9

INDUCTOR VALUES FOR WING1

Inductor	$\frac{L}{L_o}$ = .707	Computer Setting	$\frac{L}{L_o}$ = .850	Computer Setting	$\frac{L}{L_o}$ = 1.00	Computer Setting
L91	.034h	0-2-10	.041h	0-3-5	.048h	0-4-0
L93	.511	8-2-7	.613	10-1-1	.720	12-0-0
L94	.511	8-2-7	.613	10-1-1	.720	12-0-0
L95	.644	10-3-8	.773	12-4-5	.910	15-0-0
L96	.213	3-2-7	.255	4-1-3	.300	5-0-0
L97	.051	0-4-3	.061	0-5-1	.072	0-6-0
L82	.213	3-2-7	.255	4-1-3	.300	5-0-0
L83	.213	3-2-7	.255	4-1-3	.300	5-0-0
L84	.384	6-2-0	.460	7-3-4	.540	9-0-0
L85	.298	4-4-10	.357	5-4-9	.420	7-0-0
L86	.298	4-4-10	.357	5-4-9	.420	7-0-0
L87	.511	8-2-7	.613	10-1-1	.720	12-0-0
L88	.468	7-4-0	.561	9-1-9	.660	11-0-0
L61	.770	12-4-2	.925	15-2-1	1.09	15-15-0
L62	.770	12-4-2	.925	15-2-1	1.09	15-15-0

TABLE 10a

INDUCTOR VALUES FOR WINGS 2 and 3

Inductor	$\frac{L}{L_o}$=.80	Computer Setting	$\frac{L}{L_o}$=1.0	Computer Setting	$\frac{L}{L_o}$=1.2	Computer Setting
L91	.038	0-3-2	.048	0-4-0	.058	0-4-10
L93	.728	12-0-8	.910	15-0-0	1.09	15-15-0
L94	.728	12-0-8	.910	15-0-0	1.09	15-15-0
L95	.728	12-0-8	.910	15-0-0	1.09	15-15-0
L96	.240	4-0-0	.300	5-0-0	.360	6-0-0
L97	.058	0-4-10	.072	0-6-0	.086	0-7-2
L82	.240	4-0-0	.300	5-0-0	.360	6-0-0
L83	.240	4-0-0	.300	5-0-0	.360	6-0-0
L84	.432	7-1-0	.540	9-0-0	.649	10-4-1
L85	.192	3-1-0	.240	4-0-0	.288	4-4-0
L86	.192	3-1-0	.240	4-0-0	.288	4-4-0
L87	.288	4-4-0	.360	6-0-0	.432	7-1-0
L88	.240	4-0-0	.300	5-0-0	.360	6-0-0
L61	.870	14-2-6	1.09	15-15-0	1.10	15-15-10
L63	-	-	-	-	.210	3-2-6
L62	.870	14-2-6	1.09	15-15-0	1.10	15-15-10
L64	-	-	-	-	.210	3-2-6

TABLE 10b

It is to be noted that the only difference between wings 2 and 3 lies in the mass distribution. Wing 3 is a heavier wing and thus has a lower flutter frequency.

The first three mode shapes for each of the three wings, namely - first bending, first torsion, and second bending as found by measuring the "h" voltages of figure 21 at a frequency where the driving current is a minimum (maximum input impedance), are presented in figures 32, 33 and 34. The individual wings are numbered in order of mode frequencies, that is wing 1 has the highest frequencies while wing 3 has the lowest mode frequencies. Frequencies indicated on figures 32 - 34 are mechanical frequencies obtained by dividing measured computer frequencies by N = 4.

NORMAL MODES SYSTEM I. ($\frac{L}{L_o}$=.707)

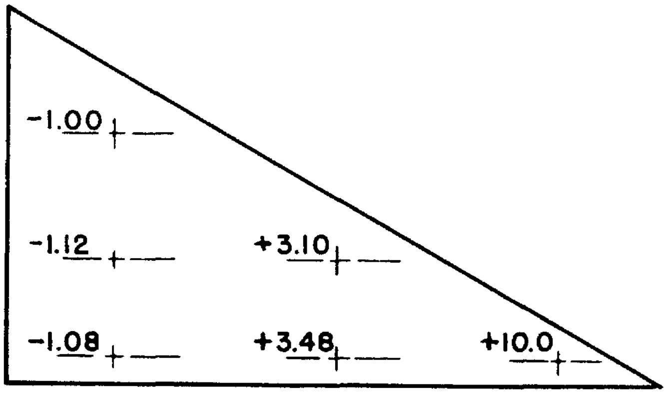

DRIVING POINT: C61 FREQUENCY: 31.25 C.P.S.

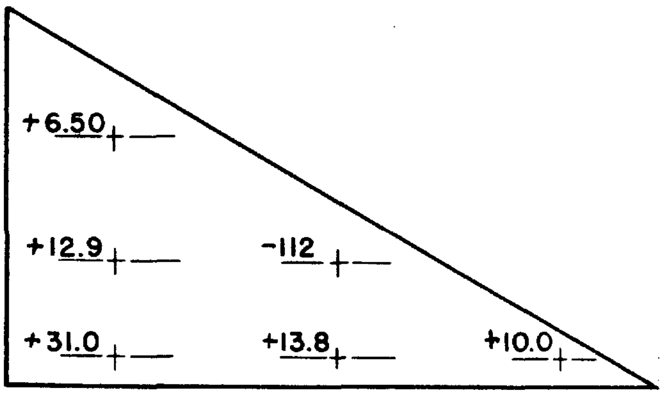

DRIVING POINT: C66 FREQUENCY: 67.0 C.P.S.

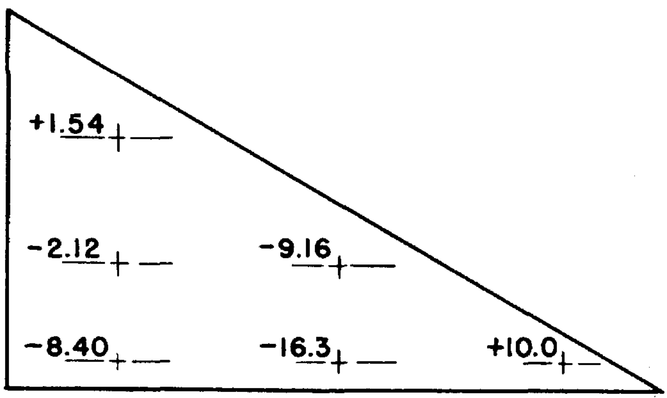

DRIVING POINT: C83 FREQUENCY: 117.3 C.P.S.

FIGURE 32

NORMAL MODES SYSTEM 2. ($\frac{L}{L_0}=1.0$)

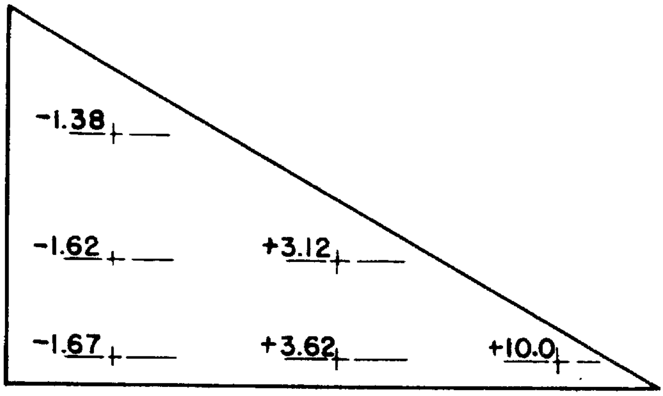

DRIVING POINT: C61 FREQUENCY: 22.88 C.P.S.

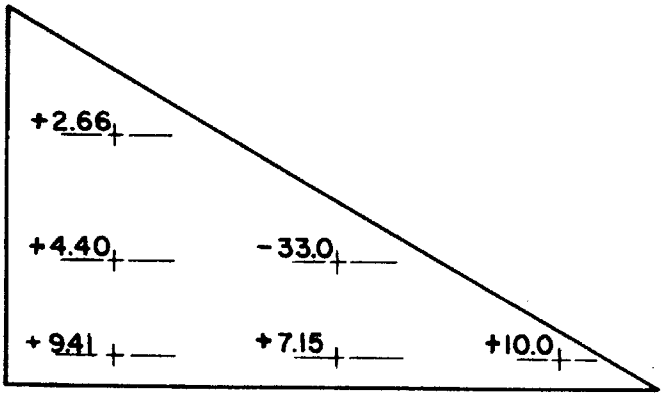

DRIVING POINT: C66 FREQUENCY: 47.25 C.P.S.

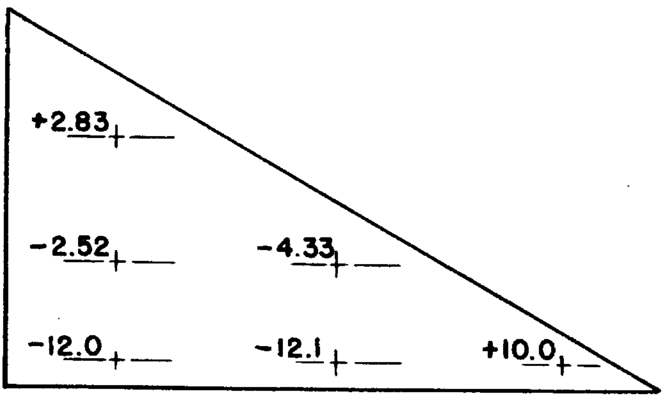

DRIVING POINT: C83 FREQUENCY: 87.0 C.P.S.

FIGURE 33

NORMAL MODES SYSTEM 3. ($\frac{L}{L_0}=1.0$)

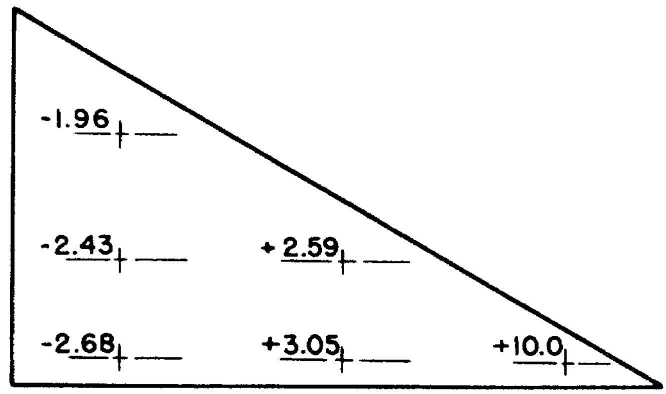

DRIVING POINT: C61 FREQUENCY: 18.5 C.P.S.

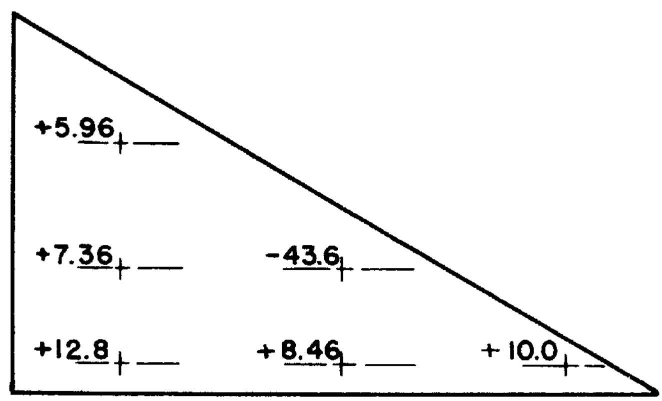

DRIVING POINT: C66 FREQUENCY: 38.5 C.P.S.

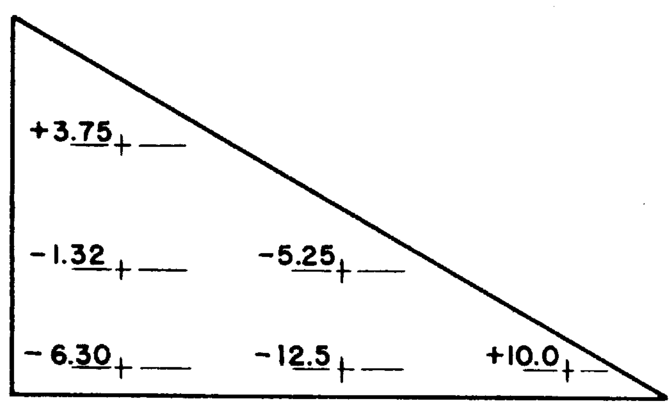

DRIVING POINT: C83 FREQUENCY: 75.75 C.P.S.

FIGURE 34

C. Flutter Results

The experimental work covered a period of five weeks. The first one and one-half weeks were spent in testing and wiring electronic equipment, while the remaining three and one-half weeks were spent working on the computer. Of this time, about 75% was used for testing, checking and actual circuit hookup, while the remainder of the time was used for taking data.

The computer flutter results are presented for the three wings (3 basic cases per wing, see section V, B) as follows:

1. Original data are presented (Polaroid camera records of voltage wave shapes and mode shapes).

2. Computed curves using above photographs are presented of frequency and damping parameter "g" (defined below) vs. stiffness for all cases.

The damping parameter "g" for a damped sine wave is defined as follows: if the envelope of the damped wave is given by:

$$e^{+g \frac{\omega_n}{2} t} \doteq 1 + g \frac{\omega_n}{2} t + \dots \qquad (46)$$

or if the increase (decrease) is given as

$$\text{per unit/cycle} = 2\pi \frac{g}{2} = \pi g$$

then

$$g = \frac{\text{per unit/cycle}}{\pi} \qquad (47)$$

Thus for example if a wave decreases 3% per cycle

$$g = \frac{-.03}{\pi} = -.00955$$

negative g representing a stable system. Figures 35 - 46 present these results. Table 11 serves as a key for interpreting the photographic records.

KEY FOR PHOTOGRAPHIC DATA

Element	System 1			System 2			System 3		
Voltage	$\frac{L}{L_o}$	Picture	Case	$\frac{L}{L_o}$	Picture	Case	$\frac{L}{L_o}$	Picture	Case
L95	.707	1-1	1	.8	1-1	1	.8	1-1	1
L95	.85	1-2	1	1.0	1-2	1	1.0	1-2	1
L95	1.0	1-2	1	1.2	1-3	1	1.2	1-3	1
L95	.707	2-1	2	.8	2-1	2	.8	2-1	2
L95	.85	2-2	2	1.0	2-2	2	1.0	2-2	2
L95	1.0	2-3	2	1.2	2-3	2	1.2	2-3	2
L95	.707	3-1	3	.8	3-1	3	.8	3-1	3
L95	.85	3-2	3	1.0	3-2	3	1.0	3-2	3
L95	1.0	3-3	3	1.2	3-3	3	1.2	3-3	3
C81	.85	1-1	1	1.2	1-1	1	1.0	1-1	1
C82	.85	2-1	1	1.2	2-1	1	1.0	2-1	1
C83	.85	3-1	1	1.2	3-1	1	1.0	3-1	1
C84	.85	3-2	1	1.2	3-2	1	1.0	3-2	1
C85	.85	2-2	1	1.2	2-2	1	1.0	2-2	1
C61	.85	3-3	1	1.2	3-3	1	1.0	3-3	1
200 cps timing wave		4-1			4-1			4-1	

TABLE 11

where Case 1 - Complete aerodynamic circuit
Case 2 - Complete aerodynamic circuit but without phase shifts (no capacitors)
Case 3 - Aerodynamic circuit without mutual terms

SYSTEM 1 TIP PITCHING VELOCITY

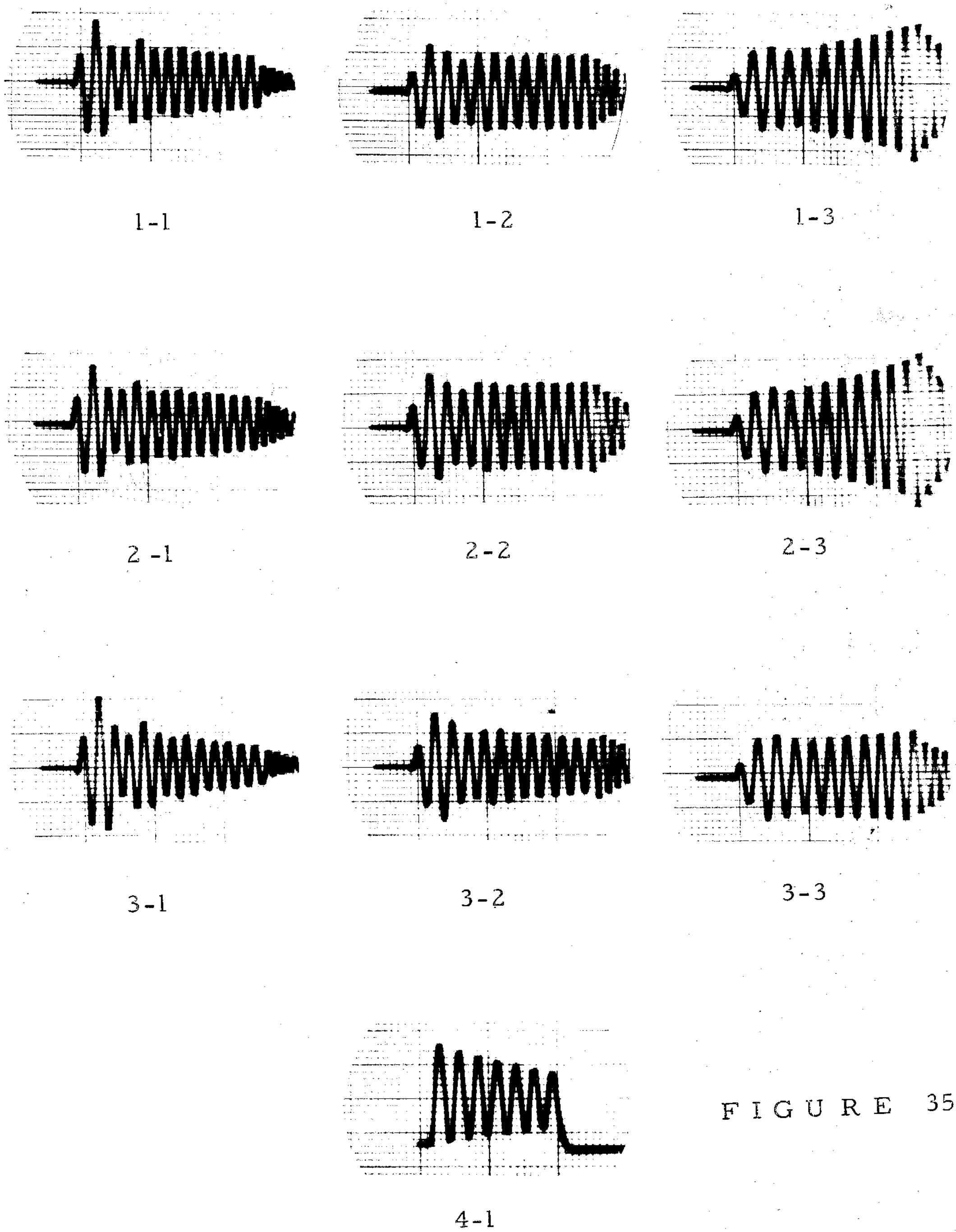

FIGURE 35

SYSTEM I.
STABILITY STIFFNESS
CHARACTERISTICS

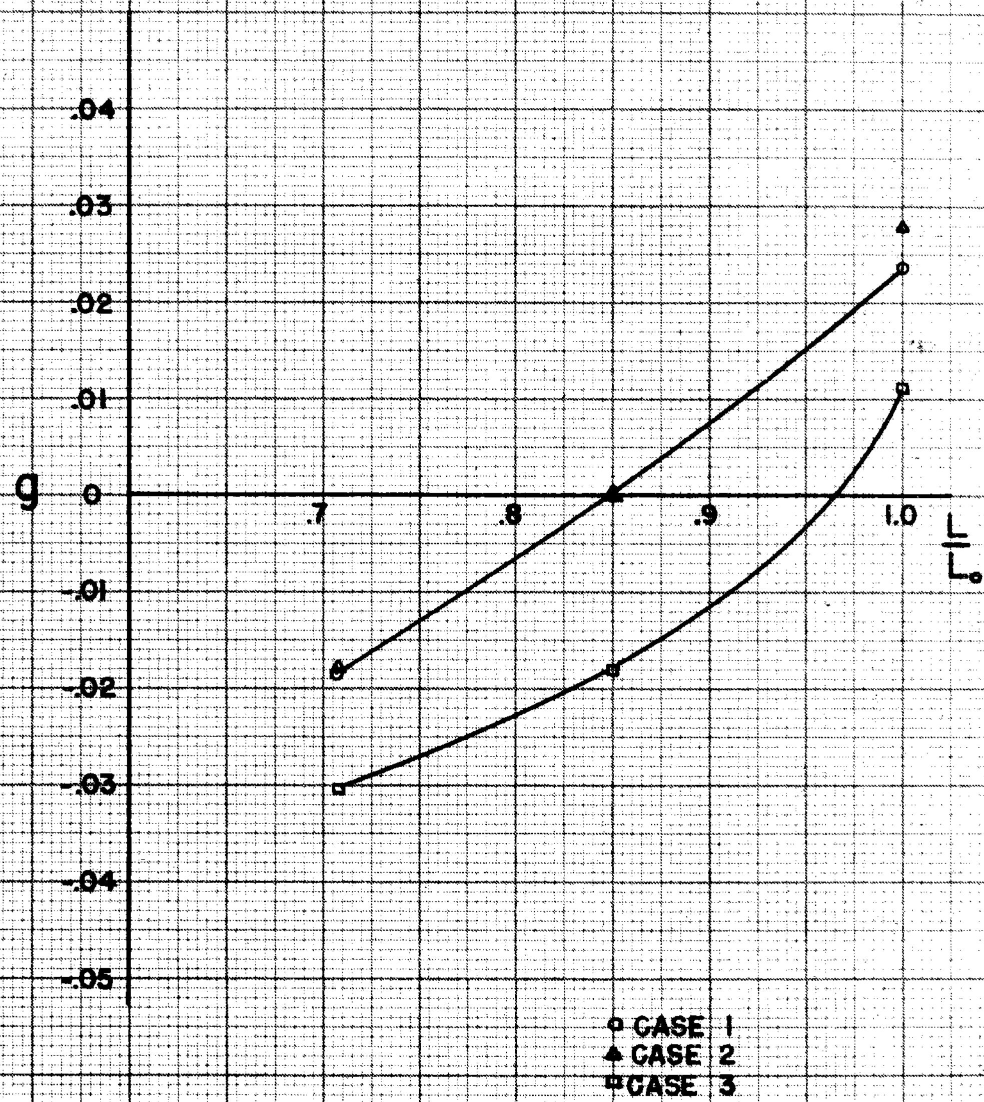

FIGURE 36

SYSTEM I.

FREQUENCY STIFFNESS CHARACTERISTICS

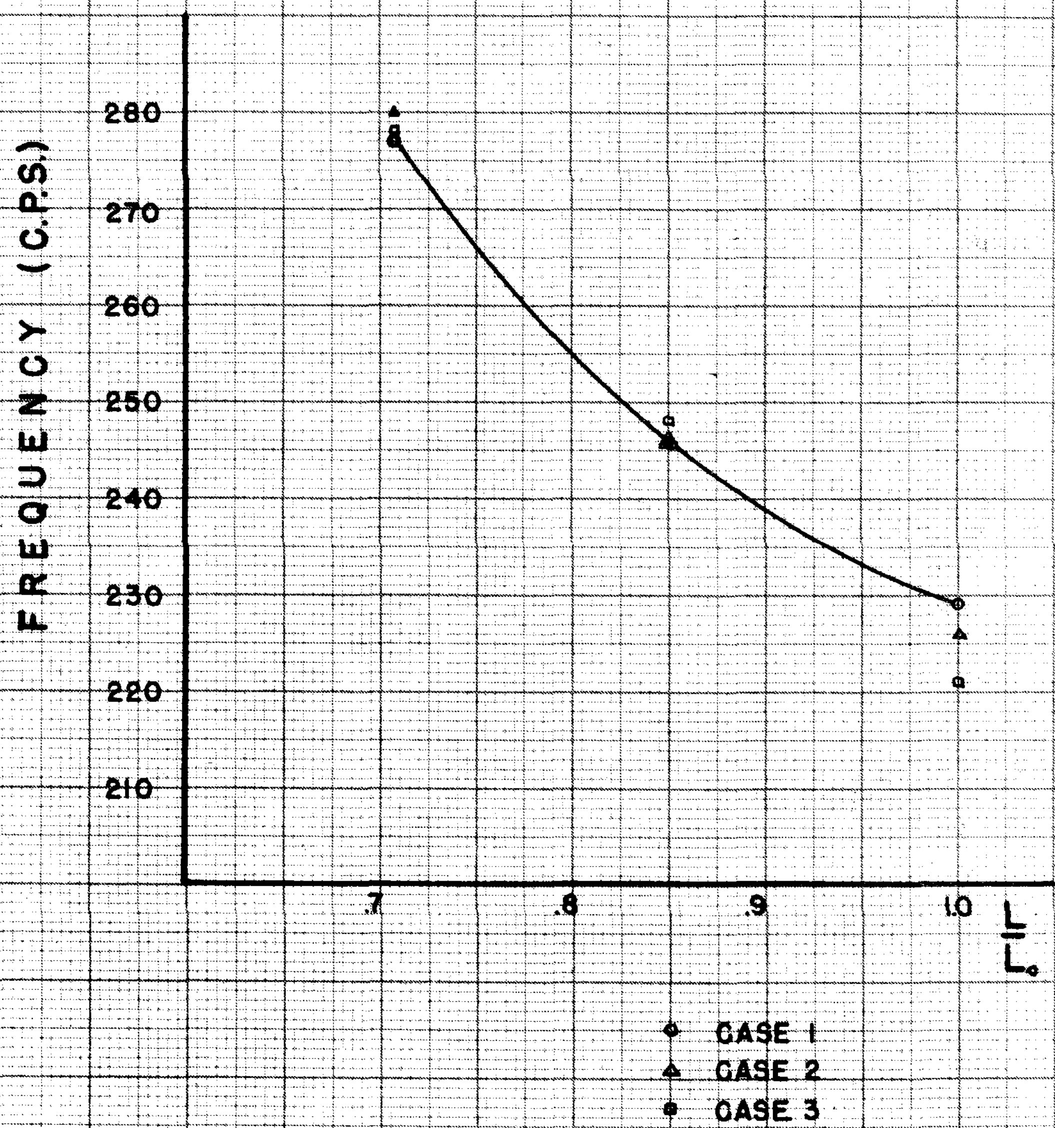

FIGURE 37

SYSTEM 1 MODE SHAPE

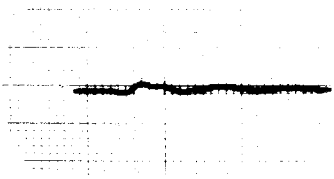

1-1

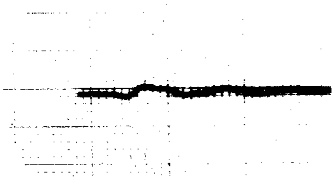

2-1

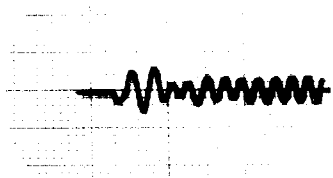

2-2

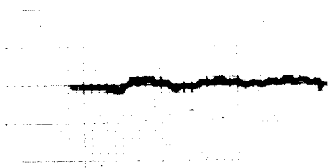

3-1

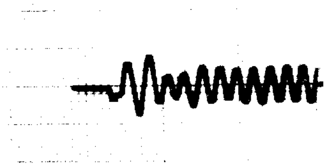

3-2

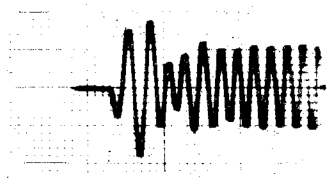

3-3

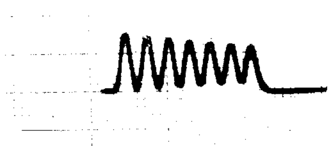

4-1

FIGURE 38

SYSTEM 2 TIP PITCHING VELOCITY

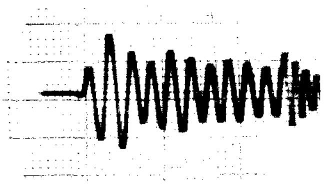

1-1

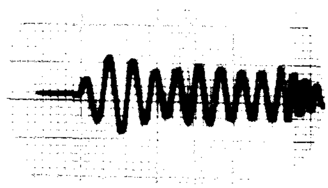

1-2

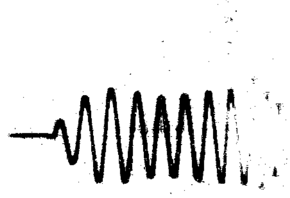

1-3

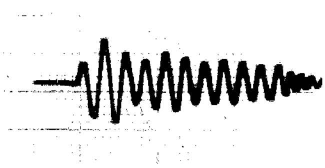

2-1

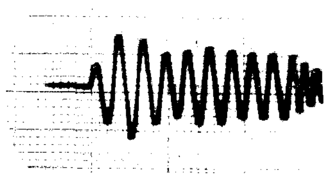

2-2

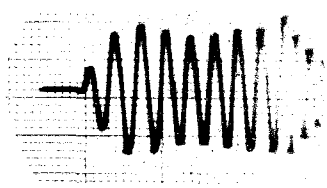

2-3

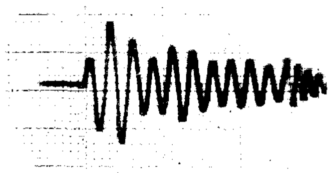

3-1

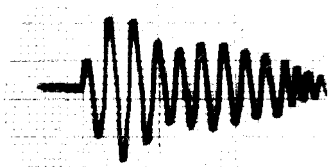

3-2

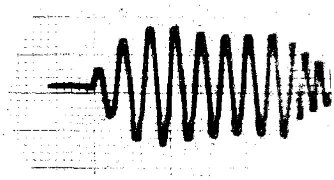

3-3

4-1

FIGURE 39

SYSTEM 2.
STABILITY STIFFNESS CHARACTERISTICS

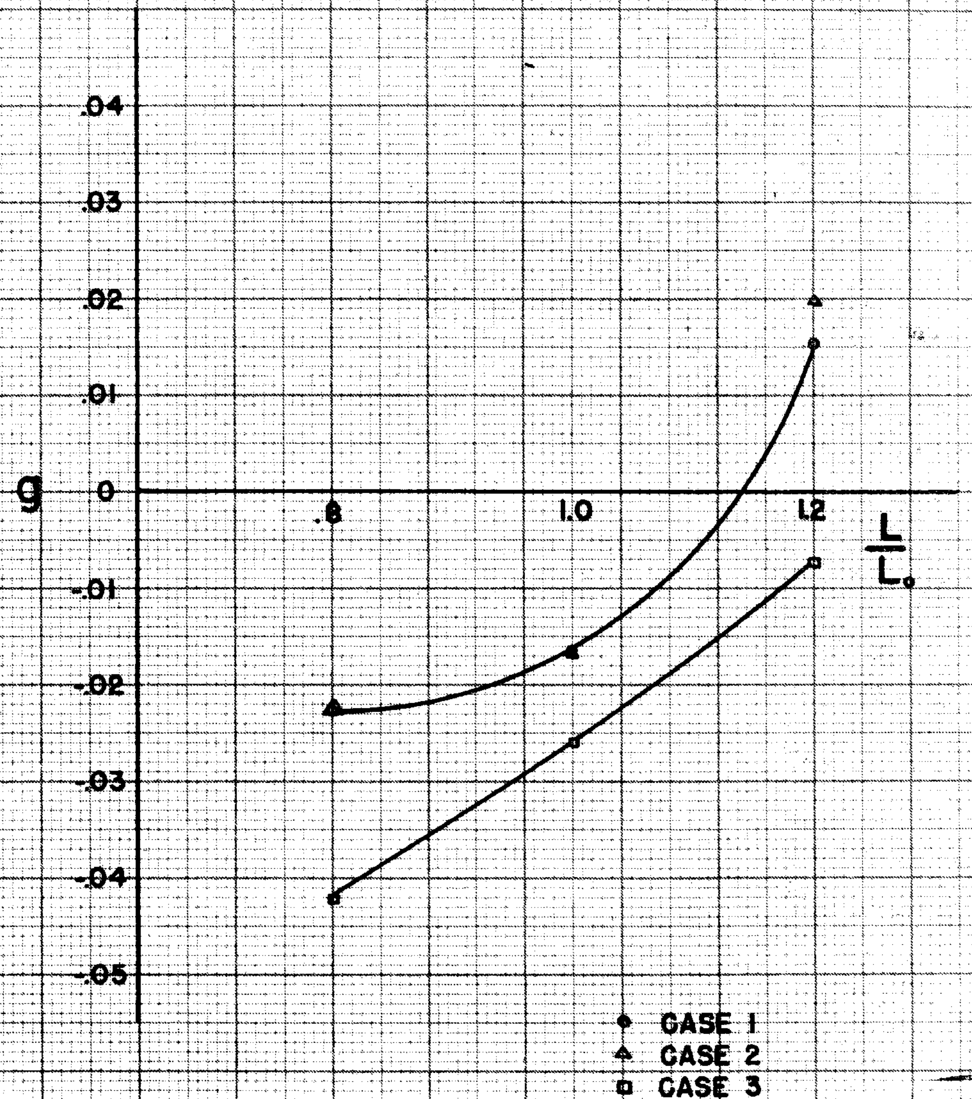

FIGURE 40

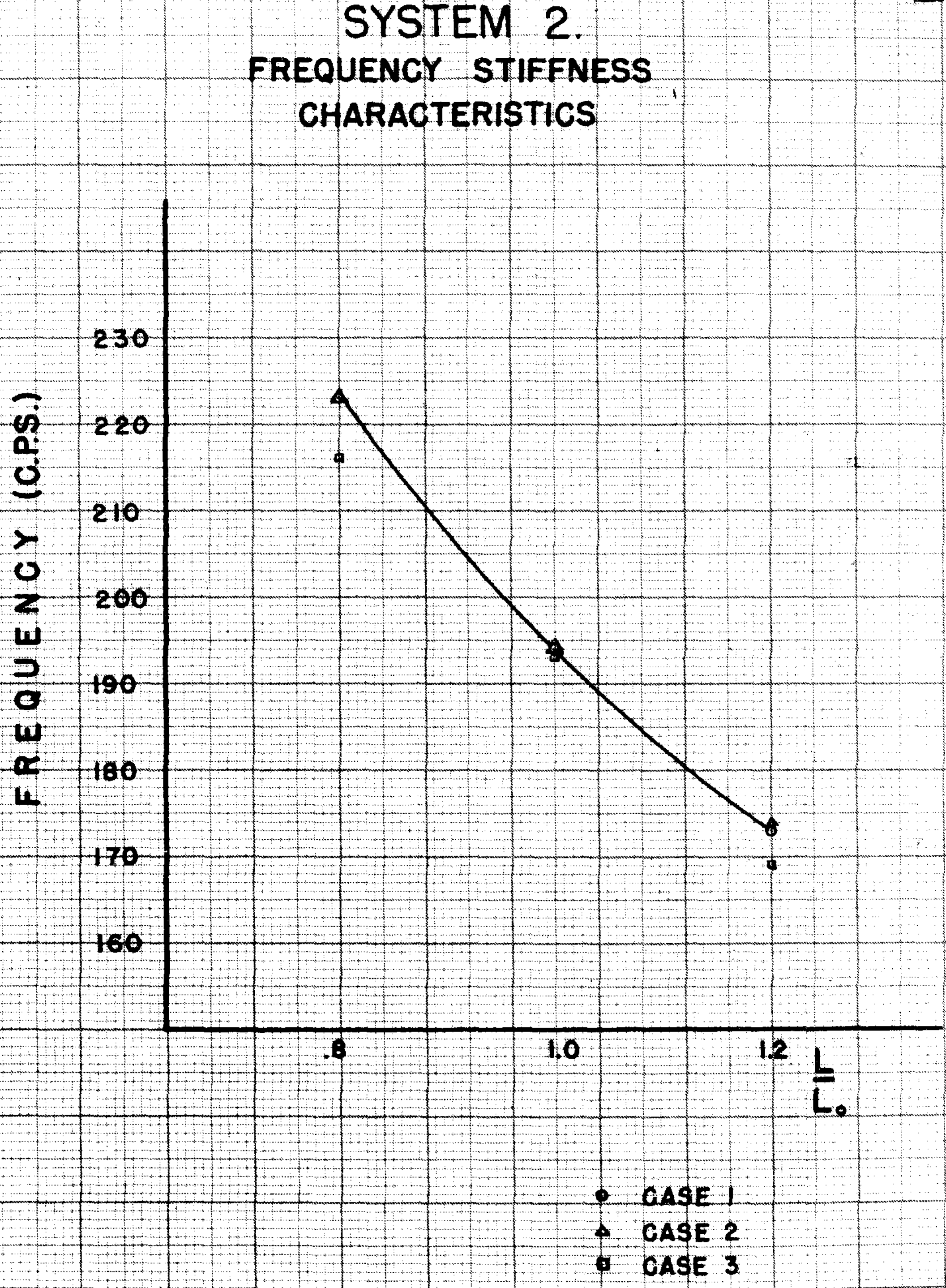
SYSTEM 2.
FREQUENCY STIFFNESS
CHARACTERISTICS
FREQUENCY (C.P.S.)
230
220
210
200
190
180
170
160
.8
1.0
1.2
L
L₀
CASE 1
CASE 2
CASE 3

FIGURE 41

SYSTEM 2 MODE SHAPE

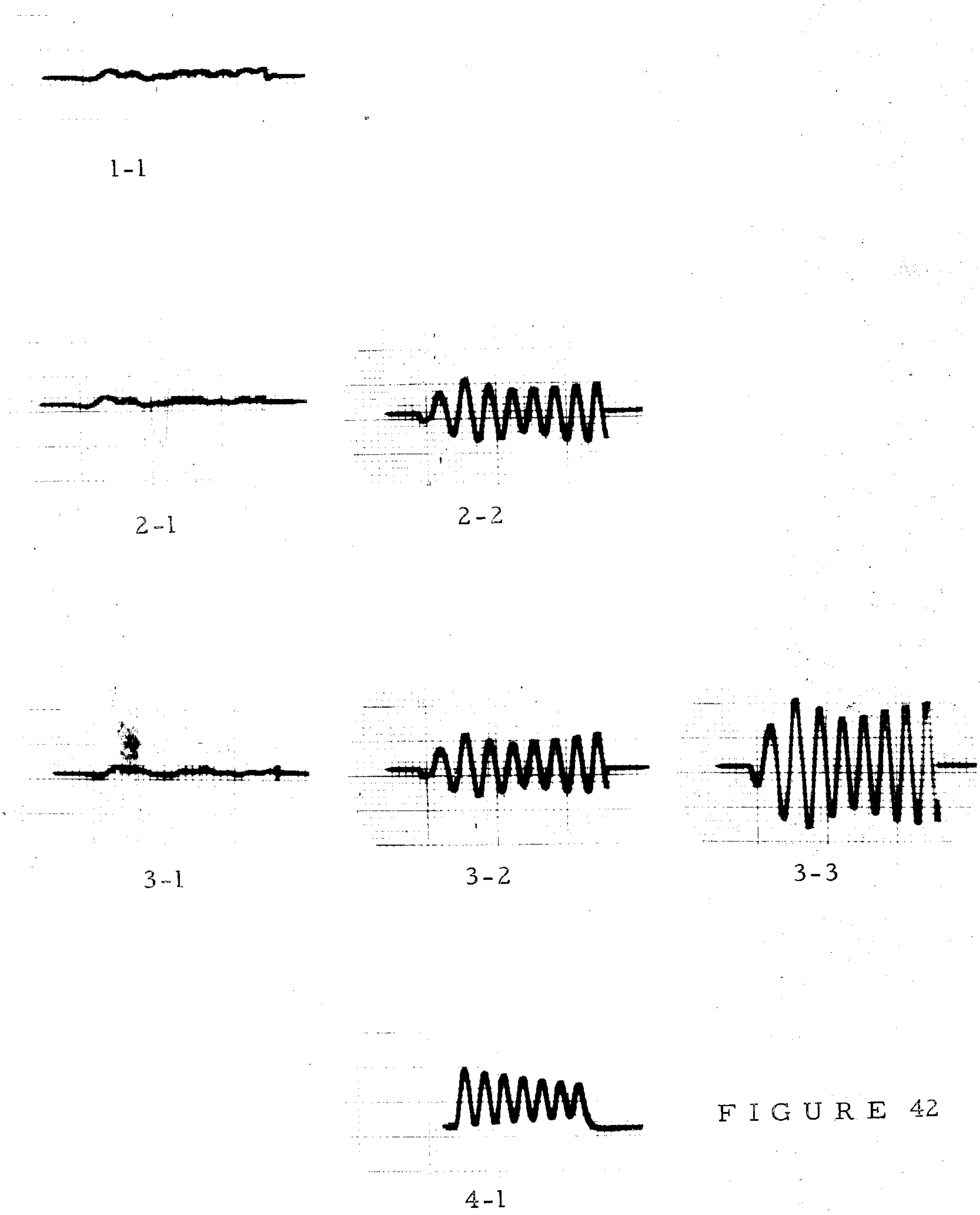

FIGURE 42

SYSTEM 3 TIP PITCHING VELOCITY

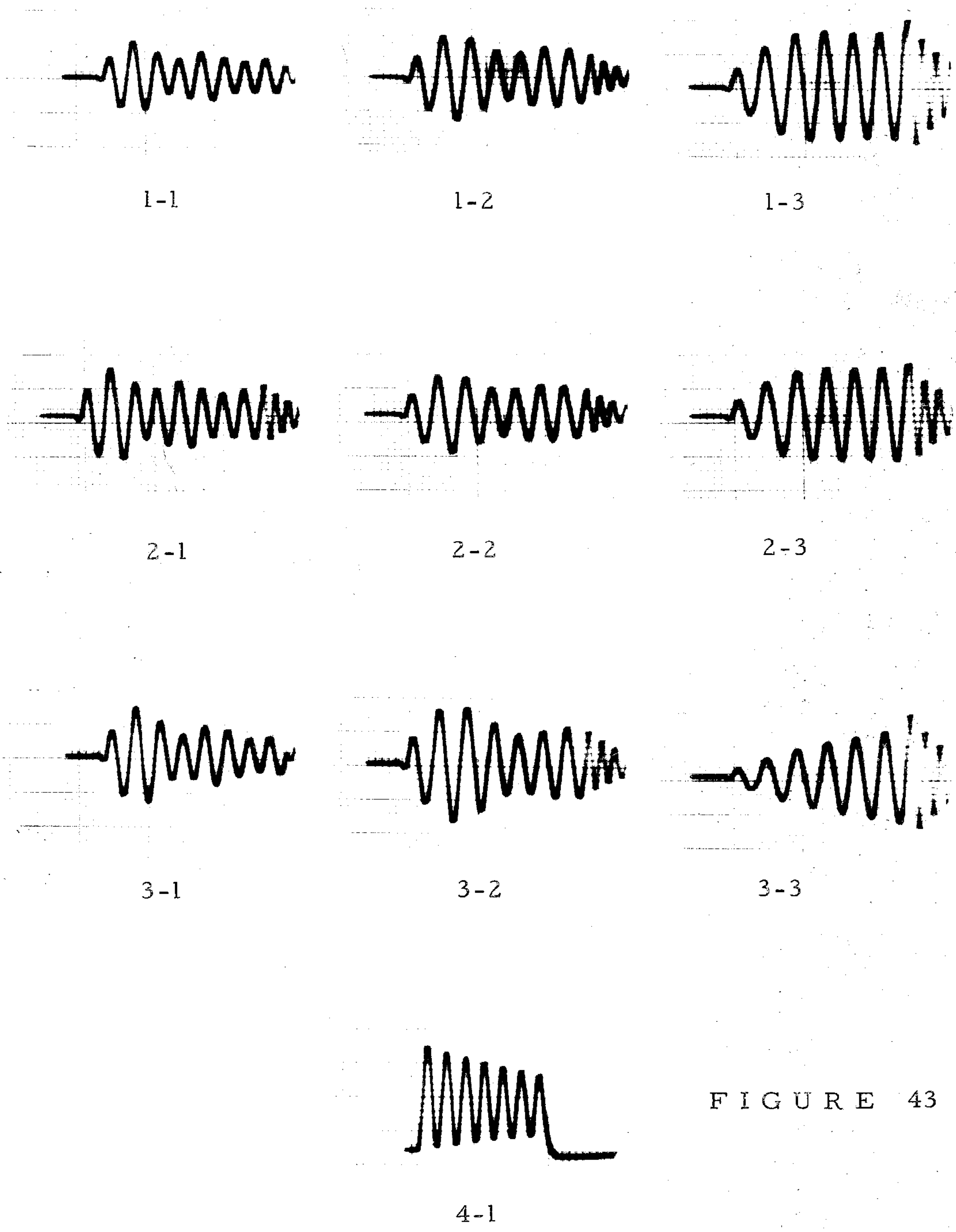

FIGURE 43

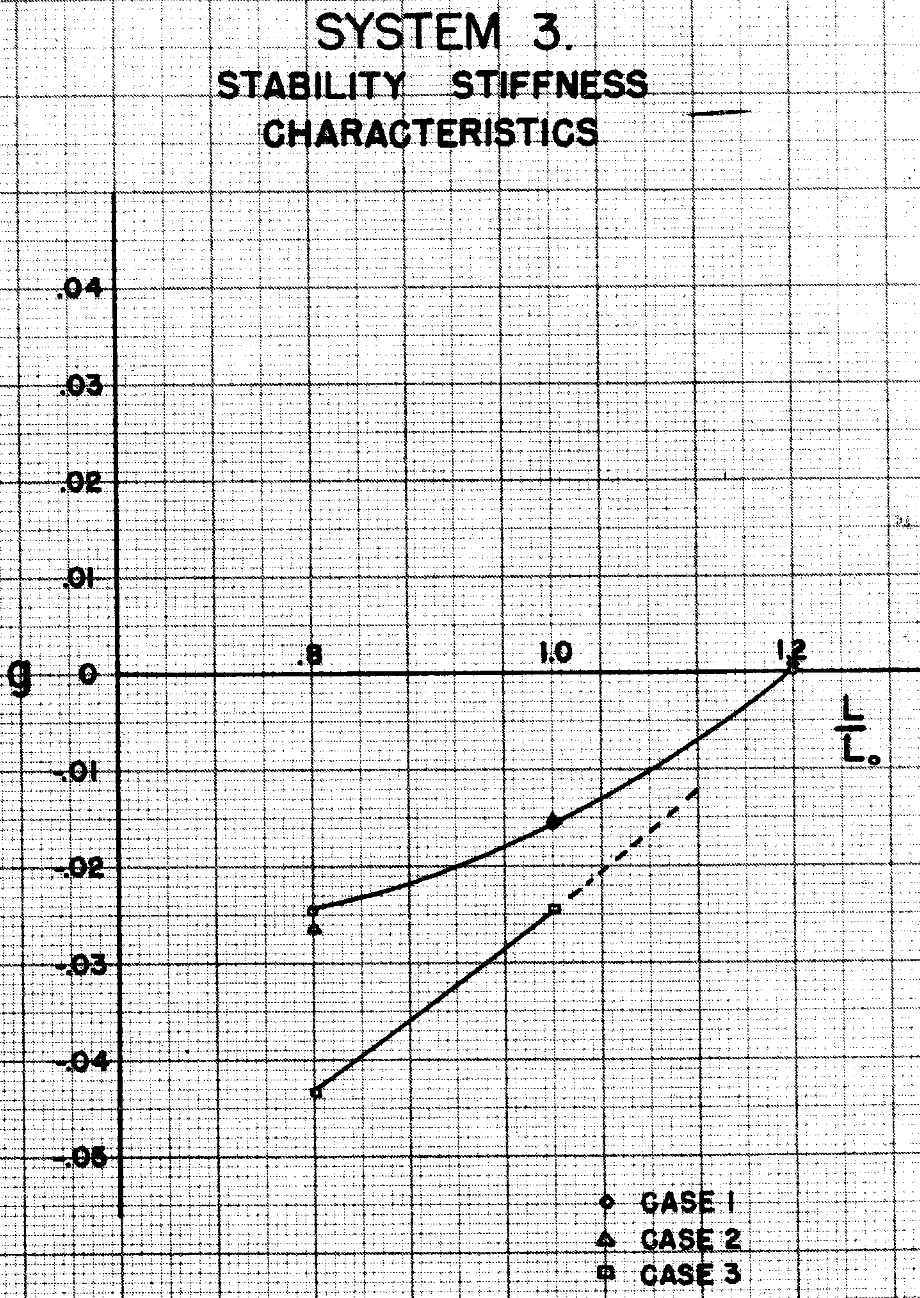
SYSTEM 3.
STABILITY STIFFNESS
CHARACTERISTICS
g
.04
.03
.02
.01
0
-.01
-.02
-.03
-.04
-.05
.8
1.0
1.2
L/L₀
CASE 1
CASE 2
CASE 3

FIGURE 44

SYSTEM 3.
FREQUENCY STIFFNESS CHARACTERISTICS

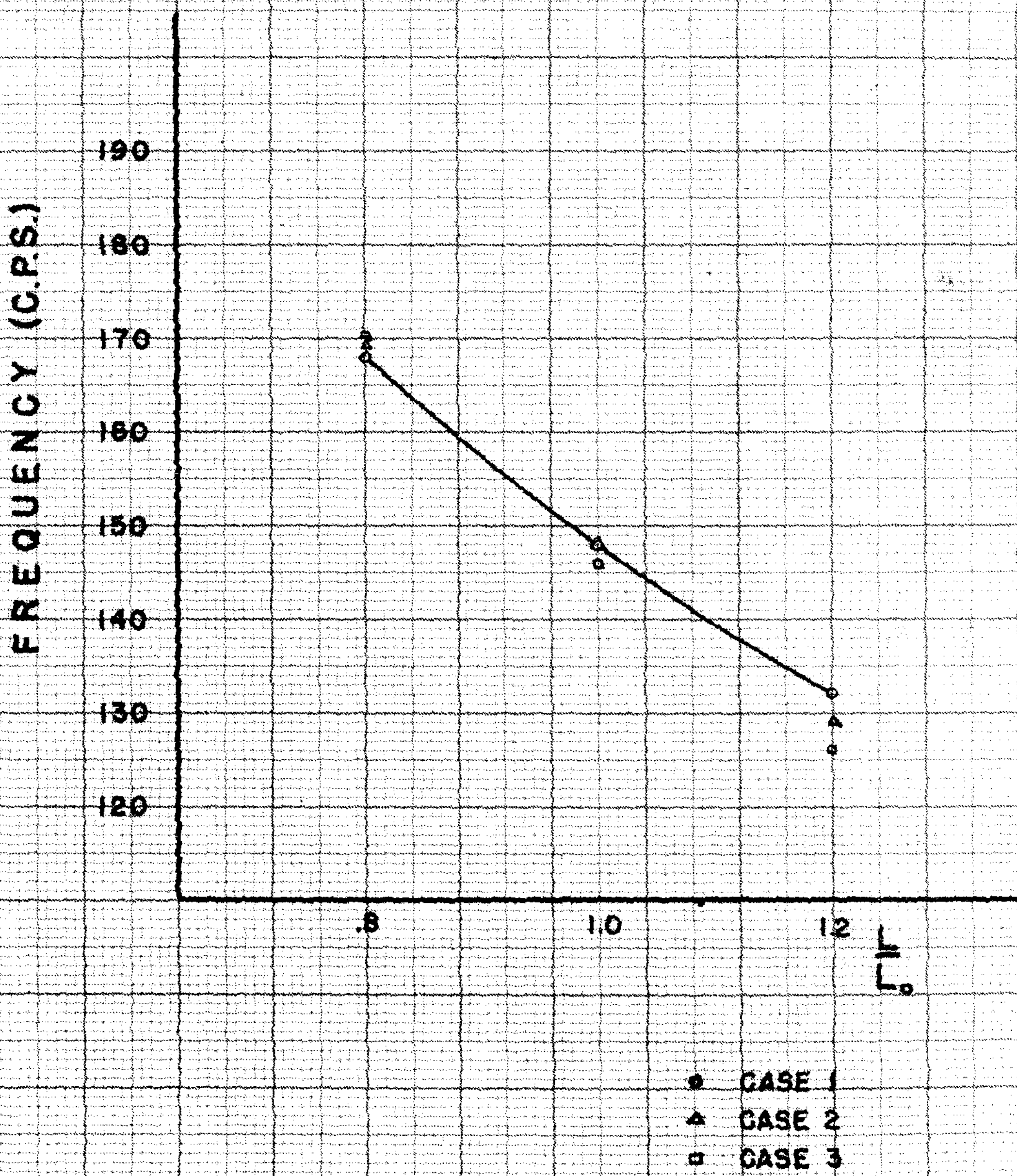

FIGURE 45

SYSTEM 3   MODE SHAPE

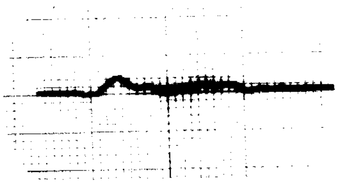

1-1

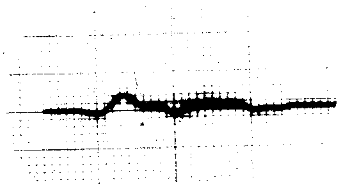

2-1

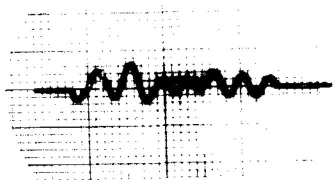

2-2

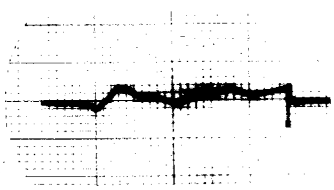

3-1

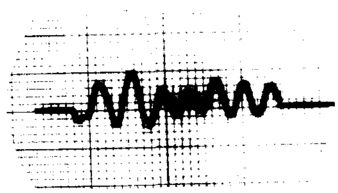

3-2

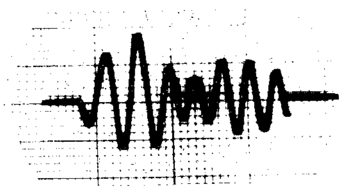

3-3

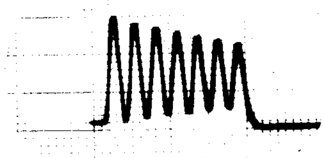

4-1

FIGURE 46

The actual steps in the experimental flutter analysis may be outlined as follows:

1. Set up and test aerodynamic lift cells as outlined in Section III.

2. Set up and test (including normal mode shapes) the elastic wing structure as outlined in Section IV.

3. Test the operation of the synchronous switches - these are used to clamp the wing circuit until the desired aerodynamic lift (transient) is applied (see figure 16).

4. Set up a disturbing function (to be applied to cells 4, 5, 6 at summer 1 inputs). Such a function is to be a damped sine wave of frequency close to the actual flutter frequency so as to excite only one root at a time (see figure 47).

5. Set up a timing wave (200 cps) as a reference (see figure 47).

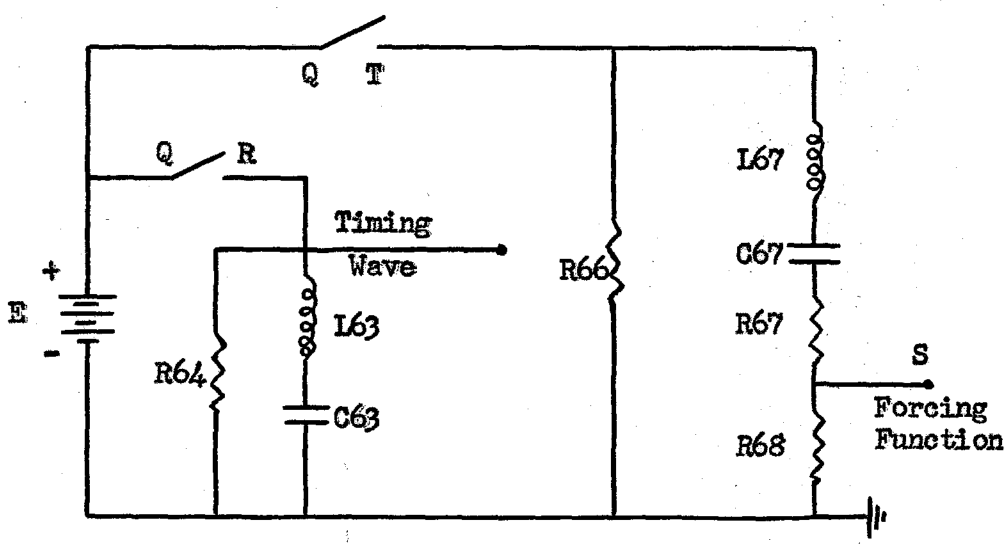

Timing: $\frac{1}{LC} = \omega^2 = 4\pi^2 = (4 \times 10^4)$ $\quad f = 200$ cps

set $\quad$ C 63 = 1 μf

L63 = .632 h $\quad$ or 10-2-8 computer setting

TIMING AND FORCING FUNCTION CIRCUIT

FIGURE 47

An analysis of the computer results shows the following:

1. An aerodynamic circuit of the form of figure 16 can be made to function properly (without parasitic oscillation difficulties).

2. The effect of the mutual terms in the lift equations is one that contributes to the instability of the wing as illustrated by the results of figures 36, 40, and 44. It is thus felt by the author, that in future studies with greater numbers of cells, that such mutual terms should definitely be included in the aerodynamic circuits.

3. The effect of the capacitors in the lag (lead) functions is negligible, hence it can be deduced that low frequency flutter is largely caused by the magnitude of the lift and not by its phase. The lag (lead) function capacitors may thus be omitted from the aerodynamic lift circuit. Such an omission not only produces a large saving of capacitors (especially for wings with large numbers of cells), but also simplifies both the associated wiring in the circuit, and the computations of the lag (lead) function parameters.

VI CONCLUSIONS AND RECOMMENDATIONS FOR FURTHER RESEARCH

The results of the electric analog computer study of the flutter of delta wings at supersonic speeds (the speed $M^2 = 1.75$ being analyzed) may again be briefly summarized as follows:

1. Circuits of the form of figure 16 can be made to produce the desired lift currents without parasitic and high frequency oscillations.

2. The mutual lift terms are significant and tend to destabilize the wing.

3. The effect of capacitors (lag or lead) in all aerodynamic circuits for the allowable frequency range is negligible.

In conclusion it should be noted that the structures analyzed were extremely crude and were so chosen as to test the performance of the aerodynamic circuit in as simple a manner as possible. Now it is fairly obvious that in order to analyze an actual wing on an electric analog computer like the one located in the Analysis Laboratory at the California Institute of Technology, a more complete wing analogy must be used. This will require more cells, and in turn, the condition of more cells will require more amplifiers (four amplifiers per cell). The practical difficulty with having more amplifiers, aside from the additional computations that must be performed, is the complicated wiring scheme that must be used. The author had only twenty-four amplifiers and fourteen lag (lead) functions mounted in four Analysis Laboratory racks, yet the physical wiring was quite involved with wires going off in all directions.

As a solution to the above problem, a rack of a new design (figure 47) is suggested. Such a rack will not only contain power supplies and amplifiers, but will also contain trays of potentiometers and places for plug-in elements. The advantages of such a rack are:

1. Only three leads per cell will have to go from the rack to the main computer plug board (one "h" lead, one "α" lead and the output lead of the current generator). All other connections will be between amplifiers and the potentiometer board.

2. By having the potentiometers mounted separately, the summer plug-in unit can be simplified, and it will be possible to have many more summer inputs on one plug-in unit. (This will be necessary when the number of aerodynamic cells will be increased.)

3. Such a rack can be physically moved to a desired position with relative ease (one such position is illustrated in figure 48).

4. Such a rack (2 will be required) is relatively inexpensive and easy to build.

SUGGESTED AERODYNAMIC TRAYS

SCALE: $\frac{3}{8}'' = 1'$

FIGURE 48

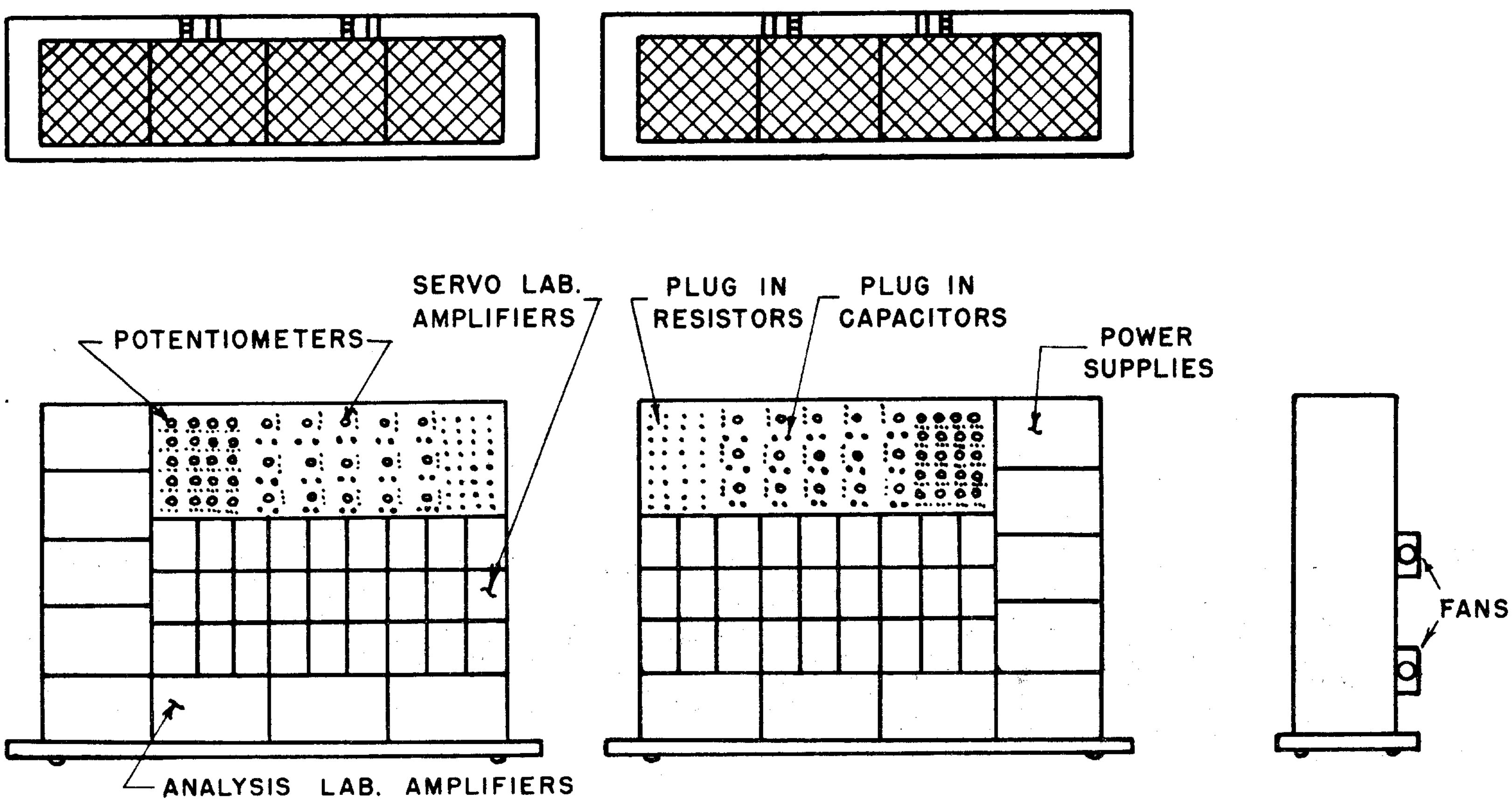

C.I.T. COMPUTER
AERODYNAMIC TRAYS

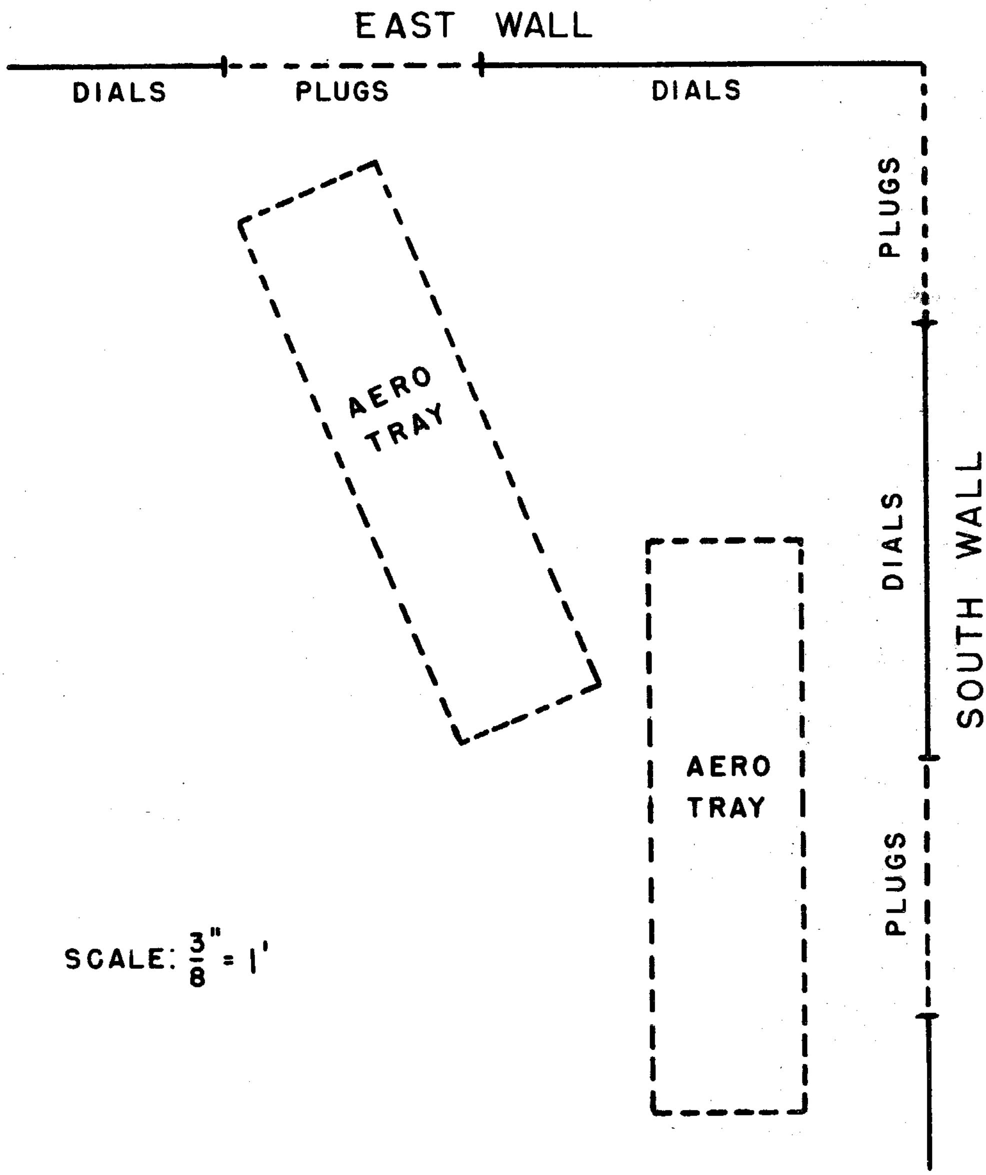

FIGURE 49

APPENDIX A

DERIVATION OF THE WAVE EQUATION

A derivation of equation (1) is given briefly at this point. The condition for irrotational flow

$$\text{Curl } \bar{v} = 0 \tag{A1}$$

implies a velocity potential

$$\bar{v} = - \text{grad } \phi \tag{A2}$$

then if the density in the stream ρ is defined as

$$\rho = \rho_o(1 + s) \tag{A3}$$

where s is a variable "condensate".

The continuity equation gives

$$\dot{\rho} + \nabla \cdot (\rho \bar{v}) = 0 \tag{A4}$$

while Newton's law for the pressure P gives

$$-\nabla P = \rho \dot{\bar{v}} + (\rho \bar{v} \cdot \nabla) \bar{v} \tag{A5}$$

Since P is only a function of ρ, equation (A5) gives

$$\rho_o \dot{\bar{v}} = - \left(\frac{dP}{d\rho}\right)_o \nabla \rho \tag{A6}$$

where $\left(\frac{dP}{d\rho}\right)_o$ is the value in the undisturbed stream, and from acoustics equals c^2, the local variable speed of sound.

Using (A6) and (A2)

$$\dot{\bar{v}} = - c^2 \nabla s = - \frac{\partial}{\partial t} (\nabla \phi)$$

or

$$\frac{\partial \phi}{\partial t} = c^2 s \tag{A7}$$

Also from (A4) and (A2)

$$\frac{\partial s}{\partial t} = \nabla^2 \phi \tag{A8}$$

Differentiating (A7) with respect to time and equating to (A8) gives

$$\nabla^2\phi = \frac{1}{\alpha^2}\frac{\partial^2\phi}{\partial t^2} \tag{A9}$$

APPENDIX B

CALCULATION OF PRESSURE FOR 6 CELL WING

$M^2 = 1.75 \quad b = 1/2' \qquad = 30^\circ$

SYMMETRICAL CASE

(1)	(2)	(3)	(4)	(5)	(6)	(7)
Cell	Formula	$x-\xi_1$	$(3)^2$	1.3463x(4)	1.7951x(3)	$\frac{p \pi \beta}{-2\rho M c W_s e^{j\omega t}} = -\pi + \bar{\omega}^2(4) + j\bar{\omega}(6)$
1a,4a,6a	24'	.0834	.006956	.009364	.14971	$(-\pi + \bar{\omega}^2\ .006956) + j\bar{\omega}\ .14971$
2a	24'	.167	.027889	.037547	.29978	$(-\pi + \bar{\omega}^2\ .02789) + j\bar{\omega}\ .2998$
3a,5a	24'	.100	.0100	.013463	.17951	$(-\pi + \bar{\omega}^2\ .010) + j\bar{\omega}\ .17951$

(1)	(2)	(3)	(4)	(5)	(6)	(7)	(8)	(9)	(10)	(11)
Cell	Formula	$x-\xi_1$	$x-\xi_2$	$(3)^2$	$(4)^2$	(5)-(6)	1.3463x(7)	(3)-(4)	1.7951x(9)	$\frac{p \pi \beta}{-2\rho M c W_s e^{j\omega t}} = \bar{\omega}^2(8) + j\bar{\omega}(10)$
1b	22'	.250	.0834	.0625	.006956	.05554	.07149	.1666	.2991	$\bar{\omega}^2\ .07477 + j\bar{\omega}\ .2991$
2b	22'	.250	.167	.0625	.02789	.03461	.04660	.0830	.1490	$\bar{\omega}^2\ .04660 + j\bar{\omega}\ .1490$
4b	22'	.250	.0834	.0625	.006956	.05554	.07149	.1666	.2991	$\bar{\omega}^2\ .07477 + j\bar{\omega}\ .2991$

TABLE 1B

TABLE 1B (continued)

(1)	(2)	(3)	(4)	(5)	(6)	(7)	(8)	(9)	(10)	(11)	(12)	(13)
Cell	Formula	$x-\xi_1$	$x-\xi_2$	A	2A	D	(6)+(7)	cot θ_1	cos $2\theta_1$	(4)/(3)	1-(11)	-(9)x(12)
1c	21'	.416	.250	-2.457	-4.914	-2.947	-7.861	-1.2251	.2002	.6010	.3990	.5009
1d	21'	.416	.250	- .6850	-1.370	- .1950	-1.565	1.2240	.1994	.6010	.3990	-.4884
1e	21'	.583	.416	-2.352	-4.704	-2.852	-7.556	- .9916	-.008389	.7136	.2864	.2840
1f	21'	.666	.583	-1.9295	-3.859	-2.258	-6.117	- .3755	-.7535	.8754	.1246	.04679
1g	21'	.770	.666	-1.706	-3.412	-1.840	-5.212	- .135	-.9636	.8649	.1351	.01824
1g'	21'	.770	.666	- .5672	-1.1344	- .1141	-1.2485	1.5697	.4226	.8649	.1351	-.2121
2c	21'	.500	.250	-2.001	-4.002	-2.380	-6.382	- .4592	-.5100	.5000	.5000	.2296
3b	21'	.167	.100	-1.965	-3.930	-2.3196	-6.250	- .4160	-.7050	.5988	.4012	.1669
4c	21'	.417	.250	-1.9675	-3.935	-2.3239	-6.259	- .4195	-.7014	.5995	.4005	.1680
4c'	21'	.417	.250	- .7570	-1.514	- .2578	-1.792	1.0585	.05677	.5995	.4005	-.4239
4d	21'	.417	.250	- .7570	-1.514	- .2578	-1.792	1.0585	.05677	.5995	.4005	-.4239
4e	21'	.750	.417	-1.123	-2.246	- .7327	-2.979	.48034	-.6251	.5560	.4440	-.2133
5b	21'	.167	.100	-1.965	-3.930	-2.3196	-6.250	- .41597	-.7050	.5988	.4012	.1669
5c	21'	.245	.167	-1.306	-2.612	-1.053	-3.665	.27116	-.8630	.6816	.3184	-.0863
5d	21'	.500	.245	- .6195	-1.239	- .1467	-1.386	1.4037	.3257	.4900	.5100	-.7159
6b	21'	.250	.0834	- .759	-1.518	- .260	-1.778	1.0538	.0523	.3336	.6664	-.7023

TABLE 1B (continued)

(1)	(2)	(14)	(15)	(16)	(17)	(18)	(19)	(20)	(21)	(22)
Cell	Formula	$(3)^2$	$(4)^2$	(14)-(15)	(.14285)((8))	(16)x(17)	(4)x(15)	(19)/(3)	(14)-(20)	(9)x(21)
1c	21'	.1731	.0625	.1106	1.1229	.1244	.01563	.03757	.1355	-.1660
1d	21'	.1731	.0625	.1106	.2236	.0246	.01563	.03757	.1355	.1658
1e	21'	.3399	.1731	.1668	1.079	.1800	.07201	.1235	.2164	-.2146
1f	21'	.4436	.3399	.1037	.8738	.09061	.1982	.2976	.1460	-.05482
1g	21'	.5929	.4436	.1493	.7445	.1112	.2954	.3836	.2093	-.02826
1g'	21'	.5929	.4436	.1493	.1783	.02662	.2954	.3836	.2093	.3285
2c	21'	.2500	.0625	.1875	.9117	.1709	.01563	.03126	.2187	-.1004
3b	21'	.02789	.0100	.01789	.8928	.01597	.00100	.005988	.02190	-.009110
4c	21'	.1739	.0625	.1114	.8941	.09960	.01563	.03748	.1364	-.05722
4c'	21'	.1739	.0625	.1114	.2560	.0285	.01563	.03748	.1364	.1444
4d	21'	.1739	.0625	.1114	.2560	.0285	.01563	.03748	.1364	.1444
4e	21'	.5625	.1739	.3886	.4256	.1654	.07252	.09669	.4658	.2237
5b	21'	.02789	.0100	.01789	.8928	.01597	.00100	.005988	.02190	-.009110
5c	21'	.06003	.02789	.03214	.5235	.01683	.004658	.01901	.04102	.01112
5d	21'	.2500	.06003	.1900	.1980	.03762	.001471	.002942	.2471	.3469
6b	21'	.0625	.006956	.0555	.2540	.01410	.0005801	.002320	.06018	.06342

TABLE 1B (continued)

(1)	(2)	(23)	(24)	(25)	(26)	(27)
Cell	Formula	-.047616 x (10)	(23) + .21428	(22) x (24)	(13) + ω^2 [(18) + (25)]	(15)/(3)
1 c	21'	-.00952	.2048	-.0340	.5009 + ϖ^2 .0904	.1502
1 d	21'	-.00949	.2048	.03395	-.4884 + ϖ^2 .0586	.1502
1 e	21'	.000399	.2137	-.04586	.2840 + ϖ^2 .1342	.2969
1 f	21'	.03588	.2502	-.01371	.0467 + ϖ^2 .0769	.5104
1 g	21'	.04588	.2602	-.007353	.01824 + ϖ^2 .1038	.5761
1g'	21'	-.02012	.1942	.06379	-.2121 + ϖ^2 .09041	.5761
2 c	21'	.02428	.2386	-.02396	.2296 + ϖ^2 .1469	.1250
3 b	21'	.03357	.2479	.002258	.1669 + ϖ^2 .01371	.05988
4 c	21'	.03340	.2477	-.01417	.1680 + ϖ^2 .08543	.1499
4c'	21'	-.002703	.2115	.03054	-.4239 + ϖ^2 .0590	.1499
4 d	21'	-.002703	.2115	.03054	-.4239 + ϖ^2 .0590	.1499
4 e	21'	.02976	.2441	.05461	-.2133 + ϖ^2 .2200	.2319
5 b	21'	.03357	.2479	-.002258	.1669 + ϖ^2 .01371	.05988
5 c	21'	.04109	.2554	.00284	-.0863 + ϖ^2 .01967	.1138
5 d	21'	-.01551	.1988	.06896	-.7159 + ϖ^2 .10658	.1201
6 b	21'	-.00249	.2118	.01343	-.7023 + ϖ^2 .02153	.02782

TABLE 1B (continued)

$$\frac{P \pi \beta}{-2\rho M c W_s e^{j\omega t}} = (26) + (32) \quad \text{where} \quad \bar{\omega} = \frac{\omega M}{c\beta^2} = 1.6035\times10^{-3}\omega$$

(1)	(2)	(28)	(29)	(30)	(31)	(32)
Cell	Formula	(3) - (27)	.5 [(9) x (28)]	(3) - (4)	.57140 (5) x (30)	$j\bar{\omega}$ [(29) - (31)]
1c	21'	.2660	-.1629	.1660	-.2330	$j\bar{\omega}$ .0701
1d	21'	.2660	.1628	.1660	-.06497	$j\bar{\omega}$ .2278
1e	21'	.2861	-.1418	.1670	-.2244	$j\bar{\omega}$ .0826
1f	21'	.1556	-.02921	.0830	-.09151	$j\bar{\omega}$ .0623
1g	21'	.1940	-.01310	.1040	-.1014	$j\bar{\omega}$ .0883
1g'	21'	.1940	.1523	.1040	-.03371	$j\bar{\omega}$ .1860
2c	21'	.3750	-.08610	.2500	-.2857	$j\bar{\omega}$ .1996
3b	21'	.1071	-.02228	.0670	-.07523	$j\bar{\omega}$ .05295
4c	21'	.2671	-.05602	.1670	-.1877	$j\bar{\omega}$ .1317
4c'	21'	.2671	.1414	.1670	-.07224	$j\bar{\omega}$ .2136
4d	21'	.2671	.1414	.1670	-.07224	$j\bar{\omega}$ .2136
4e	21'	.5181	.1244	.3330	-.2137	$j\bar{\omega}$ .3381
5b	21'	.1071	-.02228	.0670	-.07523	$j\bar{\omega}$ .05295
5c	21'	.1312	.01779	.0780	-.05821	$j\bar{\omega}$ .07600
5d	21'	.3799	.2666	.2550	-.09026	$j\bar{\omega}$ .3569
6b	21'	.2222	.1171	.1666	-.07225	$j\bar{\omega}$ .1894

REFERENCES

1. Garrick, I. E. and Rubinow, S. I.: "Theoretical Study of Air Forces on an Oscillating or Steady Thin Wing in a Supersonic Main Stream." NACA Report No. 872, (1947).

2. Garrick, I. E. and Rubinow, S. I.: "Flutter and Oscillating Air-Force Calculations for an Airfoil in a Two-Dimensional Supersonic Flow." NACA Report No. 846, (1946).

3. Stewart, H. J. and Ting-Yi Li: "Source-Superposition Method of Solution of a Periodically Oscillating Wing at Supersonic Speeds." Quarterly of Applied Mathematics, Vol. 9, (April - Jan. 1951-52), pp 31-49.

4. Baker, B. B. and Copson, E. T.: "Mathematical Theory of Huygen's Principle." Oxford, (1939).

5. Küssner, H. G.: "General Airfoil Theory." NACA TN 979, (1941).

6. Nelson, Herbert C.: "Lift and Moment on Oscillating Triangular and Related Wings with Supersonic Edges." NACA TN 2494 (Sept. 1951).

7. Pines, S. and Epstein, A.: "The Flutter Analysis of An Elastic Wing with Supersonic Edges." Republic Aviation Corporation, Report E-SAF-1.

8. McCann, G. D., Wilts, C. H., and MacNeal, R. H.: "Computer Course Notes." California Institute of Technology, (1951).

9. MacNeal, R. H., McCann, G. D., and Wilts, C. H.: "The Solution of Aeroelastic Problems by Means of Electrical Analogies." Journal of the Aeronautical Sciences, Vol. 18, No. 12, (December, 1951).

10. MacNeal, R. H.: "Theoretical and Experimental Effect of Sweep Upon the Stress and Deflection Distribution in Aircraft Wings of High Solidity." Guggenheim Aeronautical Laboratory Report, Part IV, California Institute of Technology, (June 1949).